July 2021

IMPROVEMENT OF SOLUBILITY, STABILITY, AND BIOACCESSIBILITY OF CURCUMIN USING COLLOIDAL DELIVERY SYSTEMS

bingjing zheng
University of Massachusetts Amherst

IMPROVEMENT OF SOLUBILITY, STABILITY, AND BIOACCESSIBILITY OF CURCUMIN USING COLLOIDAL DELIVERY SYSTEMS

bingjing zheng

IMPROVEMENT OF SOLUBILITY, STABILITY, AND BIOACCESSIBILITY OF CURCUMIN USING COLLOIDAL DELIVERY SYSTEMS

A Dissertation Presented

By

BINGJING ZHENG

Submitted to the Graduate School of the
University of Massachusetts Amherst in partial fulfillment
of the requirements for the degree of

DOCTOR OF PHILOSOPHY

May 2021

The Department of Food Science

IMPROVEMENT OF SOLUBILITY, STABILITY, AND BIOACCESSIBILITY OF CURCUMIN USING COLLOIDAL DELIVERY SYSTEMS

A Dissertation Presented

by

BINGJING ZHENG

Approved as to style and content by:

_____
David Julian McClements, Chair

_____
Hang Xiao, Member

_____
Matthew Moore, Member

_____
Zhenhua Liu, Member

_____
Lynne McLandsborough, Department Head
Department of Food Science

DEDICATION

To my parents, my sisters, my best friends, my son, and my husband

ACKNOWLEDGMENTS

First and foremost, I would like to express my sincere gratitude to my supervisor and mentor, Prof. David Julian McClements, an inspiratory and true scholar. Without his continued guidance and encouragement in study and research, I could not achieve this milestone.

His gentle, humble, patient, motivating, and immense knowledge always amaze and influence me. He is the true role model professional and an example of younger leads. He is the person I always look up and be my motivation. I could not imagine that I could have a better advisor than him. I would also like to appreciate the gentle guidance and support from my committee members: Prof. Hang Xiao, Prof. Guodong Zhang, Prof. Moore, and Prof. Liu. Especially Prof. Xiao, who advised and encouraged my education since my undergraduate years.

Many thanks go to Jean Alarmed, our lab manager, and our big sister. She offered the best working environment for us, which helps my experiences went smooth and organized. Her brilliant ideas of celebrations for specials, understanding, and fun make our lab as a big family and warmed my heart. Besides on her, I would also like to thanks my “family members” that I know from our lab: Bicheng, Ruojie, Tommy, Cynthia, Mahesh, Cheryl, Zipei, Dora, Xiaoyun, Fuguo, Qianchun, Xiang, Luping, Xiangyu, Li, Yi, Shengfeng, Lu, Yunbing, and Jinning, who provides me supports backups whenever I need.

Last but not the lease, my deepest appreciation goes to my members of my family: my Mom, my grandparents, and my sisters, who provided my unwavering supports. I would like to express my sincere appreciation to my husband and my son, who always being there for me.

ABSTRACT

Improving the solubility, stability and bioaccessibility of lipophilic nutraceutical, Curcumin, using colloidal delivery systems

MAY 2021
BINGJING ZHENG
B.A., University of Massachusetts Amherst
Ph.D., University of Massachusetts Amherst
Directed by: Professor David Julian McClements

Curcumin is a yellow-orange crystalline substance found in certain foods (turmeric) that is claimed to exhibit a broad range of biological activities. Its application as a nutraceutical in functional foods and beverages is often limited by its relatively low solubility in aqueous media, its chemical instability, and its low bioavailability. Recent research suggests that colloidal delivery systems can overcome these hurdles and improve the efficacy and commercial value of curcumin in the food, supplement, and pharmaceutical fields. The purpose of this research was to develop colloidal delivery systems to improve the application of curcumin as a nutraceutical in foods.

First, the chemical degradation of curcumin in oil-in-water emulsions and filled hydrogel beads (alginate and chitosan beads) was initially compared to that of curcumin in aqueous solutions (dimethyl sulfoxide, DMSO). The same amount of curcumin was encapsulated in all the delivery systems, and the emulsion and aqueous solution form of curcumin exhibited higher color intensity than the hydrogel beads. After being incubated in the samples under both acidic and neutral conditions for 15-days at 55 ºC in the dark, it was found that curcumin was more stable under acidic than neutral conditions. Interestingly, the encapsulation of curcumin in

alginate beads actually promoted its degradation at both acidic and neutral pH, but encapsulation in chitosan beads enhanced its stability at pH 7 but reduced it at pH 3. The curcumin degradation rate increased in the following order: at pH 7, chitosan beads < emulsion < alginate beads < aqueous solution; at pH 3, emulsion < aqueous solutions < chitosan beads < alginate beads.

Second, an innovative pH-driven method was used to load curcumin into emulsions and its efficacy was compared to other loading methods: oil-solubilization and heat-driven methods. The aim of using the pH-driven method was to improve the encapsulation efficiency. The oil-solubilization method involved dissolving powdered curcumin in the oil phase (60 ^{o}C, 2 h) and then forming a nanoemulsion. The heat-driven method involved forming a nanoemulsion and then adding powdered curcumin and incubating at an elevated temperature (100 ^{o}C, 15 min). The pH-driven method involved dissolving curcumin in an alkaline solution (pH 12.5) and then adding this solution to an acidified nanoemulsion (pH 6.0). Initially, the encapsulation efficiency of the curcumin in the three nanoemulsions was determined: pH-driven (93%) > heat-driven (76%) > conventional method (56%). The bioaccessibility of the colloidal delivery systems created using the pH-driven method was then compared to that in three commercial supplements that use different encapsulation technologies: Nature Made, Full Spectrum, and CurcuWin. The curcumin concentration in the mixed micelles decreased in the following order: CurcuWin ≈ pH-driven nanoemulsions > heat-driven nanoemulsions > conventional nanoemulsions >> Full spectrum > Nature Made. This result indicated our natural emulsion-based system was suitable for encapsulating and increasing the bioaccessibility of curcumin.

Third, we compared the efficacy of three different colloidal delivery systems produced using the pH-driven method: curcumin nanocrystals; curcumin-loaded nanoemulsions; and curcumin-loaded soy oil bodies. A control was also used that consisted of curcumin powder

dispersed in water. The nanoemulsions and oil bodies formed yellowish creamy dispersions that were stable to creaming, whereas the nanocrystals formed a cloudy yellow-orange suspension that was prone to sedimentation. The potential fate of the different delivery systems after ingestion was assessed using a gastrointestinal tract (GIT) model that consisted of mouth, stomach, and small intestine phases. The nanoemulsions and oil bodies were rapidly and fully digested, while the nanocrystals were not. All three systems were relatively stable to chemical transformation in the *in vitro* digestion model, but the nanocrystals gave a low bioaccessibility, whereas the other two systems had a high bioaccessibility, which was attributed to their ability to form mixed micelles that solubilized the curcumin.

Fourth, we examined the physical and chemical stability of curcumin-loaded soybean oil bodies prepared using the pH-driven method. First, the impact of pH (from 6.5 to 8) on the stability of curcumin-loaded soymilk during storage was investigated at 4 ºC for 36 days. At this low storage temperature, more than 85% of the alkaline-sensitive curcumin was retained at all three pH values, without any evidence of color fading. The impact of holding temperature (4, 20, 37, and 55 ºC) on the physicochemical stability of the curcumin-loaded soymilks was then measured during storage at pH 7 for 14 days. At 4 and 20 ºC, the emulsions remained physically stable, most of the curcumin (> 90%) was retained, and there was no evidence of color fading. At the higher temperatures, however, the rate of curcumin degradation increased. For instance, around 30% and 70% of curcumin was lost when the soymilks were stored at 37 and 55 ºC, respectively. On the other hand, the soymilks remained physically stable throughout this period.

Finally, we showed that curcumin can be successfully loaded into dairy milk using this approach, without adversely affecting milk fat globule stability. The physical and chemical stability of curcumin-loaded milk stored under different pH and temperature conditions was

assessed. The impact of pH on the stability of the curcumin-loaded milk was investigated by storing the samples at 4 ºC for 60 days at pH 6.5, 7.0 and or 8.0. At this low storage temperature, all milk samples were stable to fat globule aggregation, creaming, curcumin degradation (<13% loss), and color fading. The impact of temperature on the stability of the curcumin-loaded milk was investigated by storing samples at pH 7 for 15 days at 4, 20, 37, or 55 ºC. As expected, the extent of curcumin degradation decreased with decreasing storage temperature: 55 ºC (43%) > 37 ºC (21%) > 20 ºC (10%) > 4 ºC (5%). Interestingly, the color of the samples stored at 4, 20 and 37 ºC remained similar to that of the initial samples, but the sample stored at 55 ºC showed significant color fading. The bioaccessibility of the curcumin determined using a simulated gastrointestinal tract model was around 40%, which was attributed to some chemical degradation and binding of the curcumin reducing its stability and solubilization.

Overall, the results of this research provide valuable information that will facilitate the design and formulation of curcumin-fortified functional foods with potential health benefits.

TABLE OF CONTENTS

1. Introduction

Curcumin is a photochemical derived from turmeric, which is a perennial herb belonging to the Zingiberaceae family (Fig.1). Colloquially, turmeric is referred to as the "golden spice" because of its unique golden yellow color and earthy pungent flavor [1, 2]. In south and southeast Asian countries, turmeric has been used as a spice and pigment in food preparations for thousands of years. In addition, it has been widely used as an herbal medicine due to its perceived therapeutic benefits. Chemically, there are three major polyphenol substances that belong to the "curcuminoid" family: curcumin (diferuloylmethane); demethoxycurcumin; and bisdemethoxycurcumin. Of these, the curcumin form is the most biologically active and so has been the focus in the development of pharmaceutical, supplement, and food products [3, 4].

In functional food applications, curcumin can be considered as a natural ingredient that provides a distinctive color and flavor profile, as well as having potential health benefits [1, 2, 4]. Research in various fields has shown that ingestion of curcumin may be beneficial to health due to its wide range of biological activities, including anti-inflammatory [5, 6], antioxidant [6, 7], antibacterial, antiviral, anti-fungal [8, 9], antidiabetic, anti-tumor, and anti-cancer [3, 10, 11] activities. In cases where it is efficacious, curcumin may have advantages for the prevention or treatment of diseases because of its low cost, good safety profile, and lack of side effects. The research highlighting the potential benefits of curcumin has led to it being applied in a variety of commercial food and non-food products, including energy drinks, supplements, ointments, soaps, and cosmetics[12].

Pure curcumin is an orangey-yellow colored crystalline material, which normally comes in a powdered form. Moreover, it is a chemically-labile hydrophobic substance that has a low water-solubility (particularly under acidic or neutral conditions where it is fully protonated), poor chemical stability (especially under alkaline conditions), and low bioavailability (mainly due to

low bioaccessibility and chemical transformation due to metabolic enzymes in the gastrointestinal tract). In addition, curcumin is susceptible to chemical degradation during storage, particularly when exposed to light, high temperatures, and alkaline conditions [13]. Although curcumin is relatively stable to chemical degradation under acidic conditions, it has a very low water-solubility under these conditions, which can promote crystallization and sedimentation in aqueous delivery systems [14]. For this reason, it is important to develop effective approaches to overcome these hurdles so that curcumin can be successfully incorporated into pharmaceuticals, supplements, and functional food products.

One of the most effective means of protecting curcumin against chemical degradation, increasing its water dispersibility, and improving its bioavailability is to use modern encapsulation technologies [15, 16]. These technologies involve incorporating the curcumin into edible nanoparticles or microparticles that can then be introduced into food or supplement products [17]. These colloidal particles are assembled from food-grade ingredients, such as surfactants, phospholipids, lipids, proteins, polysaccharides, and minerals, using either spontaneous or directed processes. Numerous kinds of colloidal particles can be employed for this purpose, including micellar aggregates, liposomes, emulsion droplets, solid lipid particles, and biopolymer particles [18].

2. Literature Review

2.1 Chemistry of curcumin

Curcumin ($C_{21}H_{20}O_6$) is an asymmetric molecule with a molar mass of 368.38 g/mol (Fig. 1). Structurally, it contains three main functional groups: two aromatic ring systems containing o-methoxy phenolic groups, and one alpha, beta-unsaturated beta-diketone moiety. In aqueous solutions, curcumin undergoes keto-enol tautomerism with its conformation depending on pH: the keto form dominates under acidic and/or neutral conditions, while the enol form dominates under alkaline pH conditions (Fig. 2)[19-21]. The enol form is more chemically labile than the keto form, accounting for the poor chemical stability of curcumin in basic solutions[21].

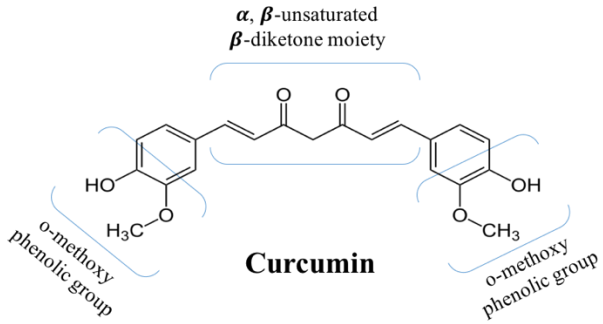

Fig.1 Chemical structure of curcumin

2.2. Biological activities of curcumin

2.2.1 Antioxidant activity

One of the main reasons that curcumin is used in many food formulations is due to its relatively strong antioxidant activity, which is believed to increase the shelf life of food products and

protect cells from free-radical induced damage. Reactive oxygen species (ROS) generated inside the human body can promote the oxidation of lipids, proteins, and DNA molecules that place critical roles in normal cellular function. A number of chronic diseases have been linked to this phenomenon, including inflammation, cardiovascular disease, diabetes, and cancer [6, 22 23]. Curcumin exhibits its antioxidant activity by acting as a free radical scavenger, singlet oxygen quencher, and chelating agent. For instance, it can donate a hydrogen atom from its □-diketone moiety to lipid alkyl or lipid peroxyl radicals, thereby reducing their activity [24, 25]. In addition, it can chelate ferric (Fe^{2+}) and ferrous (Fe^{2+}) ions, which are known to be potent pro-oxidants. Some studies have also shown that it is highly effective at inhibiting the oxidation of emulsified lipids. For instance, in linoleic acid emulsions a lower dose of curcumin (20 mM) was required to inhibit lipid oxidation than butylated hydroxyanisole (123 mM), butylated hydroxytoluene (102 mM), tocopherol (51 mM), and trolox (90 mM)[7].

2.2.2 Anti-inflammatory activity

Curcumin is also widely used as a nutraceutical in functional foods because of its relatively strong anti-inflammatory activities. In particular, it has been reported that curcumin can suppress inflammatory response enzymes and transcription factors, such as TNF-a, IL-1, IL-6, IL8, IL12, monocyte chemoattractant protein (MCP)-1, cyclooxygenase-2 (COX 2) and inducible nitric oxide synthase (iNOS), lipoxygenase, thereby inhibiting the production of inflammatory cytokines[26, 27]. The efficacy of curcumin for treating rheumatoid arthritis (a disease linked to inflammation of the joints) was compared to that of a widely used drug for this purpose (diclofenac sodium). After eight weeks, patients reported that curcumin formulation was more effective at reducing pain, swelling, and tenderness then the drug and that it exhibited less

side effects. Moreover, the patients receiving the drug reported itching and swelling around their eyes, as well as dimness of vision[28]. Animal studies have also reported that curcumin reduced inflammation and bone erosion of collagen-induced arthritis (CIA) in rats after eight weeks of treatment (110 mg/kg)[29]. Other researchers have also claimed that the anti-inflammatory activity of curcumin is responsible for its ability to inhibit tumor formation and cancer.

2.2.3 Antimicrobial effects

The antimicrobial activity of curcumin means that it has potential to inhibit food spoilage thereby prolonging shelf life, as well as deactivating pathogenic organisms thereby increasing food safety [30]. Moreover, ingestion of curcumin-rich foods has the potential to treat or prevent some infectious diseases [31]. Several mechanisms of action have been proposed for the antimicrobial activity of curcumin, including its ability to increase the permeability of bacterial cell walls, inhibit microtubule formation, impair bacterial virulence factors and interfere with key biochemical pathways [32]. For instance, studies have shown that there is an increase in cell membrane leakage for both gram-negative (*S. aureus and E. faecalis*) and gram-positive (*E.coli and P. aeruginosa*) bacteria after being treated with curcumin [33].

2.2.4 Anticancer

Curcumin has also been reported to have the ability to inhibit the growth of cancer cells by suppression of angiogenesis and induction of apoptosis [34, 35]. *In vitro* and *in vivo* studies suggest that curcumin may be able to downregulate cell growth and proliferation in various types of cancer cells, including prostate, breast, and colon cancers[34]. In the case of prostate cancer, curcumin downregulated cancer cell proliferation by attacking epidermal growth factor receptors

(EGFR) that normally down-regulate EGFT expression[36]. Curcumin has also been shown to suppress cell motility and metastasis by inhibition of bone metastatic LNCaP-derivative C4-2B prostate cancer cells[36, 37]. In the case of breast cancer, curcumin has been reported to mediate breast cancer cell apoptosis *via* suppression of NFκB, cyclinD, and MMP-1 experssion[38]. In the case of colon cancer, curcumin had been reported to reduce miR-21 promoter activity and expression by inhibiting HCT116 cells and Pko cells in the G_2/M phase, which regulates progression and metastasis of cancer cells [39, 40].

2.3. Potential Toxicity

The potential toxicity and side effects of ingesting curcumin have been investigated for decades using both animal and human models. A human feeding study reported no toxicity when up to 8 g of curcumin were ingested every day for three months, however, some of the test subjects did report minor side effects, such as diarrhea or nausea [41]. Another human study reported only minor side effects (diarrhea, rash, headache, and yellow stool) in one subject when they were fed relatively high levels (1 – 12 g per day) of curcumin for prolonged periods [42]. After reviewing the available evidence, the United States Food and Drug Admission (FDA) considers curcumin to be generally regarded as safe (GRAS)[43]. The United Nations and World Health Organization Expert Committee on Food Additives, as well as the European Food Safety Authority, allow a relatively high daily intake of curcumin: 0 to 3 mg/kg body weight/day [44, 45], which corresponds to up to about 210 mg day for an average person. This level is well above that reported to have beneficial health effects in human feeding studies[46].

2.4. Factors affecting curcumin's application

In this section, some of the main challenges that need to be addressed when formulating curcumin-based functional foods are discussed.

2.4.1 Solubility

At room temperature, pure curcumin is a crystalline material with a melting point around 183 ºC. In addition, it is a predominantly hydrophobic substance due to the non-polar regions in the aliphatic bridge, aromatic rings, and methyl groups (Figure 1) [47]. Nevertheless, it does have three hydroxyl groups, which become deprotonated at sufficiently high pH values, thereby giving it a negative charge (Figure 2). Consequently, curcumin is a predominantly hydrophobic molecule with low water-solubility under acidic and neutral conditions (where the hydroxyl groups are protonated), but a hydrophilic molecule with a relatively high water-solubility under alkaline conditions (where the hydroxyl groups are de-protonated) [48]. In particular, the solubility of curcumin increases as the solution pH is raised around and above the pK_a values of the three hydroxyl groups (7.5, 8.5 and, 9), which are located in the enolic and phenolic regions of the molecule (Figure 1 & 2). As an example, at pH ≤ 7.5, the net charge = 0, the log D = 4.1, and the water-solubility is very low (around 24 mg mL^{-1} or 0.0024%). Conversely, at pH ≥ 12.0, the net charge = -3, the log D = -2.0, and the water-solubility is very high (> 3 g mL^{-1}). As well as leading to an increase in water-solubility under alkaline conditions, deprotonation of these hydroxyl groups also promotes a color change and an increase in chemical instability (see the following sections). In most foods, the pH is in the range from about 2 to 8, so that the curcumin is a predominantly hydrophobic molecule with low-water solubility. As a result, it typically needs to be dissolved in some form of hydrophobic substance before it can be incorporated into aqueous-based foods, otherwise, it will be in a crystalline form. Having said that, the pH-dependence of the water-solubility of curcumin can be utilized in the formation of colloidal forms of curcumin, *e.g.*, in the pH-shift method (see later).

2.4.2 pH-induced color changes

The color of curcumin solutions depends on the protonation state of the three hydroxyl groups and therefore changes with pH (**Figure 2**). From pH 2 to 7, all of the hydroxyl groups are protonated and the curcumin appears golden yellow, which is the case in most foods. From pH 7 to 8.5, the enolic hydroxyl group becomes progressively deprotonated, causing the curcumin to change to a more orangey color. At still higher pH values, the other two phenolic hydroxyl groups become deprotonated causing the curcumin to have a more reddish color [4, 13, 49]. The chemical state of curcumin under specific solution conditions can therefore be elucidated by measuring the UV-visible absorption spectrum [4]. It should be noted that curcumin chemically degrades under alkaline conditions, which causes changes in its color.

2.4.3. Chemical degradation

2.4.3.1 Alkaline degradation

As mentioned earlier, the water-solubility of curcumin increases under alkaline conditions, which contributes to an increased rate of chemical decomposition. At pH values around and above the pK_a values of its hydroxyl groups, curcumin undergoes rapid hydrolytic degradation, which has been attributed to cleavage of the α, β-unsaturated β-diketone moiety. As a result, the original curcumin molecule is transformed into trans-6-(4´-hydroxy-3´-methoxyphenyl)-2,4-dioxo-5-hexanal, which itself undergoes cleavage reactions to form ferulic acid, feruloylmethane, and vanillin[4, 13, 49, 50] (Fig. 2). The color of curcumin fades due to this alkaline degradation reaction. In phosphate buffer solutions, it has been reported that around 90% of curcumin degraded within 15 minutes of incubation at neutral or alkali conditions, but the molecule was relatively resistant to degradation under acidic conditions[14, 51]. The possible

degradation of curcumin under neutral and alkaline conditions must therefore be considered when developing curcumin-enriched functional foods.

2.4.3.2 Photodegradation

Curcumin (crystalline or solubilized) also undergoes chemical degradation when exposed to light, which promotes color fading [52, 53]. The photodegradation of curcumin is also initiated at the $\boldsymbol{\alpha}$, $\boldsymbol{\beta}$-unsaturated $\boldsymbol{\beta}$-diketone moiety and leads to a variety of reaction products, including p-hydroxybenzaldehyde, vanillin, vanilic acid, ferulic aldehyde, and ferulic acid (Figure 2)[52]. Typically, the crystalline form of curcumin is more stable to photodegradation than the solubilized form, which may be because a higher fraction of the light waves is able to penetrate into a clear solution. Certain reaction products (*e.g.*, vanillin and ferulic acid) have been reported to have some antioxidant and anticancer activities, but they are less potent than the curcumin molecule itself [54-56] .

2.4.3.3 Autoxidation

Curcumin may also chemically degrade due to autoxidation reactions that occur spontaneously in aqueous solutions via a radical chain reaction[57, 58]. Initially, free radicals in the surrounding solution initiate autoxidation of the phenolic hydroxyls on the curcumin molecule, which results in the formation of an unstable intermediate that breaks down through a series of reactions to form bicyclopentadione[57, 59]. This reaction product has been shown to exhibit some anticancer activity but less than that of curcumin itself [59, 60].

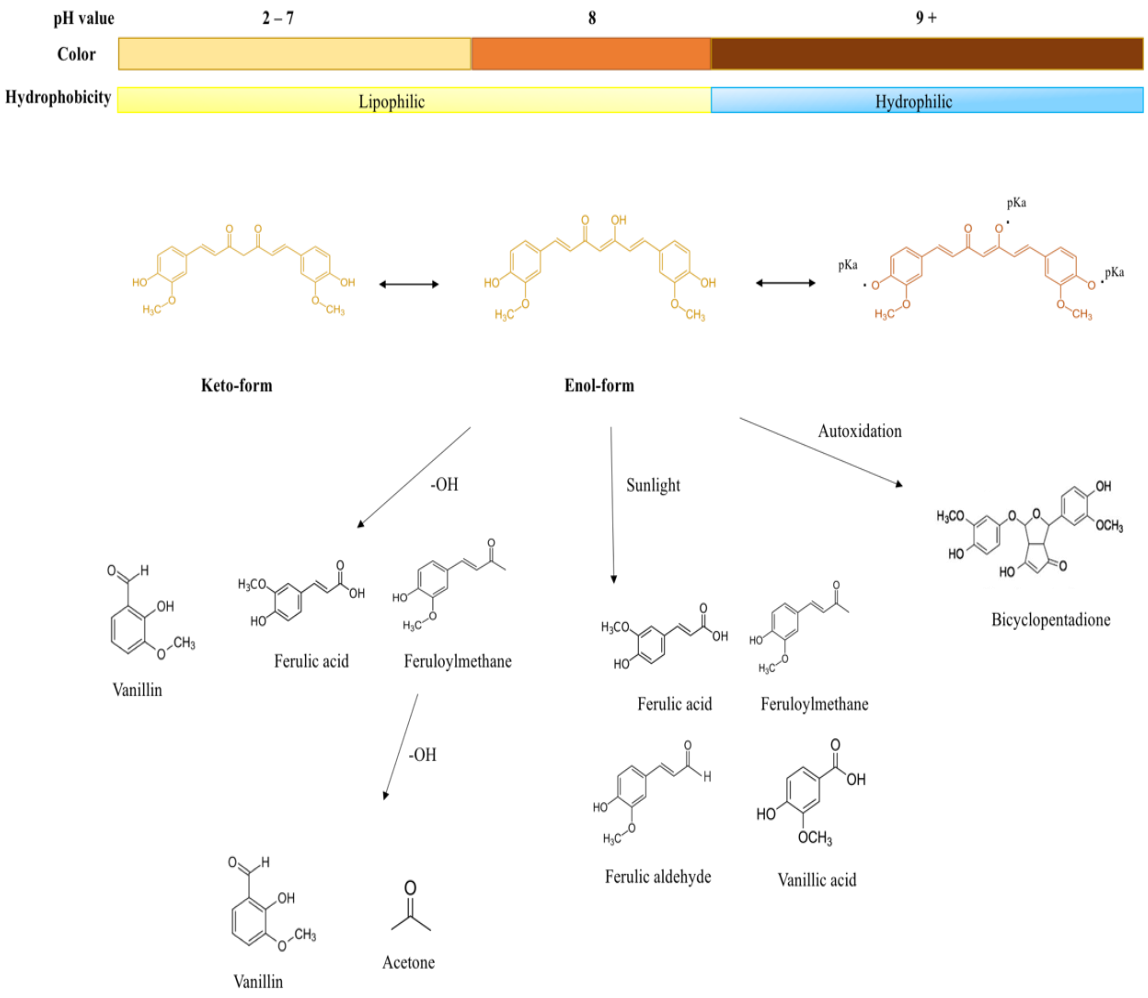

Fig. 2 the pH effects the color, hydrophobicity and molecular change in curcumin structure. It also demonstrates the chemical degradation production of curcumin under free radical, sunlight, and autoxidation.

2.4.4 Bioavailability

In this section, some of the main factors limiting the bioavailability of curcumin are highlighted (Fig. 3).

2.4.4.1 Bioaccessibility, Chemical Transformation, and Absorption

The high melting point and low water-solubility of curcumin under acidic and neutral conditions mean that pure curcumin crystals typically have a low bioaccessibility. In other words, the crystals do not readily dissolve in the aqueous gastrointestinal fluids, which reduces their ability to be transported through the mucus layer and be absorbed by the epithelium cells [34, 61]. The bioavailability of curcumin may also be limited due to chemical transformation within the gastrointestinal tract. Curcumin is resistant to degradation under acidic environments, and should therefore remain stable in the stomach. Conversely, it is prone to alkaline degradation under neutral or basic conditions and so may be unstable in the small intestine and colon. Some studies have shown that curcumin may also undergo autoxidation under physiological pH conditions [3]. Despite these potential degradation mechanisms, a rat study reported that around 90% of ingested curcumin remained in the GIT after exposure to the stomach and small intestine conditions for 30 mins, suggesting that its degradation was relatively slow within the gut [62]. The bioaccessibility and chemical stability of curcumin can be increased by encapsulating it within a lipid phase, such as a bulk or emulsified oil [47, 63]. Trapping the curcumin within a lipid phase protects it from chemical degradation by physically isolating it from reactants in the aqueous gastrointestinal fluids. Moreover, the utilization of a digestible lipid phase (such as a triglyceride) leads to the production of lipid digestion products (fatty acids and monoglycerides) that are incorporated into mixed micelles. These mixed micelles can then solubilize the curcumin within their hydrophobic interiors, thereby enhancing its bioaccessibility. Moreover, they can transport the hydrophobic curcumin molecules to the epithelium cells where they can be absorbed. After absorption, the curcumin may be metabolized within the epithelium cells and/or expelled back into the intestinal lumen due to the presence of efflux transporters within the cell

membranes [64, 65]. Some substances within foods, such as piperine in black pepper and certain catechins in green tea, are able to inhibit these efflux transporters, therefore increasing the amount of curcumin remaining in the body [66, 67]. This gives food formulators an approach to increase the potential bioactivity of curcumin using common food ingredients that act as efflux inhibitors [68].

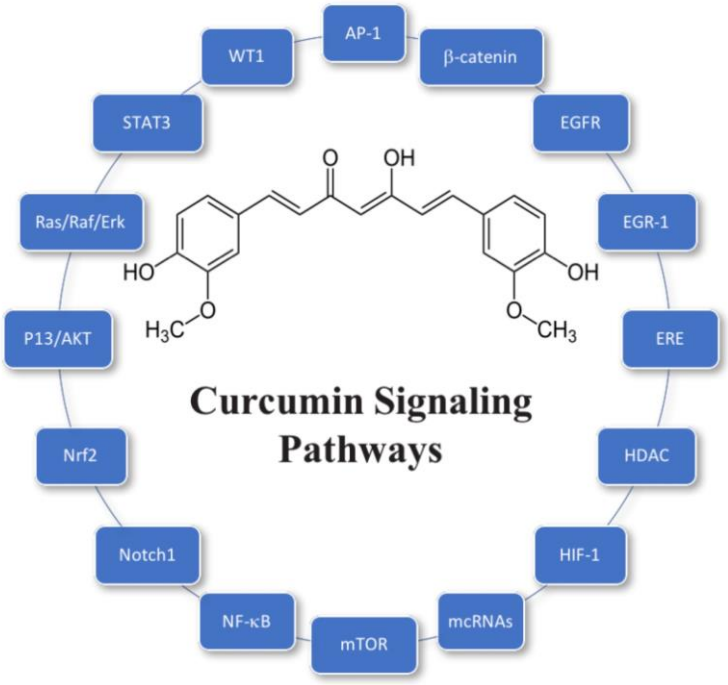

Fig 3. Proposed anticancer signaling pathways that curcumin can modulate.**Key:** AP-1, activating protein-1; EGR-1, early growth response protein-1; ERE, estrogen response element; HIF-1, hypoxia-in- ducible factor-1; mTOR, mammalian target of rapamycin; ncRNAs, non-coding RNAs; Nrf2:,NF-E2-related factor 2; PI3K/AKT, phosphatidyli- nositide 3-kinases/protein kinase B; STAT3, signal transducer and activator of transcription 3; WT1: Wilms' tumor 1. (Adapted from Kunnumakkara, 2017).

2.4.4.2 Metabolism

One of the main reasons for the poor oral bioavailability of curcumin is its rapid metabolism by metabolic enzymes inside the gut, as well as after absorption (particularly in the liver), leading to

the formation of a variety of metabolites with different biological activities to the parent molecule [61]. The human intestine and liver contain phenol sulfotransferase isoenzymes that convert curcumin into curcumin sulfates, as well as glucuronidases that convert curcumin into curcumin glucuronides [69]. In addition, a number of other metabolites may be formed, including bicyclopentadione, dihydrocurcumin, tetrahydrocurcumin (THC), hexahydrocurcumin (HHC), octahydrocurcumin (OHC), hexahydrocurcuminol, dihydroferulic acid, and ferulic acid [68, 70]. The majority of the curcumin glucuronides, curcumin sulfates, and other metabolites are fairly water-soluble and so are quickly excreted from the body *via* urine and feces[71, 72]

A number of the metabolites of curcumin have been found to exhibit some biological activity. THC has been reported to have stronger anti-inflammatory, antidiabetic, and antihyperlipidemic activity than curcumin, as well as a similar antioxidant activity[54, 73 22]. HHC has been reported to have similar or better antioxidant, anti-inflammatory, anticancer, and cardiovascular protective activities as curcumin [74-76]. OHC has also been reported to have superior anticancer properties than curcumin, by being more effective at suppressing tumor growth and inducing cancer cell apoptosis [77, 78]. In contrast, curcumin glucuronide has been reported to have a lower absorption and anticancer activity than curcumin [79]. Curcumin glucuronides and curcumin sulfates have also been reported to be less bioactive than other metabolites, as well as the parent molecule [80].

2.4.4.3 Tissue distribution

After absorption, curcumin enters the bloodstream and is rapidly distributed throughout the body, resulting in it being located in many tissues at detectable levels, including the liver, kidney, colon, brain, heart, lung, and spleen [62, 68, 81-83]. For instance, a rat study reported that a small amount of curcumin was found in the liver and kidney soon after oral administration, while about 38% was present in the large intestine after 24 hours [62]. The maximum curcumin concentration

was detected in the liver (around 45 ug/ whole tissue) and kidney (6 ug/whole tissue) after 3 hours. The amount of curcumin in the kidney has been reported to decline after about 24 hours, while that in the liver remains fairly constant for up to 4 days [82]. A rat feeding study reported that different levels of curcumin were detected in different tissues after oral administration: liver (70 nmol/mL), kidney (78 umol/mL), brain (3 nmol/mL), lungs (15 nmol/mL), heart (9 nmol/mL), and muscle tissue (8 nmol/mL)[81]. These results suggest that curcumin has the potential to work in various tissues within the human body, which means that it may be able to treat a variety of different disease conditions.

2.4.4.4 Elimination

Curcumin is eliminated from the body more through the feces than through the urine, which may be due to its relatively low water-solubility [83]. An animal study suggested that about 34% of curcumin was excreted through the feces, while less than 0.2% was secreted in the urine [82]. Nevertheless, curcumin metabolites (such as glucuronides and sulfates), which are much more water-soluble than the parent molecule, tend to be excreted through both the urine and feces[71, 72].

2.4.4.5. Pharmacokinetics

Pharmacokinetic studies have been used to study the levels of curcumin in the bloodstream of animals and humans after oral ingestion. These studies typically show that the fraction of curcumin reaching the bloodstream in an intact form is very low. For instance, in an animal study, it was reported that there was only about 0.22 ug/mL of curcumin in blood samples taken an hour after oral administration of 1.0 g curcumin per kg body weight, with this concentration declining over the following 6 hours[84]. In a human trial, only around 11 nmol/L curcumin was detected in blood plasma collected an hour after oral administration of 3.6 g of curcumin[72]. In human feeding studies, even a relatively high intake of curcumin (8 g per day) led to a relatively

low serum level (2 um/mL) in blood samples collected an hour or two after consumption[41]. These studies indicate that only a very small fraction of ingested curcumin actually gets into the systemic circulation in humans, which may limit its potential biological activity.

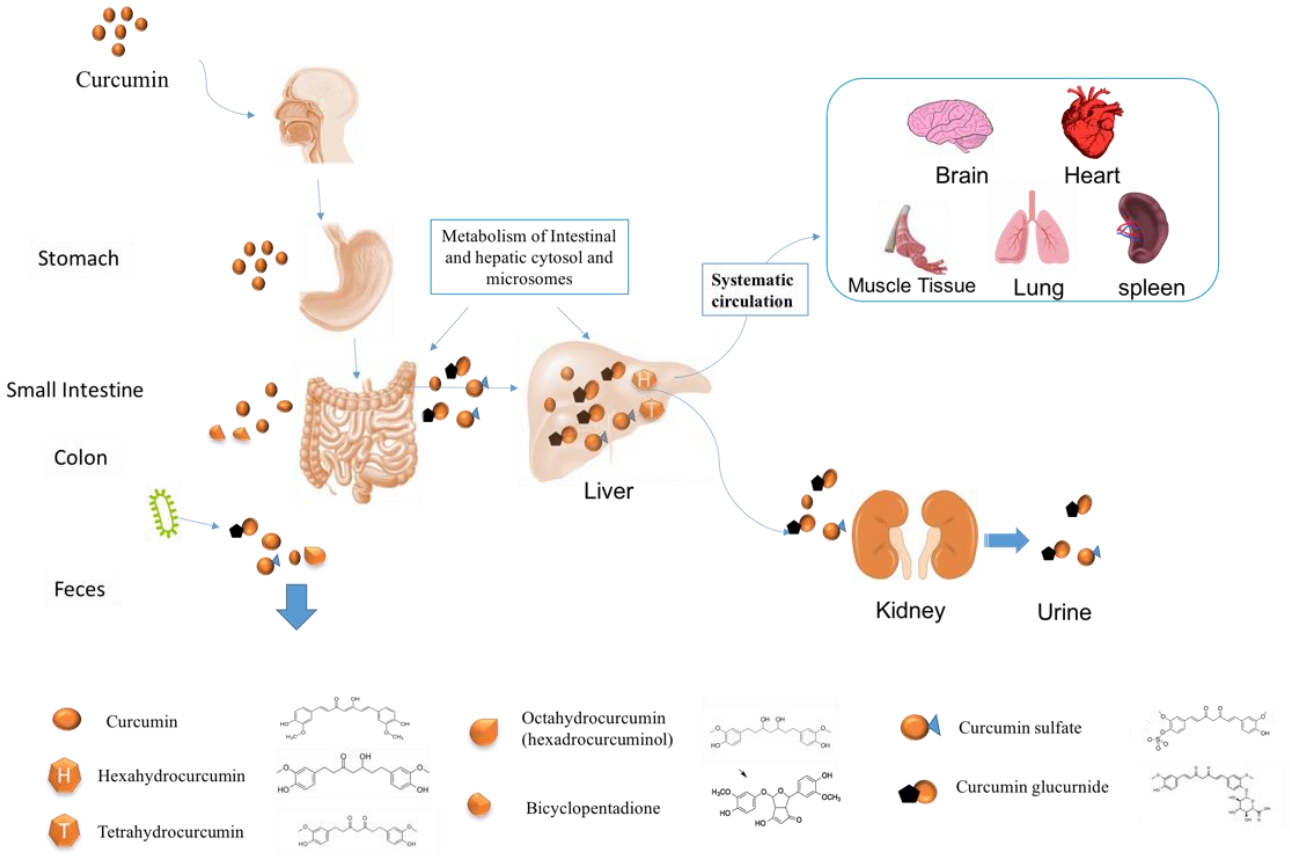

Fig.4 curcumin undergoes chemical degradation due to metabolism as it passes through the human gut and body. The metabolites formed have different bioactivates to the parent molecule

2.5. Strategies to overcome the challenges of curcumin

Potential strategies to improve the solubility/dispersibility, stability and bioavailability of curcumin are highlighted in this section.

2.5.1 Methods to enhance solubility/dispersibility of curcumin

The solubility of curcumin in both oil and water phases is important when developing effective formulations to encapsulate and deliver it. At room temperature, pure curcumin is typically in a powdered crystalline form. Consequently, it must be dissolved or dispersed within an appropriate solvent before it can be incorporated into a suitable food format. In this section, a number of approaches for introducing curcumin into solvents are highlighted.

2.5.1.1. Direct dissolution

Curcumin has a relatively low water-solubility (under neutral or acidic conditions), but it can be directly dissolved within oils and some organic solvents due to its lipophilic nature. Other than curcumin in water exhibits in the keto-form, the curcumin within the organic solvent solution has enolic form in nature (Figure 2). Some of the most common organic solvents used to directly solubilize curcumin are ethanol, methanol, chloroform, acetone, and dimethoxy sulfoxide (DMSO) [4]. These solvents are often used to dissolve curcumin prior to creating colloidal delivery systems. For instance, ethanol is often used to solubilize both curcumin and particle-forming materials, such as surfactants, phospholipids, hydrophobic proteins, or hydrophobic polysaccharides. Colloidal particles are then formed using an antisolvent precipitation method by injecting the ethanol mixture into water [85 86]. When the hydrophobic curcumin and particle-forming materials come into contact with water, curcumin-loaded particles are spontaneously formed. Curcumin has been loaded into zein nanoparticles using this method [87]. One disadvantage of using organic solvents for this purpose is that they may be environmentally unfriendly and additional costs are associated with removing and analyzing them in the final formulation [88, 89]. This problem can be overcome by using supercritical fluids (such as

supercritical carbon dioxide) to dissolve the curcumin[90, 91]. Alternatively, alkaline water can be used as a solvent, rather than an organic fluid.

As mentioned earlier, the solubility of curcumin increases substantially when the solution is raised above about pH 9 because the molecule changes from hydrophobic to hydrophilic (Figure 2). Consequently, curcumin can be solubilized in highly alkaline solutions. Curcumin-loaded colloidal particles can then be formed using a pH-shift method that involves injecting the alkaline curcumin solution into an acidified aqueous colloidal suspension. The pH decreases when these two systems are mixed together, which causes the curcumin to become more hydrophobic and move into the non-polar regions within the colloidal particles. This approach has been used to encapsulate curcumin into surface micelles [92], solid lipid particles, liposomes [93], emulsions, protein nanoparticles[94, 95], and oil bodies [95, 96]. The curcumin should only be kept for a relatively short time under highly alkaline conditions to avoid its degradation.

2.5.1.2. Mechanical action

The dissolution of crystalline curcumin in solvents can be increased by applying mechanical forces, such as stirring and sonication. Sonication is particularly suitable for this purpose because it generates intense fluctuating pressure waves that induce acoustic cavitation, leading to efficient mixing and dissolution [97, 98].

2.5.1.3. Heating

The solubility of crystalline materials in solvents usually increases as the temperature is raised. Consequently, it is possible to solubilize a higher concentration of curcumin by heating the system. This approach has been used to facilitate the dissolution of powdered curcumin into bulk oils, prior to emulsion formation [99]. It has also been used to increase the dissolution of powdered curcumin into pre-existing emulsions [100].

2.5.1.4. Encapsulation technologies

One of the most common approaches to improve the water-dispersibility of curcumin is to incorporate it within colloidal particles that have a hydrophobic interior but a hydrophilic exterior, such as micelles, microemulsions, emulsions, or hydrophobic biopolymer particles. Numerous kinds of colloidal particles that can be used for this purpose are covered in more detail in Section 6.3.

2.5.2. Methods to enhance stability of curcumin

As mentioned earlier, curcumin is susceptible to chemical transformation when exposed to certain conditions, such as alkaline pH, light, elevated temperatures, transition metals, and metabolic enzymes. For this reason, it is necessary to develop effective strategies to protect it from chemical degradation so that it can reach the target organs in an active state.

2.5.2.1. Antioxidant technologies

The rate of chemical degradation of curcumin can be inhibited by adding synthetic or natural antioxidants [101]. These authors reported that co-administration of curcumin with certain antioxidants decreased the degradation rate and increased the amount absorbed after oral administration to rats. Specifically, a number of food-grade redox active antioxidants were shown to greatly improve curcumin stability, including ascorbic acid, gallic acid, caffeic acid, rosmarinic acid, tert-butylhydroquinone (TBHQ), and Trolox. The addition of antioxidants has also been shown to enhance the stability of curcumin encapsulated within oil-in-water emulsions [102]. Hydrophilic and amphiphilic antioxidants were found to be more effective than lipophilic ones in this study, which may be because the chemical degradation of curcumin occurs more rapidly in the water phase. Overall, the authors reported the following order of efficacy for different antioxidants: Trolox ≈ ascorbic acid > ascorbyl palmitate >> control > alpha-

tocopherol. These results suggest that the stability of curcumin in food formulations can be improved by adding appropriate antioxidants.

2.5.2.2. Encapsulation technologies

The chemical degradation of curcumin occurs faster when it is surrounded by water than oil, because substances that accelerate the degradation reaction (such as hydroxyl ions) are mainly located within the aqueous phase [14]. Consequently, the stability of curcumin to chemical degradation can be improved by encapsulating it within a hydrophobic phase, which may be a bulk phase (such as oil) or colloidal particles (such as oil droplets, solid fat particles, or hydrophobic protein particles) [14, 103, 104]. Interestingly, the chemical stability of curcumin increases as the size of these hydrophobic colloidal particles increases, because then there is a slower exchange of curcumin molecules between the particles and the surrounding aqueous phase [105]. Various kinds of encapsulation technologies that may improve the chemical stability of curcumin in aqueous-based systems are discussed in Section 6.3.

2.5.2.3. Controlling environmental conditions

Curcumin is known to degrade faster when exposed to light [106], high temperatures [14], high oxygen levels [107], and alkaline environments [14]. It is therefore possible to improve its stability by controlling solution, environmental, and/or packaging conditions. For instance, the chemical stability of curcumin can be improved by incorporating it into acidic products (pH < 7) that are stored at low temperatures in the dark. Alternatively, it may be possible to exclude light and oxygen by using appropriate packaging procedures and materials, thereby further enhancing the stability of curcumin-based products.

2.5.3. Methods to enhance the bioavailability of curcumin

The bioavailability of curcumin can be enhanced by retarding its metabolism, increasing its bioaccessibility, and/or promoting its absorption. The enzymes that metabolize curcumin are located within the aqueous phase or within the cell membranes inside the human body. Consequently, the metabolism of curcumin can therefore be inhibited by trapping it inside hydrophobic phases that isolate it from the enzymes, such as those inside micellar, liposomal, microemulsion, emulsion, solid fat, or biopolymer particles. The bioaccessibility of curcumin can be increased by enhancing the amount that is solubilized within the mixed micelles present in the small intestine. This may be achieved by including surfactants, phospholipids, fatty acids, or monoglycerides within the curcumin-loaded carrier particles, as these surface-active substances, can become incorporated into the mixed micelles and increase their solubilization capacity. Alternatively, this can be achieved by including digestible lipids within the curcumin-loaded carrier particles, such as triglycerides or diglycerides. These lipids are then converted into monoglycerides and fatty acids by lipase in the human gut, thereby generating surface-active materials that can be incorporated into the mixed micelles and enhance their solubilization capacity. Finally, substances that increase the permeability of the epithelium cell membranes or that block efflux transporters can be incorporated into the curcumin-loaded carrier particles. For instance, some surfactants, fatty acids, biopolymers, and phytochemicals have been shown to increase the permeability of epithelium cells, thereby leading to enhanced absorption of hydrophobic bioactives [108-110]. As mentioned previously, certain kinds of food components, including piperine in black pepper and some catechins in green tea, can inhibit efflux transporters, thereby increasing the amount of curcumin absorbed by the body [66, 67].

2.6. Colloidal Delivery Systems

Colloidal delivery systems have been widely explored for their ability to increase the bioavailability of polyphenols, like curcumin[18]. Numerous kinds of colloidal delivery systems have been shown to be suitable for this purpose, including micelles, microemulsions, emulsions, solid lipid nanoparticles, protein nanoparticles, and biopolymer microgels. The curcumin-loaded colloidal particles can then be incorporated into functional food and beverage systems, or converted into a powdered form and used in supplements. An alternative strategy is to use excipient foods to enhance the bioavailability of curcumin. An excipient is a food that contains no bioactive components itself but breaks down in the human gut to form an environment that enhances the bioaccessibility, stability, or absorption of any curcumin co-ingested with it. Emulsified foods containing digestible lipids are particularly suitable for this purpose, including milk, creams, dressings, sauces, or yogurts[111].

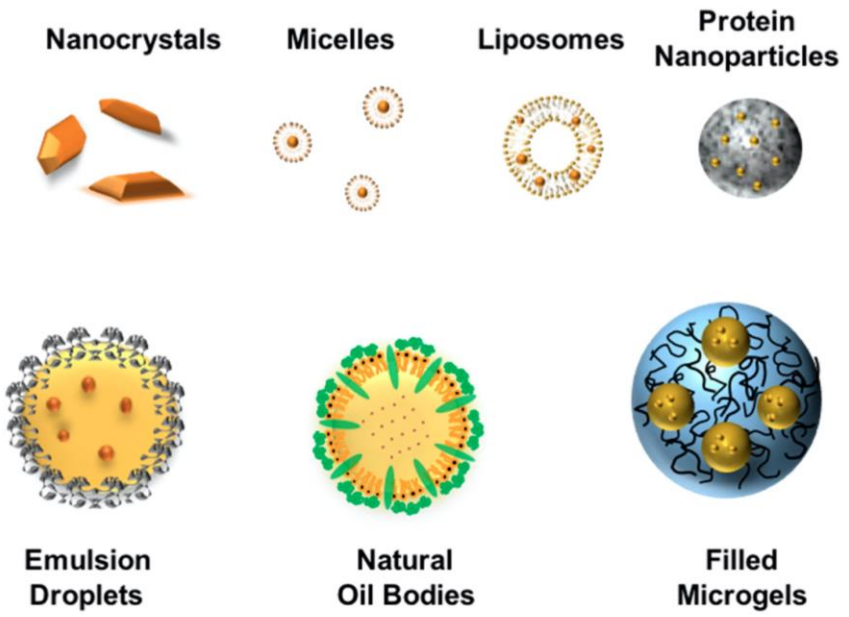

Fig. 5. Different kinds of colloidal delivery system can be used to encapsulate curcumin, thereby improving its stability and bioaccessibility. Not drawn to scale.

2.6.1. Micelles

Micelles have been widely used to improve the solubility and bioavailability of hydrophobic drug and nutraceuticals [112, 113]. They are spontaneously formed when surfactants are dispersed in water above their critical micelle concentrations. Consequently, they can often be fabricated using very simple processing methods, such as heating and/or mixing of the bioactive, surfactant, and water together. After assembly, the hydrophobic tails congregate together in the interior of the micelles, while the hydrophilic head groups point outwards towards the water. Micelles are typically formed from synthetic surfactants, but they can also be formed from certain kinds of natural surfactants, such as casein [114, 115]. Curcumin can be solubilized within the hydrophobic interior of the micelles by adding it before or after micelle formation. Typically, micelles are relatively thermodynamically stable colloidal dispersions containing relatively small (typically 5 to 20 nm) particles. As a result, they tend to be optically transparent because the particles are so small that they do not scatter light waves strongly. The viscosities of micellar systems depend on the surfactant concentration and micelle structure. At low concentrations, they tend to be fluids with low viscosities, whereas at higher concentrations, they tend to be semi-solids with high viscosities or gel-like textures. Micelles enhance the bioavailability of hydrophobic compounds (like curcumin) by increasing their bioaccessibility in the gastrointestinal fluids, as well as possibly increasing the permeability of the epithelium cells[116].

Synthetic food-grade surfactants, such as Tweens, have been widely used to solubilize curcumin [117]. The solubilization of curcumin has been reported to increase with increasing chain length and decreasing the unsaturation of the surfactant tail groups [117]. Natural surfactants, such as casein, have also been used to solubilize curcumin within aqueous solutions [118], which may be

more suitable for certain food applications. The pharmacokinetics of curcumin-fortified Tween 80 micelles and have been tested in a human feeding study. The curcumin-micelle formulation was found to have a 185-fold higher area under the curve (AUC) than free curcumin, without exhibiting any adverse side-effects [119].

2.6.2. Liposomes

Liposomes are self-assembled spherical particles consisting of one or more phospholipid bilayers [89, 120]. They therefore have a structure that is somewhat similar to biological cell wall membranes. A phospholipid molecule consists of a hydrophilic head group and a hydrophobic tail group consisting of two fatty acid chains. In a single bilayer, the phospholipid molecules are organized tail-to-tail therefore forming a thin hydrophobic domain, while the polar head groups face outwards. Liposomes containing multiple bilayers often have an onion-like structure with concentric rings of individual bilayers. Liposomes therefore have polar, non-polar, and amphiphilic regions inside the same colloidal particle, which can be useful for encapsulating one or more bioactive agents with different polarities within a single delivery system. Liposomes vary greatly in dimensions, ranging from around 25 nm to 25 um depending on the formulation and fabrication method used. Curcumin-loaded liposome typically has an orangey-yellow clear or slightly turbid look depending on the particle size [87].

Liposomes can be prepared using various methods, including passive-loading, active-loading, mechanical-dispersion, solvent-dispersion, and detergent-removal methods [120]. The preparation method used affects the nature of the liposomes formed, as well as the loading capacity of the curcumin. The characteristics of curcumin-loaded liposomes prepared using three different methods have been compared: thin film, ethanol injection, and pH-driven methods [93]. The initial diameters of the liposomes decreased in the following trend: thin film (452 nm) > pH-driven

(217 nm) > ethanol injection (115 nm). The initial encapsulation efficiency of the liposomes for curcumin decreased as follows: thin film (78%) > pH-driven (66%) > ethanol injection (39%). The physical and chemical stability of the curcumin-loaded liposomes also depended on the fabrication methods. After 30-days storage in the dark (4°C), the mean particle diameters increased to 1650, 234, and 153 nm for the thin film, pH-driven, and ethanol injection methods, while the curcumin concentration decreased by 50%, 2%, and 2%, respectively. The effect of ionic strength (0.1 to 1 M NaCl) on the stability of the liposomes was also assessed. Overall, the salt-stability of the emulsions decreased as their initial particle size increased. In particular, the liposomes prepared by ethanol-injection (which had the smallest initial size) were stable to salt addition, with little change in their appearance at any salt level after storage. Conversely, an increase in turbidity and precipitation were observed in the other liposome suspensions at high salt levels. Overall, the suggest that controlling the liposome size is important for maintaining good product stability[93]. In another study, it was shown that curcumin-loaded liposomes could inhibit the chemical degradation of curcumin, especially when exposed to transition metal ions (Fe^{3+}, Fe^{2+} Al^{3+}, and Cu^{2+}) [121].

The phospholipid source may also influence the physicochemical characteristic of curcumin-loaded liposomes. One study compared the properties of curcumin-loaded liposomes produced using a thin film/ultrasonic dispersion method that were fabricated from either milk fat globule membrane (MFGM) or soybean lecithin[122]. There were differences in the encapsulation efficiency, mean particle diameter, and -potential of the liposomes depending on lecithin type: EE = 74%, d = 212 nm ζ = +7.6 mV for MFGM; EE = 63%, d = 471 nm and ζ = -48.6 mV for soybean lecithin. Encapsulation of the curcumin was also shown to protect it from degradation when exposed to alkaline conditions, Fe^{3+}, light, heating, oxygen, and relative humidity, with the

MFGM liposomes giving slightly better protection than the soybean lecithin ones [122]. Other studies have also shown that lecithin type influences the encapsulation efficiency and stability of curcumin in liposomes [123].

The impact of liposome encapsulation on the bioavailability of curcumin has been studied using both *in vitro* and *in vivo* experiences. Interestingly, an *in vitro* gastrointestinal tract study showed that curcumin in larger liposomes (200 or 450 nm) had a higher bioaccessibility than that in smaller ones (114 nm)[93]. An animal feeding study has been used to investigate the oral bioavailability of the two curcumin-loaded liposome formulations: flexible liposomes (FL) and silica-coated flexible liposomes (SL) [124]. Pure curcumin suspended in water was used as a control. The curcumin concentrations within the blood plasma of the animals were measured up to 12 hours after oral administration. The maximum curcumin concentration occurred after 45 min for both the FL formulation and the control, with values of 129 and 71 ng/ L, respectively. Conversely, the maximum curcumin concentration occurred after 3 hours for the SL formulation with a value of 447 ng/L. Moreover, no curcumin was detected in the plasma of the animals after 4 hours for the control, while around 20 ng/L still remained after 12 hours for the encapsulated curcumin. Overall, both the SL (7.8-fold) and FL (2.4-fold) formulations gave a higher total amount of curcumin within the blood compared to free curcumin[124]. Thus, both liposome formulations were effective at increasing curcumin bioavailability.

Other researchers have also used an animal model (mice) to study the impact of liposomal encapsulation of curcumin on its bioavailability[123]. The maximum plasma concentration and time-to-reach this value depended on the formulation used: free curcumin (C_{max} =64 μg/L; T_{max} = 120 min); curcumin-loaded liposomes (C_{max} = 319 μg/L; T_{max} = 30 min); and, free curcumin + liposomes (C_{max} = 78 μg/L; T_{max}= 120 min). These results show that the bioavailability can

again be increased by delivering curcumin in the form of liposomes. Importantly, liposomal curcumin also exhibited a higher plasma antioxidation activity than the other two curcumin formulations [123], which can be attributed to its higher plasma level. Curcumin-loaded liposomes have been shown to exhibit the same cellular antioxidant activity as free curcumin when exposed to Caco-2 cells for 2 hours [121], which shows that encapsulation did not reduce the bioactivity of this nutraceutical.

2.6.3. Microemulsions

In general, microemulsions are thermodynamically stable isotropic colloidal dispersions formed from oil, water, and surfactant. Oil-in-water microemulsions contain small colloidal particles (typically 5 to 50 nm) comprised of oil and surfactant, which have a hydrophobic core and a hydrophilic shell. Any hydrophobic or amphiphilic bioactive substances can be incorporated into these colloidal particles. The fact that the colloidal particles in microemulsions are much smaller than the wavelength of light means that they are typically optically clear or only slightly turbid. Because they are thermodynamically stable systems, microemulsions should form spontaneously when the different components are mixed together but some mechanical mixing and/or heating may be required to facilitate this process. This is because there may be a kinetic energy barrier between the separated substances and the final microemulsion system that must be overcome.

Researchers have tried to optimize the formulation of curcumin-loaded microemulsions by varying the type and level of different substances used to fabricate them. For instance, one study reported that an optimum formulation consisted of DL-□-tocopherol (3.3 wt%), Tween 20 (53.8 wt%), and ethanol (6.6 wt%) [125]. This curcumin-loaded microemulsion had a clear yellow appearance, due to its small particle diameter (5 nm) and high curcumin level (14.6 mg/mL).

These curcumin-loaded microemulsions remained stable when stored under refrigerator conditions (4 ^{o}C) for a month, with no significant change in particle size or curcumin concentration. This study also showed that the encapsulated curcumin had a relatively high permeability (around 70%) when tested using an *in vitro* method [125].

Another study showed that self-micro-emulsifying drug delivery systems (SMEDDS) fabricated from oils and surfactants could be used to encapsulate and release curcumin [126]. In this case, the curcumin, oil, and surfactant are mixed together and then incorporated into capsules or pellets. This mixture spontaneously forms a microemulsion when it comes into contact with aqueous gastrointestinal fluids. These formulations exhibited excellent physical and chemical stability during storage, as well as leading to a 17-fold increase in the oral bioavailability of the curcumin (compared to the non-encapsulated form) using animal feeding studies [126]. Similar findings have been reported in other animal feeding studies using SMEDDS [127]. Overall, these results suggest that microemulsions can be designed to encapsulate curcumin, improve its stability, and enhance its bioavailability. For food applications, however, the potential limitations of this approach are the high levels of synthetic surfactant required, which can cause problems with cost, taste, and toxicity.

2.6.4. Nanoemulsions & emulsions

Nanoemulsions and emulsions typically consist of two immiscible liquids stabilized by an emulsifier, and perhaps other ingredients, such as thickening agents, gelling agents, ripening inhibitors, or weighting agents [128]. Nanoemulsions typically contain droplets with a mean diameter between about 20 to 200 nm, whereas emulsions contain droplets with mean diameters greater than 200 nm [129]. As a result, nanoemulsions may appear clear to opaque, whereas emulsions nearly always appear opaque, due to differences in light scattering. Because

nanoemulsions have a greater specific surface area (A_S), they need more emulsifier to stabilize them, since A_S is proportional to the reciprocal of the mean particle diameter (d_{32}). The physicochemical principles underlying the formation and stability of emulsions and nanoemulsions are the same, and so we will simply refer to them as "emulsions" in the remainder of this section.

For encapsulation purposes, oil-in-water (O/W) emulsions are typically used because hydrophobic substances can be encapsulated inside the droplets and then introduced into aqueous-based food and beverage products. The small droplets found in emulsions can be produced using two different approaches: high- or low-intensity methods [129]. High-intensity methods employ mechanical devices that apply intense disruptive stresses to fluids, which cause large droplets to breakdown into smaller ones, and include high-shearing, colloid mills, high-pressure homogenization, microfluidization, and sonication devices. Low-intensity methods rely on spontaneous droplet formation when oil-water-surfactant mixtures are exposed to particular conditions (compositions/temperatures), which includes phase inversion temperature and spontaneous emulsification methods [128, 129].

Emulsion-based systems have been widely used for the encapsulation, stabilization, and delivery of curcumin. Curcumin-loaded emulsions have a yellow-orange clear to milky appearance, depending on droplet concentration, droplet size, curcumin concentration, and solution pH [96]. As mentioned earlier, the emulsions look clear when the droplets are very small (< 40 nm) but milky when they are larger. The color of the emulsions depends on pH because of changes in the molecular conformation of the curcumin molecules discussed earlier [130].

Researchers have examined the impact of formulation parameters on the formation and functionality of curcumin-loaded emulsions, including oil type, emulsifier type, and curcumin-

solubilization method [131]. In particular, five oils (canola, corn, linseed, MCT, and sunflower, oil), four emulsifiers (lecithin, Tween 80, gum acacia, and whey protein), and three solubilization methods (heating, sonication, and microwaving) were investigated. Overall, heating was the most efficient method of dissolving curcumin in the oil phase, while MCT led to the highest curcumin content in the oil phase. The synthetic surfactant (Tween 80) produced curcumin-loaded MCT emulsions with relatively high curcumin contents, small particle diameters, high surface potentials, and good physical and chemical stabilities [131]. The natural emulsifiers could also produce curcumin-loaded emulsions, but they were not as stable as the ones produced by the synthetic surfactant.

Another study compared three methods of producing curcumin-loaded emulsions from all-natural ingredients (corn oil and quillaja saponin): conventional, heat-driven, and pH-driven methods. The conventional method involved dissolving powdered curcumin in an oil phase and then forming an emulsion by high-pressure homogenization. The heat-driven method involved preparing an emulsion first, and then heating it in the presence of powdered curcumin (100 C for 15 min). The pH-driven method involved mixing an acidified emulsion with an alkaline curcumin solution. The encapsulation efficiency was higher for the pH-driven method (93%) than the heat-driven method (76.2%) or conventional method (55.5%). The oil droplets in the curcumin-loaded emulsions produced using the pH-driven method had a high negative charge (-45 mV) and small particle diameter (180 nm). The bioaccessibility of the curcumin in the emulsions was determined using an *in vitro* model, and shown to be higher than non-encapsulated curcumin, as well as commercial curcumin supplements [51].

The physical and chemical stability of curcumin-loaded oil droplets has been shown to depend on their mean diameter (0.17, 0.52, or 14 μm) [132]. As expected, the rate of droplet creaming

increased with increasing droplet size because of the increase in gravitational forces. Conversely, the chemical instability of the curcumin decreased with increasing droplet size, which was attributed to the reduction in the contact area between the oil and water phases. Overall, curcumin bioaccessibility did not depend strongly on droplet size because of the competing effects of increased solubilization but decreased chemical stability of curcumin in smaller droplets.

An animal (mouse) study examined the impact of oil droplet size (50,100 and 200 nm) on curcumin bioavailability, anti-inflammatory activity, and anti-allergic effects [133]. Interestingly, a higher curcumin concentration was found in the blood for the 100 nm droplets ($C_{max} \approx 11$ ng/mL, T_{max} = 2hr) than for the 50 nm or 200 nm ones ($C_{max} \approx 5$ ng/mL, T_{max} = 2-hour). The 100 nm droplets also exhibited higher anti-inflammatory and anti-allergic effects[133]. Again, these effects may be due to conflicting influences of particle size on bioaccessibility, stability, and absorption.

2.6.5. Solid lipid particles

Solid lipid nanoparticles (SLNs) are similar in composition and structure to oil-in-water emulsions, except that the lipid phase is crystalline at the application temperature [134, 135]. The size of the lipid particles in the SLN suspensions vary from around 20 to 1000 nm depending on the formulation and preparation method used. Suspensions in the lower particle size range (< 50 nm) appear transparent, whereas those containing larger particles appear cloudy or opaque [136]. SLNs are typically prepared using the same methods as emulsions (high-pressure homogenization, sonication, or microfluidization), except homogenization is usually carried out at a temperature appreciably above the melting point of the lipid phase. In principle, a solidified lipid core is more effective at retaining and stabilizing curcumin than a liquified one. However, the system must be carefully designed to inhibit particle aggregation and curcumin expulsion

when the lipid phase crystallizes[134, 135]. In addition, solidified lipid phases are typically digested more slowly than liquid ones, which may lead to prolonged release of any encapsulated substances.

Curcumin has been successfully encapsulated within SLNs coated by biopolymers (caseinate or caseinate/pectin) [137]. The size, charge, and stability of these SLNs could be controlled by optimizing the formulation and preparation methods used. Curcumin has also been encapsulated within SLNs coated by soy lecithin and Tween 80 [138]. Initially, the SLNs had a relatively small diameter (134 nm) and a high encapsulation efficiency for curcumin (92%). After incubation for 12 months at a refrigerated temperature (5 °C), the particle size only increased slightly (160 nm) and the curcumin content only decreased slightly (3%). These results suggest that the SLNs were suitable for curcumin encapsulation under low-temperature storage conditions. The researchers also investigated the pharmacokinetics of curcumin after oral administration to rats. Encapsulation of curcumin within the SLNs led to a 48-fold increase in plasma concentration and a 39-fold increase in the area under the curve compared to a control (powdered curcumin in water), leading to an appreciable increase in oral bioavailability.

The efficacy of Curcumin-loaded solid lipid nanoparticles (Cur-SLNs) and nanostructured lipid carriers (Cur-NLCs) has been compared using *in vitro* and *in vivo* studies [139]. Cur-SLNs were prepared using cetyl palmitate as a lipid source leading to a highly regular crystalline structure, whereas Cur-NLCs were formulated using oleic acid and cholesterol as a lipid source leading to a more irregular solid structure. The storage stability, antioxidant activity, pharmacokinetics, and cytotoxicity of the Cur-SLNs and Cur-NLCs were then compared. The entrapment efficiency and storage stability of the Cur-NLCs were higher than that of the Cur-SLNs, but their antioxidant activities were similar. In an animal (rat) pharmacokinetic study, the area under the

curve (AUC) in the plasma was 5-fold and 2-fold higher for Cur-NLCs and Cur-SLNs than the control, indicating that both delivery systems increased the bioavailability. Thus, NLCs appeared to be more effective at increasing the efficacy of curcumin than SLNs. *In vivo* studies with humans have shown that curcumin-loaded SLNs can appreciably increase the bioavailability of curcumin [140].

2.6.6. Biopolymer particles

Biopolymer particles are typically assembled from proteins and/or polysaccharides using an appropriate method. The method employed depends on the nature of the biopolymers themselves, as well as the required characteristics of the colloidal particles formed (such as composition, size, shape, charge, and stability). The final particles usually contain biopolymer molecules held together by attractive forces, such as hydrophobic, electrostatic, or hydrogen bonding interactions. The most common methods of inducing the assembly of biopolymer molecules are ionotropic, cold-set, heat-set, or enzymatic gelation. The most common particle-forming methods include injection, emulsion templating, electrostatic complexation, antisolvent precipitation, and thermodynamic incompatibility methods [141]. Biopolymer particles can be prepared with mean diameters ranging from around 100 nm to 1 mm depending on the fabrication method used.

Biopolymer particles can be formed from proteins or polysaccharides that have antioxidant properties, thereby protecting labile nutraceuticals from chemical degradation [94]. They can also be designed to retain nutraceuticals under one set of environmental conditions, but then release them under another set [141]. For example, biopolymer particles could be designed to retain curcumin during storage, mouth, and stomach conditions, but then release it in under small intestinal conditions.

Curcumin-loaded lipid droplets have been encapsulated within hydrogel beads made from either alginate (370 μm) or chitosan (255 μm) using an injection-gelation method [142]. The anionic alginate was cross-linked with cationic calcium ions, whereas the cationic chitosan was cross-linked with anionic tripolyphosphate ions. Interestingly, encapsulating the curcumin-loaded lipid droplets within the hydrogel beads actually reduced its chemical stability. Moreover, there were some swelling and shape changes in the beads during storage. Curcumin has also been encapsulated within wheat protein microgels (510 nm) formed by heating the system at a controlled pH [143]. The protein microgels had a relatively high encapsulation efficiency (90%), good sedimentation stability, and high antioxidant activity, which may be important for commercial applications.

Encapsulating curcumin within biopolymer microgels may be an advantage in applications where sustained or triggered release is required. An *in vitro* study showed a faster and higher release of curcumin from free oil droplets than from oil droplets trapped in either carrageenan beads or alginate beads [144]. Similarly, the release of curcumin under simulated gastrointestinal conditions has been shown to be reduced when it is encapsulated within whey protein microgels [143] or pectin microgels [145]. These results suggest that biopolymer microgels may be useful for prolonging the release of curcumin, rather than increasing its bioavailability.

The water-dispersibility and antioxidant activity of curcumin have been increased by incorporating it within the hydrophobic cores of casein-micelles [146]. In a human study, it was shown that the oral bioavailability of curcumin could be increased substantially by loading it into γ-cyclodextrin complexes [147].

2.6.7. Nature-derived colloidal particles

The growing interest in developing more sustainable and healthy food products has led many food scientists to explore the possibility of using nature-derived colloidal particles to encapsulate curcumin. Recently, it was shown that curcumin could be encapsulated within the milk fat globules in bovine milk[130] and the oil bodies in plant-based milks [148]. The curcumin was loaded into these nature-derived colloidal particles using the pH-shift method. First, curcumin is dissolved in a highly alkaline aqueous solution (pH 12), which is then mixed with an acidified milk product. The final pH of the mixed system is designed to be neutral or below, leading to a decrease in the water-solubility of the curcumin, which causes it to move into the hydrophobic core of the colloidal particles (milk fat globules or oil bodies). The authors showed that the curcumin-loaded milks had good storage stability and a high curcumin bioaccessibility, as determined by an *in vitro* digestion method [130, 148].

2.7. Conclusion

Curcumin has been used as an edible health-promoting substance for thousands of years as part of traditional medicinal practices in Asia. More recently, modern scientific methods have demonstrated that curcumin exhibits a broad spectrum of biological activities that may be beneficial to human health, including antioxidant, antimicrobial, anti-inflammatory, and antitumor activities. Even so, there are a number of challenges that have to be addressed when formulating curcumin-based functional foods or therapeutics, including its low water solubility, chemical stability, and bioavailability. In this article, we highlighted some of the methods that can be used to overcome these problems, including antioxidant, encapsulation, and storage strategies. In particular, we focused on the utilization of colloidal delivery systems, such as micelles, liposomes, microemulsions, emulsions, solid lipid nanoparticles, biopolymer particles,

and nature-derived colloidal particles. Each of these delivery systems has its own advantages and disadvantages for specific applications and it is important to select the most appropriate formulation. For instance, there are differences in the appearances, textures, mouthfeels, flavors, shelf-lives, and environmental histories of different curcumin-fortified functional food products (such as soft drinks, milky drinks, sauces, dressings, and bakery goods), which require different kinds of encapsulation technologies. In the future, it will be important to compare different formulations in terms of their cost, ease-of-manufacture, robustness, pharmacokinetics, bioavailability, bioactivity, sustainability, and environmental impact. The most suitable formulation for a specific application can then be selected.

CHAPTER 3

3. Impact of delivery system type on curcumin stability: Comparison of curcumin degradation in aqueous solutions, emulsions, and hydrogel beads

3.1. Introduction

Turmeric, a member of the ginger family, has been used as a dietary spice, yellow dye, preservative and traditional medicine in the south and southeast of Asia for thousands of years [31]. Turmeric consists of three major curcuminoids: curcumin; demethoxycurcumin; and, bisdemethoxycurcumin [3]. Curcumin is the most bioactive constituent within turmeric and has been reported to have various pharmaceutical functions, including antioxidant, antibacterial, anti-inflammatory, anti-tumor and anti-cancer activities [3, 149, 150]. Curcumin is generally regarded as safe (GRAS) by the United States Food and Drug Administration (FDA) due to its low toxicity even when ingested at relatively high levels [41]. For these reasons, curcumin has been widely investigated for its potential application as a bioactive agent in functional foods, supplements, and pharmaceuticals [151, 152]. Curcumin has a desirable yellowish color that also makes it suitable for use as a natural colorant in some food products [1].

The effectiveness of curcumin as a nutraceutical or natural colorant in food applications depends on its ease of use, chemical stability, and bioavailability. Curcumin is a hydrophobic substance that has low water-solubility, poor chemical stability (especially in alkaline solutions), and low bioavailability [3]. Under alkaline conditions, hydroxyl ions convert curcumin (diferuloylmethane) into trans-6-(4′-hydroxy-3′-methoxyphenyl)-2,4-dioxo-5-hexanal, ferulic acid, feruloylmethane, and vanillin, which leads to a reduction in its desirable yellow color [13, 49]. Therefore, there is a need for delivery systems to improve the water-dispersibility, chemical stability and bioavailability of curcumin [153-155].

Previous studies have demonstrated that the functional attributes of curcumin can be improved by encapsulating it within emulsion-based delivery systems, such as emulsions (d > 200 nm) or nanoemulsions (d < 200 nm) [103, 156-159]. Encapsulation of the hydrophobic curcumin molecules within lipid droplets improves their dispersion in aqueous solutions, and helps protect them from chemical degradation by limiting their interactions with reactive substances in the aqueous phase (such as hydroxyl ions). Moreover, the presence of a digestible lipid within the delivery system can increase curcumin bioavailability by forming mixed micelles in the gastrointestinal fluids that solubilize and transport the curcumin to the epithelium cells [132, 160]. An advantage to using nanoemulsions rather than emulsions for curcumin encapsulation is that they have better physical stability and a higher bioavailability [160]. Conversely, an important limitation of using nanoemulsions is that they have a large specific surface area, and so curcumin is more exposed to reactive substances in the aqueous phase that may promote their degradation [132]. This problem may be overcome by encapsulating curcumin-loaded lipid droplets inside hydrogel beads [160-163]. The hydrogel beads should be designed to protect the curcumin from degradation in foods and the gastrointestinal tract, but then release it at an appropriate location where it can be absorbed and exhibit its bioactive effects. A number of previous studies have examined the impact of curcumin encapsulation on its bioavailability and bioactivity [3, 132], but there have been few studies on the impact of encapsulation on its storage stability.

The objective of the current study was to determine the impact of delivery system type on the chemical stability of curcumin when stored under either neutral or acidic conditions. Two different types of food-grade delivery system were investigated: emulsions (curcumin-loaded lipid droplets) and filled hydrogel beads (curcumin-loaded lipid droplets trapped in microgels). The efficacy of these delivery systems was established by comparing them to a system consisting

of curcumin dispersed in an aqueous solution. Hydrogel beads with different characteristics were fabricated using two different types of ionic polysaccharide: alginate and chitosan; These two polysaccharides were selected because they have opposite charges [164]. Alginate is an anionic polysaccharide composed of 1,4′-linked β-D-mannuronic acid and α-L-guluronic acid units, whose negative charge comes from de-protonated carboxylic groups [165, 166]. Chitosan is a cationic polysaccharide that consists of D-glucosamine and *N*-acetyl glucosamine units, whose positive charge comes from protonated amino groups [167]. The results of this study may be useful for the rational formulation of foods, supplements, and other products containing curcumin.

3.2. Materials and methods

3.2.1. Materials

Corn oil was purchased from a local supermarket (Mazola, ACH Foods, Cordova, TN). The following chemicals were purchased from the Sigma-Aldrich Chemical Company (St. Louis, MO): curcumin powder (C 1386, purity 76% assayed by HPLC); alginic acid (A2033) (sodium salt extracted from brown algae, medium viscosity, viscosity of 1% dissolved in water = 15-20 mPa s); chitosan (448877, medium molecular weight, viscosity of 1 wt. % dissolved in 1% acetic acid = 200-800 mPa s); Tween 80 (P1754); Nile Red (N3013). All other chemicals were of analytical grade and were purchased from the Fisher Chemical Company (Thermo Fisher Scientific). Double distilled water, obtained from a water purification system (Nanopure Infinity, Barnstead International, Dubuque, IA), was used to prepare all solutions, emulsions, and hydrogels.

3.2.2. Preparation of curcumin in different delivery matrices

3.2.2.1. Aqueous solutions

Curcumin powder (9 mg) was dissolved in 30 ml dimethyl sulfoxide (DMSO) solution. Aqueous solutions of curcumin with different pH values were prepared by pouring 90% (v/v) phosphate buffer solution (5 mM, pH 3.0 or 7.0) into 10% curcumin solution. The final systems contained 3 mg of curcumin per 100 mL of 10% DMSO solution.

3.2.2.2. Emulsions

A stock emulsion was prepared from 10% (w/w) oil phase (corn oil) and 90% (w/w) aqueous phase (1% w/w Tween 80, 10 mM Phosphate Buffer, pH 6.5). Initially, the oil and aqueous phases were blended together for 2 min using a high shear mixer to form a coarse emulsion (M133/1281-0, Biospec Product, Inc., ESGC, Switzerland), and then they were passed five times through a high-pressure homogenizer at an operating pressure of 12,000 psi (Microfluidizer M-110Y, Microfluidics, Newton, MA USA). The resulting emulsions were stored at 4 °C before being used.

Curcumin powder (0.3 mg/ml) was added to the stock 10% w/w oil-in-water emulsion and the resulting system was stirred for 2 hours at 85 °C to fully dissolve the curcumin (SWB-10L-2, Major Science, Inc., CA, USA). This emulsion was then diluted 10-fold using either pH 3 or pH 7 phosphate buffer solution (5 mM), and the resulting systems were adjusted back to the required pH. The final systems therefore contained 1% w/w oil phase and 3 mg of curcumin per 100 mL of emulsion.

3.2.2.3. Curcumin-loaded filled alginate beads

An aqueous alginate solution was formed by dispersing 1.6% (w/v) alginate in double distilled water and then stirring overnight. A 1% (w/w) curcumin emulsion was then mixed with

this alginate solution (1:1 v/v) and then stirred for 1 hour in the dark. Curcumin-loaded filled alginate beads were formed by injecting the mixture of curcumin-loaded lipid droplets and alginate into a 10% (w/v) calcium chloride solution using an encapsulation device (Encapsulator B-390, BUSHI, Switzerland). This device had a vibrating nozzle with a diameter of 120 μm, an operating frequency of 1400 Hz, and an electrode potential of 1000 V. The beads were kept in the calcium chloride solution for at least half an hour with constant stirring to ensure crosslinking. The beads were then washed three times with double distilled water to remove any residual crosslinking solution, and then filtered overnight in a refrigerator. The resultant filled alginate beads were stored at 4 °C in the dark before use.

3.2.2.4. Curcumin-loaded filled chitosan beads

Chitosan powder (1.6 % w/v) was dissolved in 100 mM acetic acid and stirred overnight. Any insoluble matter was removed by centrifuging the chitosan solution at 2000 rpm for 5 min (Sorvall ST 8, Thermo Fisher Scientific, Inc., PR, China), so as to avoid blocking the nozzle of the encapsulation device. The filled-chitosan beads were then prepared using similar conditions as the filled-alginate beads: 120 μm nozzle size; operating frequency 1400 Hz; and, electrode potential of 900 V. The filled chitosan beads were formed by injecting a mixture of curcumin-loaded lipid droplets and chitosan into 100 mM sodium tripolyphosphate solution (pH 3) using the encapsulation device. The resulting beads were then kept in the gelling solution and stirred for at least 30 min at ambient temperature to ensure crosslinking of the chitosan molecules. The hardened beads were then washed with distilled water to remove excess crosslinking solution from their surfaces, and then filtered overnight in a refrigerator.

Eventually, both types of hydrogel beads were placed in either acidic or neutral phosphate buffer solutions (5 mM, pH 3 or 7) to determine the impact of pH and storage time on curcumin stability and bead properties.

3.2.3. Calculation of oil content in beads

The oil content of the filled hydrogel beads was calculated using the following expression:

$$\text{Oil content (g oil per g beads)} = W_{inital} \times C_{oil} / W_{final} \quad (1)$$

Here, $W_{initial}$ is the weight of the filled beads before filtration (g); C_{oil} is the percentage of oil in the original mixture used to prepare the beads; and W_{final} is the weight of the filled beads after filtration (g).

3.2.4. Storage study

Four delivery matrices were prepared to investigate their impact on the color stability of curcumin: (i) aqueous solutions (DMSO); (ii) emulsions; (iii) filled alginate beads; and, (iv) filled chitosan beads. All the samples containted the same final amount of curcumin (3 mg per 100 mL). Each system was distributed into a number of test tubes, so that a separate sample could be used for analysis at each incubation time. The samples were stored under both acid (pH 3.0) and neutral (pH 7.0) conditions at 55 °C for 14 days in the dark.

3.2.5. Color measurement

The tristimulus color coordinates of the samples were determined using an instrumental colorimeter (ColorFlex EZ 45/0-LAV, Hunter Associates Laboratory Inc., Virginia, USA): *L** (lightness/darkness); *a** (redness/greenness); and, *b** (yellowness/blueness). A test sample (10 ml) was placed in a petri dish, and then illuminated with D65-artificial daylight (10 standard

angle) using a white background plat. In this study, only the b^* values were used because they best represented changes in the yellow color of curcumin due to chemical degradation.

3.2.6. Particle characterization

The mean particle diameters and particle sizes distributions of the samples were measured using static light scattering (Mastersizer 2000; Malvern Instruments, Worcester- shire, UK). Small aliquots of sample were added to 5 mM buffer solutions (same pH as sample) placed in the instrument measurement cell and stirred at 1200 rpm to ensure homogeneity. The refractive indexes of the dispersed and continuous phases used in the calculations were 1.474 and 1.330, respectively. The data is reported as either the full particle size distribution or the volume-weighted mean particle diameter (d_{43}). The electrical charges (ζ-potentials) of the samples were analyzed using particle electrophoresis (Nano-ZS, Malvern Instruments, Worcestershire, UK). All samples were diluted with buffer solution (same pH as sample) before measurement. The particle sizes and electrical charges of curcumin solutions (DMSO) could not be measured because they did not contain colloidal particles that scattered light sufficiently strongly.

3.2.7. Bead swelling

Weighed filtered wet beads were immersed in either acid (pH 3) or neutral (pH 7) phosphate buffer solutions at 55 °C, and then their mean particle diameters (d_{43}) were measured by static light scattering at the first and last days of storage. The percentage increase in the diameter of the beads due to swelling was then calculated using the following expression:

$$\text{Swelling percentage (\%)} = [(d_{final} - d_{initial}) / d_{initial}] \times 100 \qquad (2)$$

3.2.8. Microstructure analysis

The microstructures of the samples were characterized using confocal scanning fluorescence microscopy (Nikon D-Eclipse C1 80i, Nikon, Melville, NY). All images were

acquired using a 10× eyepiece and a 20× objective lens. Samples were stained with Nile Red (1%) to highlight the location of the lipid regions. Images of the curcumin solutions were not measured because they were homogeneous systems that did not have any observable structure.

3.2.9. Statistical analysis

All data are shown as the mean ± standard deviation (SD) of measurements, were carried out in triplicate experiments using freshly prepared samples. The statistical comparisons were preformed using the student's t-test by commercial software (SPSS 16). P-values lower than 0.05 were considered to be significantly different.

3.3. Results and discussion

3.3.1 Properties of initial curcumin-loaded delivery systems

The different kinds of curcumin delivery system were prepared as described earlier: curcumin solution; curcumin emulsion; curcumin-loaded filled alginate beads; and, curcumin-loaded filled chitosan beads. The physicochemical and structural properties of the different delivery systems were then measured.

3.3.1.1. Curcumin solution

The overall appearance and yellowness (*b** value) of aqueous solutions containing curcumin were measured by digital photography (Fig. 1a) and instrumental colorimetry (Table 1). The aqueous curcumin solutions turned a transparent orange-brown color after adjustment to pH 7, but remained a transparent yellow color after adjustment to pH 3 (Fig. 1a). Despite their different visual appearances, the two solutions had fairly similar *b**-values (Table 1). Curcumin is known to be more structurally stable in acidic solutions than in neutral or alkaline solutions [1]. At relatively high level of hydroxide ions in the aqueous phase under neutral or alkaline

conditions rapidly degrades curcumin, which leads to a rapid color change [1, 13]. The initial aqueous solutions containing curcumin did not contain any colloidal particles and therefore it was not possible to measure the particle size, charge, or microstructure.

3.3.1.2 Curcumin emulsion

The 1% w/w oil-in-water emulsions containing curcumin initially had a homogeneous cloudy yellow appearance at both pH values (Fig. 1a). Moreover, the *b**-values were very similar for the emulsions under both acidic and neutral conditions, being around +60.4 (Table 1). Notably, the curcumin-loaded emulsions did not have the orange-brown color that was observed in the aqueous solutions at neutral pH (Fig. 1a). This result suggests that encapsulation of the curcumin within lipid droplets protected it from chemical degradation induced by hydroxyl ions or other constituents in the aqueous phase.

Static light scattering and particle electrophoresis were used to measure the initial mean particle diameter and surface potential of the droplets in the curcumin emulsions. The pH of the aqueous phase did not affect the mean droplet diameter (D_{43}= 0.27 ± 0.01 μm) or the particle size distribution (Fig. 1b), but it did affect the surface potential (Table 1). The curcumin-loaded lipid droplets had a relatively strong negative ζ -potential at pH 7 (ζ = −20.3 mV), but a slightly positive ζ -potential at pH 3 (ζ = +0.2 mV). The pH dependence of the ζ -potential of lipid droplets coated by a non-ionic surfactant can be attributed to two effects. First, there may be preferential adsorption of anionic hydroxyl ions to the droplet surfaces at relatively high pH values, and adsorption of cationic hydrogen ions at relatively low pH values [168]. Second, the oil or surfactant ingredients used to formulate the emulsions may contain ionic impurities, such as free fatty acids, that give the lipid droplets a charge [128].

The microstructure of the curcumin emulsions, determined by confocal fluorescence microscopy, indicated that the lipid droplets were evenly distributed throughout the system at both pH values (Fig. 1c). The individual lipid droplets could not be discriminated using this form of optical microscopy because they were below the limit of resolution.

3.1.3 Filled alginate beads

The individual curcumin-loaded filled alginate beads were opaque spheres that had a milky yellow appearance. After these beads were dispersed in aqueous solutions they rapidly moved to the bottom of the test tubes and formed cloudy yellow sediments, with the sediment layer being thicker at pH 7 than pH 3 (Fig. 1a). The rapid downward movement of the beads can be attributed to the fact that they were relatively large and their densities were greater than that of the surrounding water [128]. The fact that a thicker sediment layer was formed at pH 7, suggests that the beads were more swollen under neutral conditions than under acidic conditions, which was confirmed by light scattering measurements (see later). The alginate bead suspensions had similar yellow colors ($b^* \approx 28$) at both pH values (Table 1), but these b^* values were only about half of those of the emulsions. This effect may have been because the scattering of light by the beads decreased the color intensity [169].

The initial particle size distributions of the filled alginate beads in both the acidic and neutral solutions were monomodal (Fig. 1b), but the beads in the pH 7 solution (D_{43}= 404 μm) were appreciably larger than those in the pH 3 solution (D_{43}= 371 μm) (Table 1). This difference in bead dimensions can be related to changes in the electrostatic interactions in the systems [164, 166]. At pH 7, the alginate molecules have a relatively high negative charge because this pH is well above the pK_a value of the carboxyl groups (around pH 3.5) on the alginate chains. Consequently, there will be a relatively strong electrostatic repulsion between the anionic

alginate chains that make up the hydrogel network, thereby causing the beads to swell. Conversely, the alginate molecules are less highly charged when the solution pH is below the pK_a value of the carboxyl groups, and therefore there will be a weaker electrostatic repulsion between the alginate chains, causing the beads to be less swollen under acidic conditions [170]. As mentioned earlier, this effect would account for the fact that the thickness of the sediment layer at the bottom of the test tubes was greater at pH 7 than at pH 3 (Fig. 1a).

The electrical characteristics of the filled alginate beads also depended on solution pH (Table 1). The surface potential of the beads was appreciably more negative at pH 7 (−17.4 mV) than at pH 3 (−12.7 mV), which can again be attributed to the change in the electrical charge on the alginate molecules when the pH is altered from above to below the pK_a values of the carboxyl groups [166].

The microstructure of the filled alginate beads was characterized using confocal fluorescence microscopy at both pH values (Fig. 1c). Filled alginate beads incubated in both acidic and neutral pH conditions had similar structures, consisting of large spheres with lipid droplets (stained red) distributed inside. There was no evidence of any lipid droplets in the aqueous phase surrounding the alginate beads, which indicated that the encapsulation efficiency was high.

3.3.1.4. Filled chitosan beads

The individual filled chitosan beads also had a milky yellow appearance when observed by eye, which can be attributed to selective absorption of light waves by the encapsulated curcumin molecules. When the filled chitosan beads were suspended in aqueous buffer solutions they rapidly moved downwards and formed a sediment at the bottom of the test tubes. However, in this case the sediment layer was thicker at pH 3 than at pH 7 (opposite to the alginate beads),

and the sediment layer formed was thinner than for the alginate beads. Again, the rapid sedimentation of the chitosan beads can be attributed to their relatively large size and high density. The fact that a thinner sediment layer was formed for the chitosan beads than for the alginate beads can be attributed to the fact that the latter beads were more swollen (trap more water). Moreover, the thicker sediment layer formed under acidic conditions can be attributed to the fact that the chitosan beads were more swollen at pH 3 than at pH 7. Indeed, the light scattering measurements confirmed that the mean particle diameter of the chitosan beads incubated at pH 3 (D_{43}= 255 μm) were larger than those incubated at pH 7 (D_{43}= 239 μm) (Table 1). This effect can again be attributed to the impact of electrostatic interactions on the swelling behavior of the beads [171, 172]. At a pH well below the pK_a value of the amino groups (≈ 6.5), the chitosan chains have a high positive charge, and so there is a strong electrostatic repulsion between them, which leads to swelling of the beads. Conversely, at a pH above the pK_a value, the chitosan chains have a lower positive charge, and so there is a weaker electrostatic repulsion between them, leading to less swelling. The instrumentally determined yellow color (*b** value) of the chitosan bead suspensions was fairly similar at both pH values, and was appreciably less than that measured in the emulsions (Table 1). As discussed earlier, this latter effect may have been because the hydrogel beads scattered light, thereby leading to some color fading.

The surface potential (ζ-potential) of the chitosan beads was highly dependent on the pH of the buffer solution in which they were incubated (Table 1). The chitosan beads initially had a relatively high negative charge at pH 7 (-22.7 mV), but a small positive charge at pH 3 (+0.8 mV). The electrical charge on the chitosan molecules in solution is known to change from highly positive at acidic pH to slightly positive at neutral pH [173]. The fact that the chitosan beads had a strong negative charge at pH 7 in our study may therefore have been due to the fact that the

chitosan molecules were cross-linked with tripolyphosphate ions ($P_3O_{10}^{5-}$), and so the net charge was dominated by the strongly anionic multivalent ions rather than by the weakly cationic chitosan molecules.

The particle size distributions (Fig. 1b) of the chitosan beads were monomodal at both pH 3 and 7, but as mentioned earlier, the beads were slightly larger under acidic than under neutral conditions (Table 1), which was attributed to a greater degree of electrostatic repulsion between the chitosan chains. The morphology of the chitosan beads was observed by confocal fluorescence microscopy, which indicated that they had a more irregular shape and were smaller than the alginate beads (Figure 1c). The smaller dimensions of the chitosan beads suggest that the polysaccharide molecules were more densely packed within the hydrogel matrix, which may account for the thinner sediment layer formed by these systems than for the alginate beads (Fig. 1a). The lipid droplets (stained red) appeared to be exclusively located inside the chitosan beads, which suggested that they had a high encapsulation efficiency.

3.3.1.5 Comparison of delivery systems

Our results indicate that encapsulation of curcumin within the lipid droplets inhibited the color change from yellow to brown-orange that was observed at pH 7 in the aqueous solutions. This effect was observed in both the emulsions and in the filled hydrogel beads. The origin of this effect can be attributed to differences in the molecular environment of the curcumin in the different delivery systems. In the aqueous solutions, the curcumin is exposed to relatively high levels of hydroxyl ions at neutral pH, which promotes its chemical degradation. In the lipid droplets, the curcumin is surrounded by oil molecules, and is therefore more protected from direct contact with the hydroxyl ions.

The different characteristics of the various delivery systems will determine the type of products that they can be utilized in. Aqueous solutions could be used in optically transparent products, whereas emulsions could be used in optically opaque products. The fact that the emulsions had good creaming stability means that that could be used in either low or high viscosity products. Conversely, the filled hydrogel beads could only be used in optically opaque high viscosity products, otherwise they would rapidly sediment. Alternatively, the delivery systems could be converted into a powdered form (*e.g.*, by spray or freeze drying), and then incorporated into solid products (such as capsules, tablets, or foods).

1a

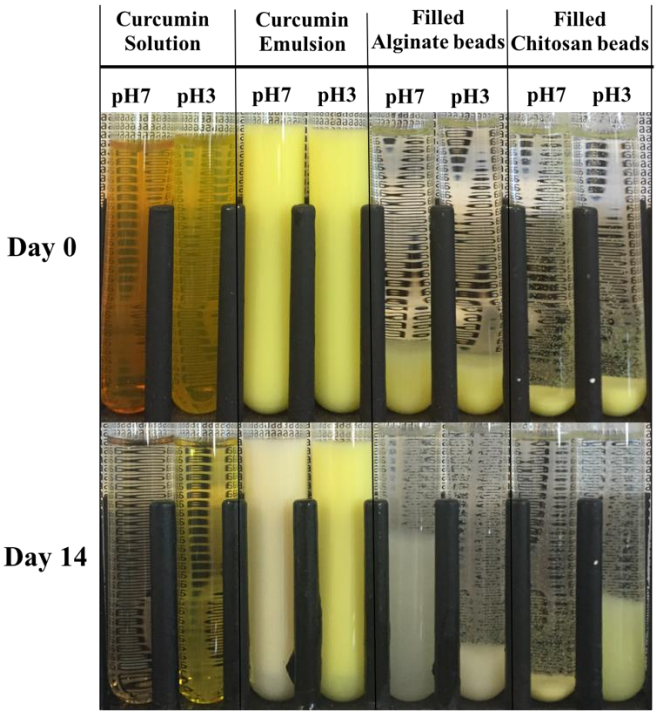

1b

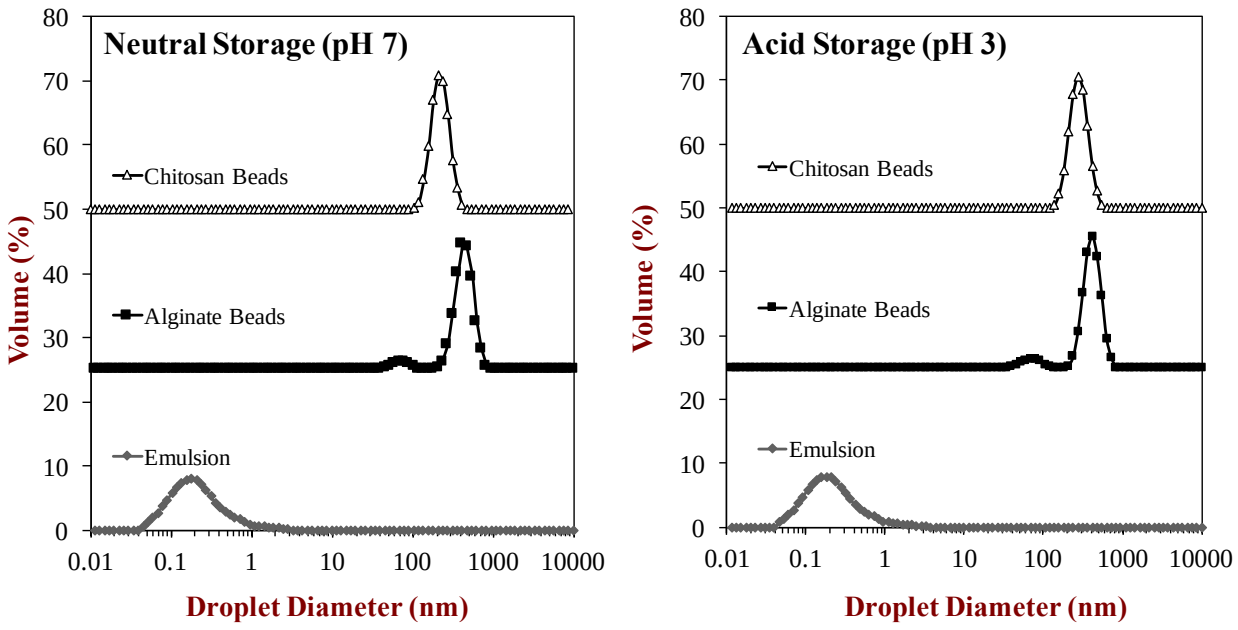

1c

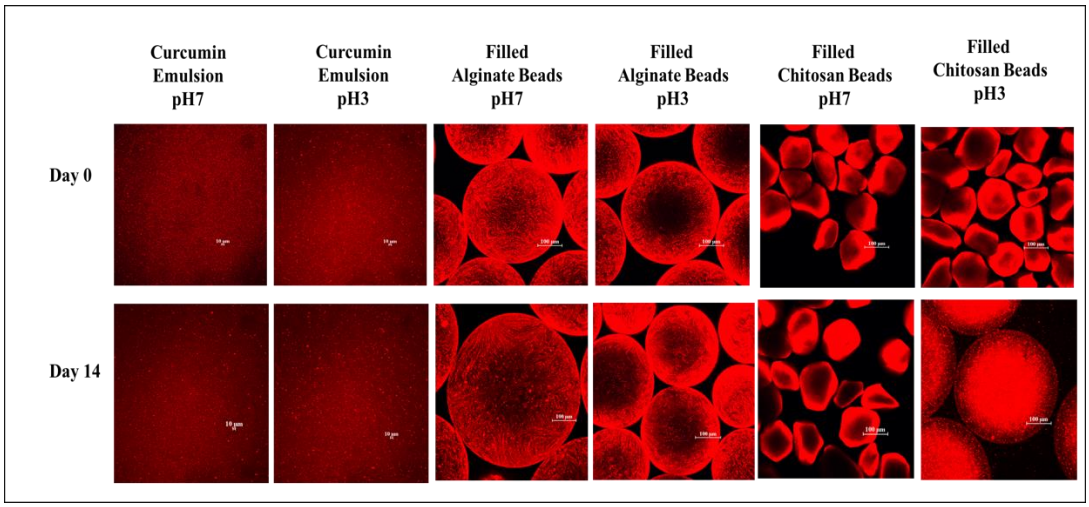

Fig. 1 a) Appearances, b) Particle size distributions c) microstructure of different curcumin-loaded delivery systems before and after being storage under acidic or neutral conditions at 55°C for 14 days. The delivery systems consisted of curcumin dispersed in aqueous solutions, emulsions or filled hydrogel beads. a) The picture on the right shows the presence of sediments at the bottom of the test tubes containing the aqueous solutions. C)The microstructures were obtained using confocal fluorescence microscopy, and the lipid phase appeared red due to the presence of Nile red.

Table.1 The impact of pH on the initial yellow color (b^*), mean particle diameter (D_{43}) and electrical characteristics (ζ-potential) of curcumin-loaded delivery systems: aqueous solutions; emulsions; filled alginate beads; and, filled chitosan beads. Samples designated with different letters (a, b, c) were significantly different (Duncan, $p<0.05$).

	Aqueous Solution		Emulsion		Filled Alginate Beads		Filled Chitosan Beads	
	pH 7	pH 3	pH 7	pH 3	pH 7	pH 3	pH 7	pH 3
*b**	65.5±2.8 [a]	67.5±3.1 [a]	60.4±3.1 [b]	60.4±3.5 [b]	26.5±4.6 [d]	28.6±2.1 [d]	34.3±1.5 [c]	33.1±2.9 [c]
D_{43} (μm)			0.27±0.03 [d]	0.27± 0.04 [d]	404±15 [a]	371±10 [b]	239±21 [c]	255±19 [c]
ζ (mV)			−20.3±0.7 [b]	0.28±0.55 [e]	−17.4±2.1 [c]	−12.7±1.0 [d]	−22.7±1.9 [a]	0.74±0.58 [e]

3.3.2. Influence of delivery system type on storage stability of encapsulated curcumin

The impact of delivery system type on the chemical stability of curcumin was investigated by incubating the samples in acidic (pH 3) and neutral (pH 7) conditions at 55 °C for 14 days and then measuring the change in color (Fig. 2). The initial rate of color degradation was estimated by calculating the slope of the lines in the initial region where the plots were approximately linear (Fig. 3). In addition, the changes in the physicochemical and structural properties of the particles in the delivery systems were measured throughout storage.

3.2.1. Curcumin solution

Visual observation of the aqueous solutions containing curcumin after 14-days storage indicated that a noticeable color change occurred at both pH values, with much more extensive color fading at pH 7 than pH 3 (Fig. 1a). There was also an appreciable decrease in the yellowness of the curcumin solutions measured using a colorimeter, with the *b** value decreasing to 17% of its original value at pH 3 and to 73% of its original value at pH 7 (Fig. 2). Moreover, the initial rate of color fading was appreciably higher at neutral conditions than at acidic conditions (Fig. 3). These results are in agreement with previous studies that have reported that curcumin is much more unstable to chemical degradation at neutral or alkaline conditions, than at acidic conditions [19]. Curcumin may be more stable in acidic solutions because the phenolic group is protonated, which stabilizes its conjugated diene structure, whereas it is de-protonated at

pH 7, which destabilizes it [49, 50, 174]. The curcumin solutions did not become completely colorless at the end of the storage period, which suggests that some of the reaction products formed during their chemical degradation were colored. Moreover, there was evidence of some curcumin precipitation in the aqueous solutions during storage, with a thin layer of sediment being observed at the bottom of the test tubes (Fig. 1a).

3.3.2.2. Curcumin emulsions

Visual observation of the curcumin emulsions indicated that appreciable color fading occurred when they were stored at pH 7, but there was little change when they were stored at pH 3 (Fig. 1a). Instrumental color measurements also showed that there was much more color fading at neutral conditions than at acidic conditions, with the *b**-value decreasing to 33% of its original value at pH 7 but to 93% of its original value at pH 3 (Fig. 2). In addition, the initial rate of color fading was much faster at pH 7 than pH 3 (Fig. 3). The rate and extent of color fading was considerably less in the emulsions than in the aqueous solutions at both pH values, which suggested that encapsulation of curcumin within the hydrophobic interior of lipid droplets protected it from chemical degradation. No sediments were observed at the bottom of the test tubes containing the curcumin-loaded emulsions, which suggests that the presence of the lipid droplets also prevented curcumin precipitation.

The mean particle diameter of the lipid droplets in the emulsions was similar at both pH values, and did not change appreciably during the 14-day storage period, remaining around D_{43}= 0.27 ± 0.01 μm (data not shown). The confocal fluorescence microscopy images of the emulsions taken after 14-days storage also indicated that they were stable to aggregation, with small droplets being evenly distributed throughout the images (Fig. 1c). The surface potential of the lipid droplets also did not change appreciably during storage, with the ζ-potential remaining

around -0.4 ± 0.5 mV at pH 3 and around -21.2 ± 1.0 mV at pH 7 (data not shown). Overall, these results indicate that the emulsions were stable to droplet aggregation under the experimental storage conditions used. It should be noted that a small amount of creaming was observed in the emulsions after 14-days storage (Fig. 1a), which may have been because there was a small population of relatively large droplets that moved upwards due to gravity.

Table 2. Influence of acidic and neutral incubation on the diameters of hydrogel beads. Samples designated with different letters (a, b, c) were significantly different (Duncan, $p<0.05$).

	Initial Bead Diameter (μm)	Final Bead Diameter (μm)	% of Swelling
Alginate beads (pH 7)	404±15 ^{a}	480±7 ^{A}	+19.3±3.7
Alginate beads (pH 3)	371±10 ^{b}	331±9 ^{C}	−10.8±3.8
Chitosan beads (pH 7)	239±21 ^{cD}	245±26 ^{cD}	−1.9±5.0
Chitosan beads (pH 3)	255±19 ^{cD}	436±18 ^{B}	+72±11

3.3.2.3. Filled alginate beads

The curcumin encapsulated in the alginate beads was highly unstable to chemical degradation when stored at both acidic and neutral conditions, with the degradation rate being faster at pH 7 than at pH 3 (Fig. 2). The initial rate of color degradation was actually much higher in the filled alginate beads than in either the aqueous solutions or the emulsions at pH 3 (Fig. 3), which suggests that the local molecular environment inside the alginate beads actually promoted curcumin degradation under acidic conditions. Conversely, the initial rate of curcumin degradation was much less in the alginate beads than in the aqueous solutions at pH 7, but considerably higher than in the emulsions (Fig. 2). Since both the emulsions and filled alginate beads contained curcumin-loaded lipid droplets, this result suggests that the microenvironment inside the alginate beads also promoted curcumin degradation at neutral conditions. The local

pH inside a hydrogel can be appreciably different from the pH in the surrounding aqueous phase [175], which may have altered the stability of the curcumin to degradation. However, further studies are needed to identify the precise molecular origin of this interesting finding.

The impact of pH on the physicochemical and structural properties of the filled alginate beads during storage was also measured (Fig. 4). As mentioned earlier, the initial diameter of the alginate beads was higher at pH 7 than at pH 3 because of the stronger electrostatic repulsion between the alginate chains within the hydrogel matrix [164, 166]. At pH 7, the mean particle diameter of the alginate beads increased appreciably during storage, from around 404 μm initially to 482 um after 14-days storage, which corresponds to a 19% increase in dimensions. Conversely, at pH 3, the mean particle diameter increased slightly during the first three days of storage, but then decreased appreciably at longer storage times. Overall, the mean particle diameter of the alginate beads incubated under acidic conditions decreased from around 371μm initially to 331 μm after two-weeks storage, which corresponds to a 11% decrease in size. The swelling of the alginate beads under neutral conditions and shrinkage under acidic conditions was also observed in the confocal fluorescence microscopy images (Fig. 1c). These images also showed that the beads remained spherical throughout storage, and that the lipid droplets remained trapped inside them.

The swelling of the beads at pH 7 may have occurred because of slow molecular rearrangements of the alginate chains within the hydrogel matrix during storage as they tried to increase the distance between their neighbors driven by the strong electrostatic repulsion between them. Alternatively, swelling may have occurred at neutral pH because some of the calcium ions leached out of the hydrogel matrix into the surrounding aqueous phase due to ion exchange with sodium ions from the phosphate buffer, thereby allowing the alginate chains to

move further apart from each other [170]. The shrinkage of the alginate beads at pH 3 may have occurred because the alginate molecules underwent molecular rearrangements during storage that allowed them to adopt a more compact structure, since there would be less electrostatic repulsion between them at this pH. Alternatively, some of the alginate molecules at the surfaces of the hydrogel beads may have degraded or dissociated under acidic conditions, and then moved into the surrounding aqueous phase *i.e.*, surface erosion [170].

At pH 3, the surface potential (ζ -potential) of the alginate beads remained relatively constant throughout storage (Fig. 5), which suggested that there was little change in the composition or structure of the bead surfaces. Conversely, at pH 7, the ζ -potential of the alginate beads became more negative during storage (Fig. 5), which suggested that there was some change in their surface composition or structure. This increase in negative charge supports the hypothesis that some of the cationic calcium ions may have leached out of the hydrogel beads during storage.

3.2.4. Filled chitosan beads

The chemical stability of curcumin was appreciably different when it was encapsulated in chitosan beads than in alginate beads (Fig. 2). At pH 7, encapsulation of curcumin in the filled chitosan beads greatly retarded the rate and extent of color degradation compared to the aqueous solution and emulsion. Moreover, the chemical degradation rate was much slower in the chitosan beads than in the alginate beads (Fig. 3). These results clearly show that the molecular environment of curcumin plays a key role in determining its chemical stability. At pH 7, the biopolymer network within the chitosan beads would be expected to be relatively compact, as highlighted by the small particle size (Fig. 1b), thin sediment layer formed (Fig. 1a), and high packing density of the lipid droplets within the beads observed by confocal microscopy (Fig. 1c).

Consequently, one would expect the pore size of the biopolymer network inside the beads to be relatively small under these conditions, which may have inhibited the ability of aqueous phase components to interact with the curcumin-loaded lipid droplets. Alternatively, the high level of amino-groups associated with the chitosan chains may have enhanced the chemical stability of the encapsulated curcumin, since recent studies suggest that the interaction of curcumin with amino groups may inhibit its degradation around neutral pH [176]. At pH 3, the color loss occurred more rapidly when the curcumin-loaded lipid droplets were encapsulated within chitosan beads rather than being freely dispersed within the aqueous phase (Figs. 2 and 3), which suggests that the presence of the chitosan network actually promoted curcumin degradation. On the other hand, the stability of the curcumin was appreciably higher in the chitosan beads than in the alginate beads. The origin of these effects is currently unknown, but again highlights the importance of the molecular environment of the chitosan on its stability.

The physicochemical and structural properties of the chitosan beads were also measured during storage. At pH 7, the mean particle diameter of the beads remained relatively constant throughout storage (Fig. 4), which was supported by the confocal microscopy images taken after 14-days storage (Fig. 1c). Moreover, the thickness of the sediment formed at the bottom of the test tubes was fairly similar at the beginning and end of storage (Fig. 1a). Taken together, these results suggest that the chitosan beads did not swell, shrink, or dissociate when stored under neutral conditions. Conversely, there was a progressive increase in the mean particle diameter of the chitosan beads during the first 10 days of storage at pH 7 (Fig. 2). Indeed, the mean particle diameter of the beads increased from around 255 μm initially to 436 μm after 14-days, which corresponds to an increase in diameter of about 72% (Table 1). Interestingly, the confocal microscopy images indicated that the chitosan beads changed from relatively small irregular

particles at the beginning of the storage period to large spheres at the end (Fig. 1c). However, the lipid droplets still remained trapped within the chitosan beads at the end of the incubation period. The swelling of the chitosan beads under acidic conditions was also demonstrated by the large increase in the thickness of the sediment layer at the bottom of the test tubes after 2-weeks storage (Fig. 1a). The high degree of swelling observed in the chitosan beads at pH 3 may have been because of the strong electrostatic repulsion between the strongly cationic chitosan molecules. Consequently, the structural organization of the chitosan chains within the hydrogel beads changed over time so that they could get further apart [177]. Alternatively, some of the tripolyphosphate molecules may have diffused out of the beads during storage, thereby decreasing the number of cross-links between the chitosan molecules.

The electrical characteristics of the chitosan beads changed appreciably during storage at both pH values, which suggested that their surface composition or structure changed. At pH 3, the ζ -potential of the chitosan beads became progressively more positive during storage (Fig. 5), which may have occurred because some of the negatively charged tripolyphosphate ions diffused out of the beads. At pH 7, the ζ -potential of the chitosan beads became less negative during storage (Fig. 5), which again may be indicative of the loss of tripolyphosphate ions. The leaching out of these ions during storage would therefore account for the observed increase in bead dimensions during storage, since there would be fewer cross-links between the chitosan molecules.

Fig. 2

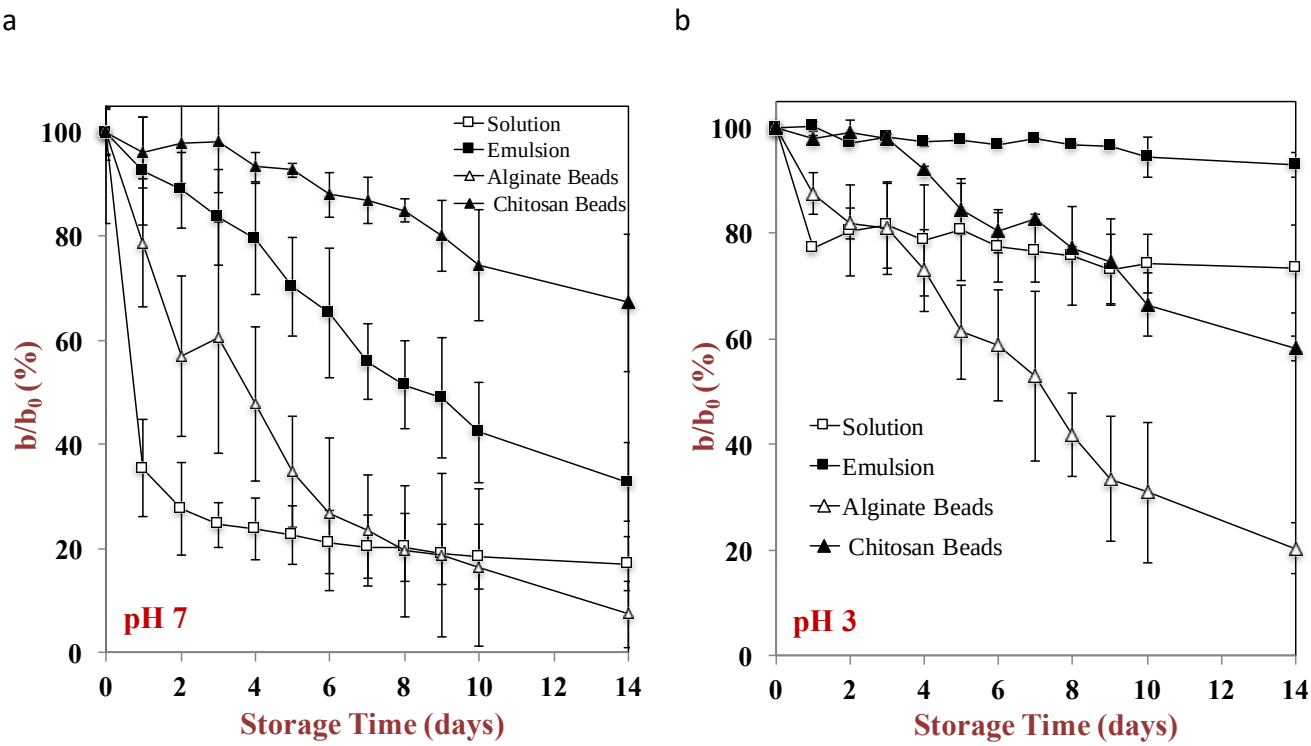

Fig.2. Influence of acidic and neutral pH conditions on yellow color (*b**) degradation in different types of curcumin-loaded delivery systems during storage at 55 °C.

Fig. 3

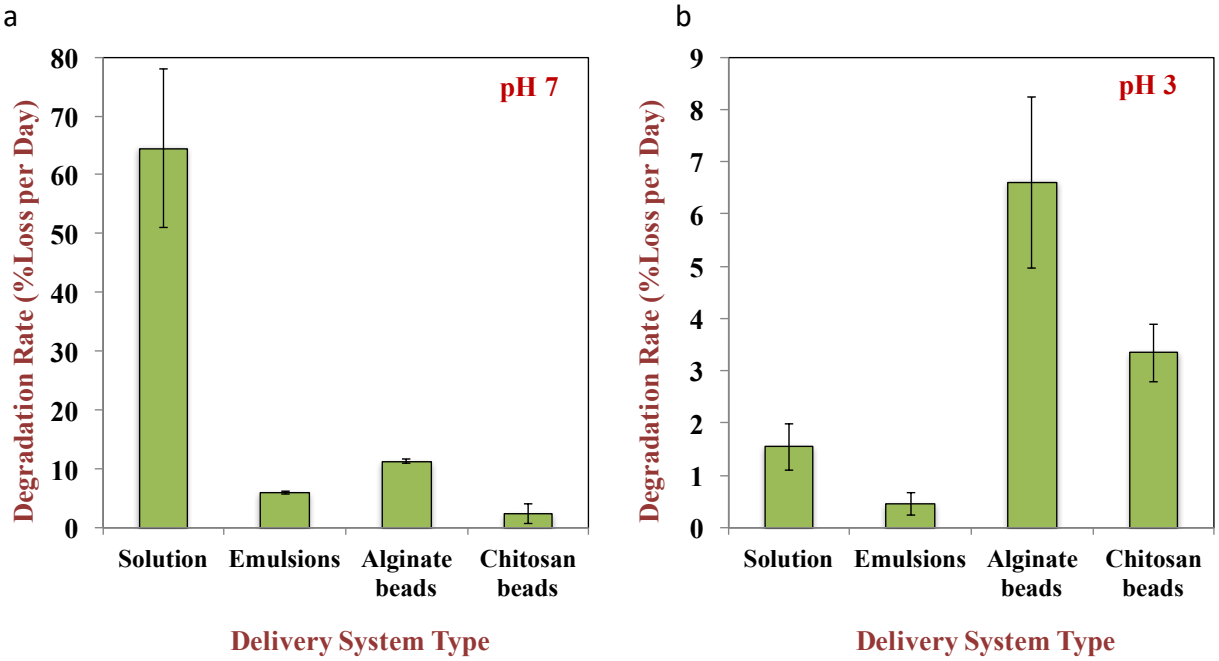

Fig.3. Influence of acidic and neutral pH conditions on the initial rate of color degradation in different types of curcumin-loaded delivery systems during storage at 55 °C.

Fig. 4

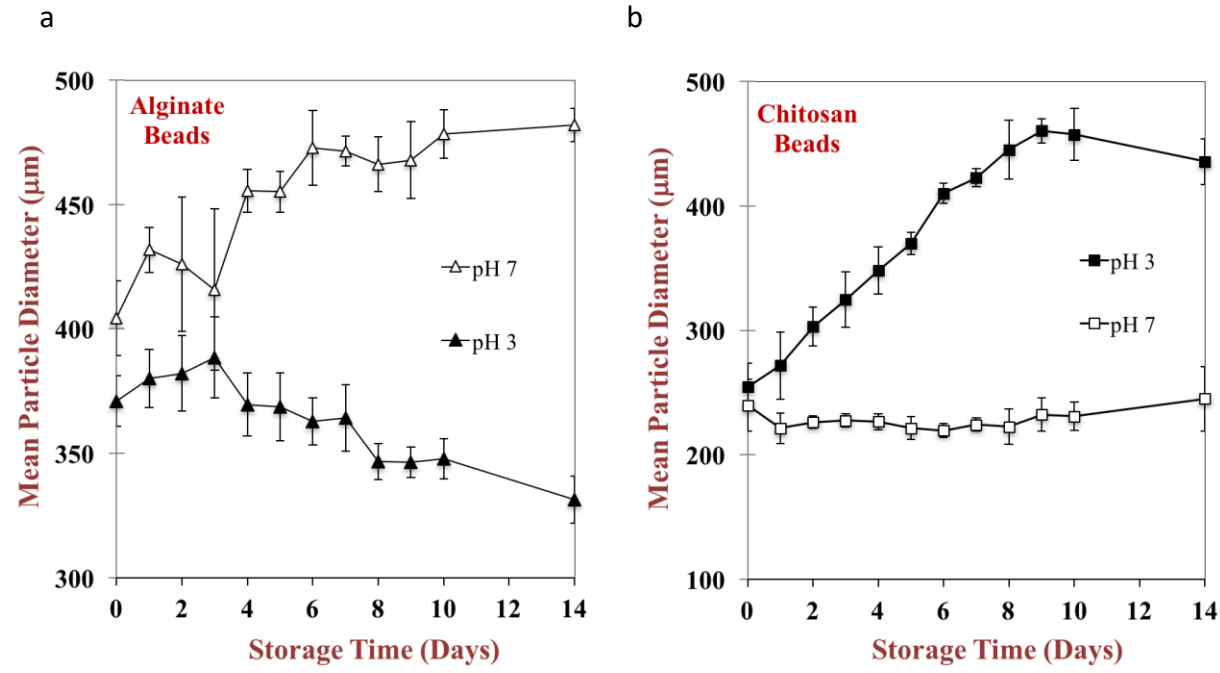

Fig. 4. Influence of storage pH on the mean particle diameter of curcumin-loaded filled alginate or chitosan beads during storage at 55 °C.

Fig. 5

a b

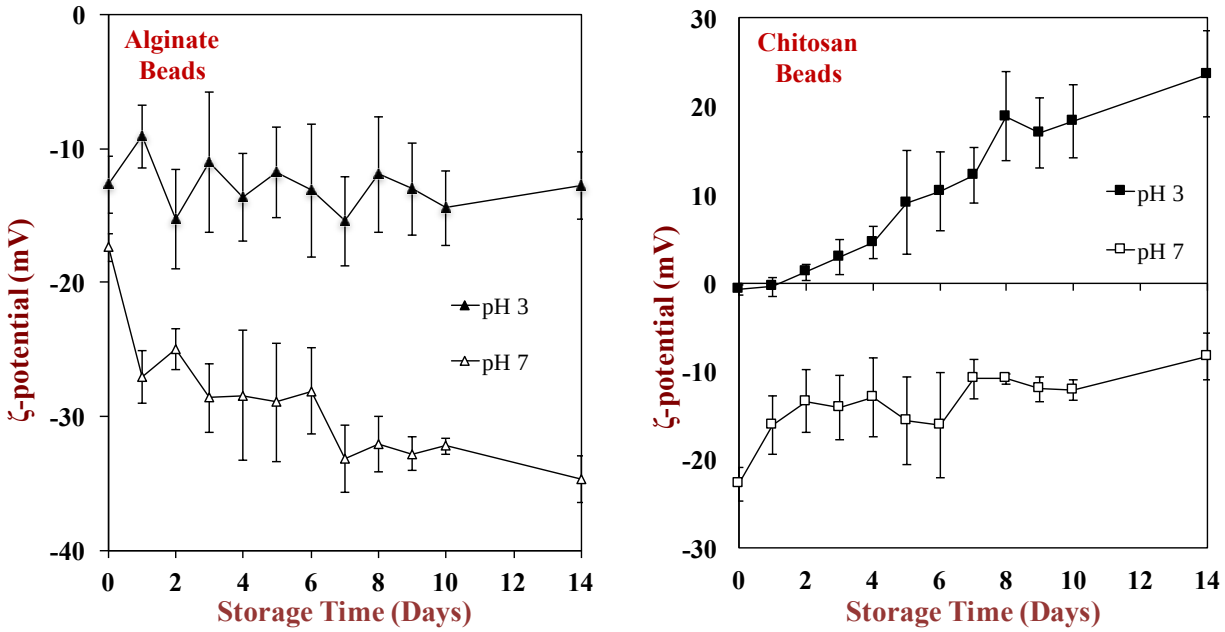

Fig. 5. Influence of storage pH on the surface potential (ζ-potential) of curcumin-loaded filled alginate or chitosan beads during storage at 55 °C.

3.3.2.5 Comparison of delivery systems

Our results indicate that there were major differences in the chemical and physical stability of the different delivery systems during storage. The aqueous curcumin solutions were highly unstable to color fading and precipitation, and would therefore be unsuitable as delivery systems for commercial applications. The curcumin-loaded emulsions had good physical stability at both pH values, and provided the best protection against chemical degradation at pH 7 of all the systems studied. Consequently, they would be the most suitable delivery systems for application in commercial products with pH values around neutral. However, the curcumin-loaded emulsions were prone to rapid color fading at pH 7, and would therefore not be suitable for application in neutral products.

Compared to the emulsions, the alginate beads appeared to accelerate curcumin degradation at both pH values, and would therefore be unsuitable as delivery systems. Moreover, there were appreciable changes in the dimensions of the alginate beads during storage, which might also be undesirable for many commercial applications (see below). The chitosan beads also appeared to be less suitable than the emulsions for encapsulation of curcumin under acidic conditions, since there was a more rapid degradation rate (Fig. 3). On the other hand, the rate of color loss was appreciably lower in the filled chitosan-beads than in the emulsions at pH 7, which suggested that this type of bead may be more suitable for application in commercial products with pH values around neutral. However, appreciable swelling of the chitosan beads occurred during storage at pH 3. Changes in the dimensions of hydrogel beads during storage may have a number of important implications for their practical applications as delivery systems. Typically, the apparent shear viscosity or elastic modulus of hydrogel suspensions increases/decreases when they swell/shrink because this increases/decreases the disperse phase volume fraction [178, 179]. The optical properties and stability to gravitational separation of hydrogel beads may also be altered appreciably when their particle dimensions change [180]. The pore size of the hydrogel matrix within the beads will increase/decrease when they swell/shrink, which may impact the retention and release of any encapsulated components [164, 166]. The pH dependent changes in the dimensions of the hydrogel beads may be particularly important when they are used to control the delivery of bioactive components within the human gastrointestinal tract, where the pH changes appreciably as one moves through the mouth, stomach, small intestine and colon [170]. Consequently, there may be undesirable alterations in the texture, appearance, stability, and release properties of the hydrogel beads during storage.

3.4. Conclusion

This study has provided some valuable insights into the design and development of curcumin delivery systems. It is often assumed that encapsulation of a bioactive component within a delivery system will improve its chemical stability, but as shown in this study, this is not always the case. For instance, encapsulation of curcumin-loaded lipid droplets within alginate beads actually decreased their chemical stability under both acidic and neutral conditions. Consequently, it is important to carefully select the most appropriate delivery system for each application. In this study, it was shown that oil-in-water emulsions were the most effective delivery systems for curcumin at pH 3, since they gave the best protection against chemical degradation and remained physically stable. Moreover, they are simpler, quicker and cheaper to fabricate that filled hydrogel beads, which would be an advantage for many commercial applications. On the other hand, filled chitosan beads appeared to give the best protection against curcumin degradation at pH 7. However, these beads were prone to substantial swelling during storage, which would limit their application in some products. In future studies, it would be interesting to identify the molecular basis for differences in the stability of curcumin in different molecular environments.

Chapter 4

4. Impact of delivery system type on curcumin bioaccessibility: comparison of curcumin-loaded nanoemulsions with commercial curcumin supplements

4.1. Introduction

Curcumin, a bioactive constituent found in turmeric, has been shown to have anti-oxidative and anti-inflammatory properties that provide the basis for its application as a nutraceutical or pharmaceutical to inhibit or treat certain diseases, such as rheumatoid arthritis, cystic fibrosis, inflammatory bowel disease, and colon cancer [3, 150, 181]. In foods, curcumin can also be used as a natural pigment because it has a desirable yellow-orange color. Curcumin has a relatively low toxicity and is generally regarded as safe (GRAS) by the United States Food and Drug Administration (FDA). The potentially beneficial biological activities exhibited by curcumin has led the pharmaceutical, supplement, and food industries to develop forms suitable for oral ingestion, such as pills, capsules, powders, foods, and drinks [1, 13, 132, 182]. However, there are a number of hurdles that have to be overcome before curcumin can be utilized in these products, including its high melting point, low water-solubility, alkaline degradation, and low oral bioavailability [183].

The oral bioavailability and bioactivity of curcumin is known to depend on the physical form that it is delivered in. Studies have reported that encapsulation of curcumin within colloidal particles enhances its bioavailability [132, 146, 183-186]. Many of the conventional technologies used to incorporate curcumin into colloid dispersions utilize either heating or organic solvents, which both have technical challenges [13, 187, 188]. The main disadvantage of using heating methods is that curcumin chemically degrades at high temperatures, which leads to a loss of its biological

activity [13, 184]. On the other hand, the main disadvantage of using organic solvent methods is that they are environmentally unfriendly and costly [88, 189]. Consequently, there is interest in developing alternative approaches for incorporating curcumin into colloidal delivery systems.

Recently, a novel pH-driven method has been developed to incorporate hydrophobic molecules, such as curcumin, into colloid delivery systems without using heating or organic solvents [92-94, 190]. This method is based on the fact that the water-solubility of curcumin is highly dependent on solution pH. Curcumin is practically insoluble in water under acidic and neutral conditions, but highly soluble under alkaline conditions because it is a weak *Brønsted* acid with three labile protons at high pH values (pK_a = 7.5, 8.5, and 9.5) [4, 13, 191]. Consequently, the water-solubility of curcumin increases when the pH increases above neutral because the molecules becomes progressively more negatively charged. Conversely, when the pH of an alkaline curcumin solution is reduced, the negative charge on the curcumin is reduced and it becomes insoluble. The pH-driven method utilizes this phenomenon to load curcumin into oil-in-water emulsions. The curcumin is first dissolved in an alkaline solution, which is then mixed with an acidified emulsion. When the pH of the entire system decreases the curcumin becomes insoluble and is driven into the interior of the oil droplets.

The main objective of the current study was to compare the pH-driven method of loading nanoemulsions with curcumin with two more commonly used methods: the conventional method and the heat-driven method. The conventional method involved dissolving powdered curcumin in an oil phase and then blending this with an aqueous phase to form a curcumin-loaded nanoemulsion. The heat-driven method involved forming a nanoemulsion first, then adding powdered curcumin, and then incubating the mixed system at an elevated temperature to cause the curcumin crystals to dissolve and move into the oil droplets. The loading capacity and

bioaccessibility of curcumin in nanoemulsions prepared using the three different loading methods was compared. In addition, the efficacy of the nanoemulsion-based delivery systems prepared in this study were compared to those of three commercial formulations in terms of their ability to increase curcumin bioaccessibility. Due to the increasing trend towards clean-labels in the food industry, all-natural ingredients were utilized to fabricate the curcumin-loaded nanoemulsions. The results of this study should have important implications for the design and formulation of more efficacious nutraceutical delivery systems.

4.2. Material & Methods

4.2.1 Materials

Corn oil was purchased from a local supermarket and used without further purification (Mazola, ACH Foods, Cordova, TN). Curcumin supplements produced by Nature Made (Nature Made Nutritional Products, Mission Hills, CA), Full Spectrum (Solgar, Inc., Leonia, NJ), and CurcuWin (Relentless Improvement® LLC, Reno, NV) were also purchased from an on-line supplier (Amazon.com). The following chemicals were purchased from the Sigma-Aldrich Chemical Company (St. Louis, MO): curcumin (C1386-10G, purity ≥65%); mucin from porcine stomach (M2378-100G); pepsin from porcine gastric mucosa (P7000-25G); lipase from porcine gastric mucosa (L3126-100G); porcine bile extract (B8831-100G); sodium hydroxide (SS266-4L), and Nile Red (N3013-100MG). Quillaja saponin (Q-Naturale® 200) was provided by Ingredion Inc. (Westchester, IL).

The three commercial curcumin supplements had different physical forms. The Nature Made (NM) and CurcuWin (Win) products were powders, whereas the Full Spectrum (FS) products was a liquid. The NM product appeared to be prepared by directly adding powdered curcumin into capsules with other inactive ingredients. However, the Win product appeared to

be prepared using a patented technology (UltraSol®) from Omniactive Healthy Technologies (Canada), which involves incorporating curcumin into food-grade nanoparticles with antioxidants. The FS product was a water-soluble form containing curcumin stabilized by a synthetic surfactant (Polysorbate 80).

4.2.2 Preparation protocol

The curcumin nanoemulsions were prepared using three different approaches: the conventional method; heat-driven method; and, pH-driven method.

4.2.2.1. Conventional method

Curcumin-loaded nanoemulsions were produced using the conventional method by dispersing powdered curcumin into an oil phase (corn oil) prior to homogenization. A weighed amount of curcumin powder was added to the oil phase (3 mg/g) and then the mixture was incubated at 60 °C for 2 hours to ensure fully dissolution. The aqueous phase was prepared by mixing Quillaja saponin (2% w/w) with phosphate buffer solution (10 mM, pH 6) for 5 min. A coarse emulsion was then formed by blending 10% (w/w) of curcumin-loaded oil with 90% (w/w) of aqueous phase for 2 min using a high-speed blender (M122.1281-0, Biospec Products, Inc., ESGC, Switzerland). A nanoemulsion was then formed by passing the coarse emulsion five times through a high-pressure homogenizer (Microfluidizer M-110Y, Microfluidics, Newton, MA USA) with a 75-μm interaction chamber (F20Y) at an operating pressure of 12,000 psi. The resulting curcumin nanoemulsion was stored at 4 °C in the dark before being used. The nanoemulsions were then diluted 1:1 (w/w) using double distilled water so that the final system contained 0.15 mg curcumin per g emulsion for the *in vitro* studies.

4.2.2.2. Heat-driven method

Curcumin-loaded nanoemulsions were prepared using the heat-driven method by mixing powdered curcumin with heated nanoemulsions. The stock nanoemulsions were fabricated by homogenizing 10% (w/w) oil phase (corn oil) and 90% (w/w) aqueous phase (2 % w/w Q-naturale, 10 mM phosphate buffer, pH 6) using the same approach as described for the conventional method. Powdered curcumin (0.3 mg/g) was then added to the stock nanoemulsion and the resulting mixture was incubated at 100 °C for 15 min in the dark with constant stirring. This system was then diluted 1:1 (w/w) with double distilled water to obtain a final system containing 5% oil and 0.15 mg curcumin /g emulsion.

4.2.2.3 pH-driven method

The curcumin-loaded nanoemulsions fabricated using the pH-driven method were prepared by mixing an alkaline solution of dissolved curcumin with a stock nanoemulsion, which was slightly acidic (pH 6). An alkaline curcumin solution (6 mg/g, pH 12.5) was prepared by adding powdered curcumin into an alkaline solution (0.1N sodium hydroxide) and then stirring for 2 min in the dark at ambient temperature. The alkaline curcumin solution was then added to a stock nanoemulsion (prepared using the same method as for the heat-driven method) to reach a final concentration of 0.3 mg curcumin per g emulsion. The mixed nanoemulsion formed has immediately adjusted back to pH 6 and then stirred for 30 min in the dark at ambient temperature. Again, the samples were diluted with double distilled water to obtain a final system containing 5% oil and 0.15 mg curcumin per g emulsion.

4.2.2.4 Commercial curcumin supplements

Initially, the curcumin concentration of each product was determined based on a standard curve prepared using pure curcumin. The curcumin was extracted from each sample using

chloroform. The samples were diluted with double distilled water to obtain final systems containing 0.15 mg of curcumin per g sample.

4.2.3 Optical properties

The optical properties of curcumin dispersions prepared using different fabrication methods was characterized by measuring their color coordinates. An instrumental colorimeter (ColorFlex EZ 45/0-LAV, Hunter Associates Laboratory Inc., Virginia, USA) was used to determine the color coordinates: L^* (lightness/darkness); a^* (redness/greenness); and b^* (yellowness/blueness). An aliquot of sample (10 mL) was placed in a Petri dish, and then illuminated using D65-artificial daylight (10° standard angle) with a black background. Three replicate measurements were taken and averaged to represent the final results. Only the b^* and L^* values are reported here because they best represent the yellow color and lightness of the curcumin-loaded systems.

4.2.4 simulated gastrointestinal digestion

4.2.4.1 General

A gastrointestinal tract (GIT) model was used to analyze the effect of delivery system type on the potential gastrointestinal fate of curcumin. The model mimicked the mouth, stomach, and small intestine stages of the GIT. An equal amount of each sample (30 mL) was transferred into a glass beaker and then incubated at 37 °C in a shaking incubator (Innova Incubator Shaker, Model 4080, New Brunswick Scientific, New Jersey, USA). Each sample contained 0.15 mg curcumin per g sample, while all the emulsions containing the same level of oil (5% w/w).

2.4.2 Oral phase

An artificial saliva stock solution (ASSS) was prepared and used within 2 days of the study. The ASSS was fabricated by mixing sodium chloride (1.594 g/L), ammonium nitrate

(0.328 g/L), potassium phosphate (0.636 g/L), potassium chloride (0.202 g/L), potassium citrate (0.308 g/L), uric acid sodium salt (0.021 g/L), urea (0.198 g/L), lactic acid sodium salt (0.146 g/L) with double distilled water (1 L) and storing at 4°C overnight. Then, a stock simulated saliva fluid (SSF) was prepared by adding 90 mg mucin into 30 g ASSS and stirred overnight at 4 °C before the digestion study.

For the oral phase study, the initial sample (30 mL) and SSF (30 mL) were heated to 37 °C for 10 min prior to starting. The two samples were then transferred into a glass beaker after incubation and the pH was adjusted to 6.8. The resulting mixture was then placed into a shaking incubator operating at 100 rpm and 37 °C for 2 min to mimic oral conditions.

4.2.4.3 Stomach phase

Initially, a simulated gastric fluid work solution (SGFWS) was prepared by adding pepsin (3.2 mg/g) into stimulated gastric fluid (SGF) and then stirring for 40 min at room temperature. The SGF was produced by fully dissolving sodium chloride (2 g/L) and hydrochloric acid (83.3 mM/L or 7 mL/L) into double distilled water at room temperature. The remaining SGF solution was placed into the refrigerator (4°C) before experiments. The sample and SGF were preheated to 37 °C for 10 min before each study. Samples (40 g) collected from the mouth phase were mixed with SGF (40 g) and then adjusted to pH 2.5. The samples were then continuously agitated for 2 hours using an incubator shaker set at 100 rpm and 37 °C.

4.2.4.4 Small Intestine phase

Initially, three solutions containing intestinal constituents were prepared and incubated in a water bath (37°C): stock simulated intestinal fluids (SIF); bile salt solution; and, lipase solution. The stock SIF was prepared by fully dissolving calcium chloride (5.5 g) and sodium chloride (32.87 g) in 150 ml double distilled water. The bile salt solution was prepared by mixing

porcine bile extract (53.57 mg/mL) with phosphate buffer (5 mM, pH 7) overnight at room temperature with continuous stirring. The lipase solution (24 mg/ mL) was prepared 30 min before utilization by mixing powdered lipase with phosphate buffer (5 mM, pH 7).

Samples collected from the stomach phase (60 g) were transferred into a water bath at a temperature of 37 °C. An automatic titration unit (Metrohm, USA Inc.) was used to monitor and maintain a neutral pH in the sample. First, the sample was adjusted to pH 7, subsequently, 3 mL SIF containing (0.5 M $CaCl_2$ and 7.5 M NaCl) and 7 mL bile salt solution (containing 375 mg bile extract) was added to the sample, which was then adjusted back to pH 7. Finally, 5 mL of lipase solution (containing 120 mg lipase) was added to this mixture and the automatic titration device was started. The volume of alkaline solution (0.25 M NaOH solution) required to maintain a neutral pH was recorded throughout the digestion period. All solutions were preheated to 37 ^{o}C for 5 min before being used.

The amount of NaOH solution required to neutralize the free fatty acids (FFA) released was recorded and used to estimate the fraction of FFA released [192]:

$$FFA(\%) = 100 \times \frac{V_{NaOH} m_{NaOH} M_{lipid}}{2\ W_{liquid}}$$

Here, FFA (%) is the percentage of released FFAs; V_{NaOH} is the volume of titrant required to neutralize the FFA; m_{NaOH} is the molarity of sodium hydroxide; M_{lipid} is the molecular weight of the oil used (grams per mole); and the "2" represents the fact that two FFAs are released from a triglyceride, and W_{lipid} is the mass (gram) of the oil in the digestion system.

4.2.5 Particle characterization

A laser light scattering instrument (Mastersizer 2000, Malvern Instruments Ltd., Malvern, Worcestershire, U.K.) was used to measure the particle diameter and particle size distribution of the samples. A particle electrophoresis device (Zetasizer Nano, Malvern Instruments, Worcester-

shire, U.K.) was used to determine the ζ-potential values of the particles. The initial, mouth and small intestine samples were diluted with phosphate buffer (5 mM, pH 7), while the stomach samples were adjusted with acidified double distilled water (pH 2.5) to avoid multiple scattering effects.

4.2.6 Microstructure analysis

A confocal scanning laser microscope (Nikon D-Eclipse C1 80i, Nikon, Melville, NY) was used to characterized the microstructure of the samples with a 200× magnification (20× objective lens 10× eyepiece). The oil regions in the samples were stained by adding a hydrophobic fluorescence dye in the form of Nile red solution (1 mg/mL ethanol).

4.2.7 Curcumin concentration determination

The level of curcumin in the initial samples, mixed micelle fraction, and total digest fraction were measured. The curcumin concentration in the samples was quantified using an UV-visible spectrophotometer at a wavelength of 419 nm (Cary 100 UV−vis, Agilent Technologies, Santa Clara, CA, USA). Samples were collected after the small intestine phase and split into two portions: the mixed micelle fraction and the total digest fraction. The mixed micelle fraction was transferred into a centrifuge tube and centrifuged (18,000 rpm, 25 °C) for 50 min (Thermo Scientific, Waltham, MA). The clear top layer of these samples was collected to represent the “mixed micelle fraction” where the curcumin was solubilized. The total digest fraction was used directly without any centrifugation. The concentration of curcumin in each fraction was determined by adding chloroform and then then centrifuging at 3000 rpm for 10 min. The hydrophobic curcumin moved into the chloroform layer. The concentration of the curcumin in the separated chloroform layers was then determined using a standard curve

prepared by measuring the absorbance of known curcumin samples (Supplementary information Fig. 1).

The *bioaccessibility* of curcumin, which is the fraction in the small intestine that was solubilized in the mixed micelle phase (and therefore potentially available for absorption), was calculated using the following equation:

$$Bioaccessibility\ (\%) = 100\ \times \frac{C_{micelle}}{C_{digest}}$$

The *stability* of curcumin, which is the fraction remaining in the original state in the small intestine phase, was calculated using the following equation:

$$Stability(\%) = 100\ \times \frac{C_{digest}}{C_{initial}}$$

Here, C_{micelle} is the concentration of curcumin in the mixed micelle faction; C_{digest} is the concentration of curcumin in the total digest; and, $C_{initial}$ is the curcumin concentration in the initial sample.

4.2.8 Statistical analysis

All experiments were performed on at least three freshly prepared samples. The resulting data are measured as the mean ± standard deviation calculated from this data. Statistical differences among samples were determined using statistical analysis software (SPSS, IBM Corporation, Armonk, NY, USA), with $p< 0.05$ being considered as a significant difference.

4.3. Results & discussion

4.3.1 Influence of curcumin loading method

Initially, the impact of the three different loading methods on the formation and properties of the curcumin-loaded nanoemulsions was investigated: the conventional; heat-driven; and, pH-driven.

4.3.1.1 Influence of loading method on encapsulation efficiency

An equal amount of curcumin powder (150 μg/mL) was used to prepare each nanoemulsion. However, the total amount of curcumin encapsulated within the nanoemulsions after fabrication was different: 140 μg/mL for the pH-driven method; 114 μg/mL for the heat-driven method; and, 83 μg/mL for the conventional method (Table 1). Consequently, the encapsulation efficiency of the pH-driven method (93%) was considerably higher than that of the heat-driven (76%) or conventional (56%) methods. There are a number of potential reasons for these differences. First, the pH-driven method is carried out at ambient temperature and so there is little thermal degradation of the curcumin. In contrast, both the heat-driven (100 °C for 15 min) and conventional (60°C for 2 h) methods required a thermal processing step that could damage the curcumin. The fact that the amount of curcumin was lower in the nanoemulsions prepared using the conventional method suggests that the prolonged heating time used caused more extensive thermal degradation. Second, the different loading methods may have resulted in different amounts of curcumin crystallization during the nanoemulsion preparation procedure. Previous studies have shown that curcumin dissolved at high temperatures may crystallize when the system is cooled [5, 187]. In our study, we observed an orange precipitate at the bottom of the nanoemulsions prepared using the conventional method, which was presumably due to the formation and sedimentation of curcumin crystals (Fig 1a). In contrast, no orange precipitate was observed for the heat-driven and pH-driven methods, which suggests that loading the

curcumin after the nanoemulsions have been formed inhibited crystallization, possibly because the lipid droplets always had small dimensions. The solubility of substances is known to increase as the size of the particles they are contained within decreases due to a thermodynamic effect related to increased specific surface area [193].

The colorimetry measurements of the nanoemulsions supported the loading measurements. All samples had positive *b*-values and high *L*-values corresponding to materials with a yellowish color and strong lightness. As expected, the intensity of the yellow color of the nanoemulsions decreased with decreasing encapsulation efficiency: $b^* = 93$, 87, and 73 for the pH-driven, heat-driven, and conventional methods, respectively.

Table 1

	Conventional	**Heat-Driven**	**pH-Driven**
Initial curcumin concentration (μg/mL)	83.3 ± 10.8 ^{a}	114.3 ± 8.5 ^{b}	139.7 ± 3.8 ^{c}
Loading capacity (%)	55.5 ± 7.2 ^{a}	76.2 ± 5.2 ^{b}	93.2 ± 2.3 ^{c}
L^*	121.2 ±0.5^{c}	118.9 ± 0.2^{b}	117.8 ± 0.3^{a}
b^*	72.7 ± 0.5 ^{a}	87.0 ± 0.2 ^{b}	92.2 ± 1.8 ^{c}
D_{32} (μm)	0.17 ± 0.02 ^{a}	0.20 ± 0.00 ^{b}	0.18 ± 0.01 ^{ab}
ζ- potential (mV)	-45.2 ± 1.3 ^{a}	-44.6 ± 1.7 ^{a}	-45.3 ± 1.8 ^{a}

Table 1. The influence of the fabrication method on the initial curcumin concentration, loading capacity, tristimulus color value (b^*), mean particle diameter (D_{32}) and electrical characteristics (ζ- potential) of curcumin lipid nanoparticles. Samples designated with different letters are significantly different (Duncan, $p<0.05$).

Fig. 1

a

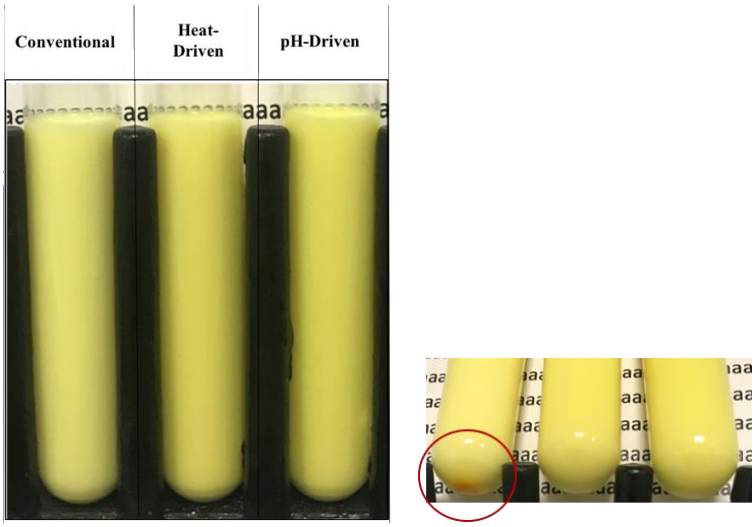

b

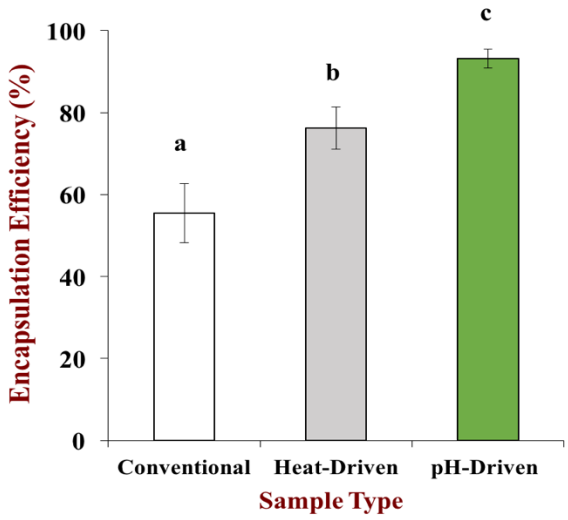

Fig. 1. a. Appearances of curcumin-loaded lipid nanoparticles prepared using different methods. b. the percentage of curcumin loading capacity of different methods on lipid nanoparticle. The lowercase letter means significantly different (Duncan, $p < 0.05$) between samples.

4.3.1.2 Influence of loading method on gastrointestinal fate of curcumin nanoemulsions

The impact of loading method on the gastrointestinal fate of the curcumin-loaded nanoemulsions was monitored using a simulated GIT. The particle size distribution (Fig. 2), mean particle diameter (Fig. 3), microstructure (Fig. 4) and ζ -potential (Fig. 5) of samples

collected from nanoemulsions exposed to mouth, stomach and intestinal phase were fairly similar to each other. This similarity can be attributed to the fact that all the nanoemulsions initially contained similar droplet sizes, compositions, and charges.

4.3.1.2.1 Initial

Initially, the particle size distributions (PSDs) of the curcumin-loaded nanoemulsions was monomodal and the mean particle diameters were relatively small (d_{32} < 200 nm) (Figures 2 and 3). The confocal microscopy images indicated that the lipid droplets were evenly distributed throughout the samples, indicating they were stable to flocculation. Interestingly, the light scattering data and the microscopy images indicated that the nanoemulsions prepared using the heat-driven method contained slightly larger droplets than the other two systems. This may have been because these nanoemulsions were held at a high temperature during their preparation, which may have caused some droplet aggregation. Indeed, previous studies have shown that lipid droplets coated with quillaja saponins undergo some aggregation at elevated temperatures [194].

All the curcumin-loaded lipid droplets initially had a relatively high negative surface potential (ζ > -40 mV) (Table 1), which can be attributed to the presence of carboxylic acid groups that have pK_a values around pH 3.5 [194, 195]. This relatively high surface potential is important for nanoemulsion stability because it generates a strong electrostatic repulsion between the lipids droplets [128]. The fact that all the samples had similar surface potentials suggests that the interfacial composition was not highly dependent on the curcumin-loading method used.

4.3.1.2.2 Oral phase

The PSDs of all the nanoemulsions were still monomodal after exposure to simulated oral conditions, but the mean particle diameter increased compared to the initial samples (Figs. 2 and 3). Moreover, the confocal microscopy images indicated that there were some larger particles in

the samples (Fig. 3), which is indicative of droplet aggregation. The magnitude of the surface potential on the particles in the samples changed from around -40 mV to around -30 mV after exposure to the simulated saliva. These effects can be attributed to the presence of mineral ions and mucin molecules in the saliva. The mineral ions screen the electrostatic repulsion between the lipid droplets while the mucin molecules can promote depletion and/or bridging flocculation [196-198].

4.3.1.2.3 Stomach phase

The PSDs became bimodal after exposure to the stomach phase with a population of relatively small particles and another population of relatively large particles (Fig. 2). As expected, this led to an increase in the mean particle diameter of the samples compared to the mouth phase (Fig. 3). The confocal microscopy images indicated that many of the lipid droplets in these samples were clustered together (Fig 3). Taken together, these results are characteristic of the lipid droplet aggregation that is often observed under simulated gastric conditions [196, 199]. The surface potentials of the particles became slightly positive (≈ +1 mV) after exposure to the stomach phase due to the relatively low pH and high ionic strength of the simulated gastric fluids (Fig. 5). Specifically, the low pH leads to protonation of the carboxylic acid groups on the adsorbed surfactant molecules while the mineral ions cause electrostatic screening [132, 199].

4.3.1.2.4 Small Intestine

The PSDs of all the samples were relatively broad after exposure to the simulated small intestinal phase (Fig. 2), which reflects the fact that there are many kinds of colloidal particles present after digestion, including micelles, vesicles, calcium-fatty acid soaps, and undigested lipid droplets [200]. The mean particle diameter of the samples in the small intestine phase was fairly similar to that in the stomach phase (Fig. 3) but does not reflect the broad range of particle sizes present. The confocal microscopy images indicated that most of the lipid droplets had been

digested, but that there were some relatively large lipid-rich particles present. The surface potential of the particles was negative (-20 mV) due to the fact that most of the constituents making up the colloidal particles in the neutral intestinal fluids are anionic, such as bile acids, free fatty acids, saponins, and peptides.

4.3.1.3 Influence of loading method on lipid digestion profile

In this section, the impact of the curcumin loading method on the lipid digestion profiles of the nanoemulsions was investigated using an automatic titration unit. The volume of sodium hydroxide (NaOH) solution required to maintain neutral pH in the samples when they were exposed to simulated small intestinal conditions was monitored. This volume was then used to calculate the fraction of FFAs released. Overall, the FFA release profiles of the three nanoemulsions were very similar (Fig. 6). The amount of FFAs released increased rapidly during the first 10 min and then gradually increased for the remainder of the digestion period. These results are consistent with previous studies that have also reported that the small lipid droplets in nanoemulsions are rapidly digested by lipase because of their high surface area [132, 160, 201]. Overall, these results indicate that the curcumin loading method used to prepare the nanoemulsions did not have a major impact on lipid digestion.

4.3.1.4 Influence of loading method on physiochemical characteristics of mixed micelles

The impact of the curcumin loading method on the properties of the mixed micelles formed at the end of the small intestine phase was also investigated. Initially, the raw digest was centrifuged to remove any large particles such as insoluble calcium-fatty acid soaps and undigested lipid droplets. The size and electrical characteristics of the particles remaining in the clear mixed micelle phase were then measured. The mean particle diameter of the mixed micelles collected from all three curcumin nanoemulsions was fairly similar: $d_{32} = 146 \pm 2$ nm,

136 ± 2 nm and 158 ± 2 nm for the conventional, heat-driven, and pH-driven methods, respectively. Similarly, the surface potentials of the mixed micelles from each sample were also relatively similar: ζ-potential = -21 ± 3 mV, -26 ± 3 mV and -21 ± 2 mV, respectively. The negative charges on the mixed micelles can be attributed to the fact that they were mainly comprised of neutral (monoacylglycerols) and anionic (bile salts and free fatty acids) molecular species [132, 200]. These results suggest that the loading method did not have a major impact on the nature of the mixed micelles formed after digestion.

4.3.1.5 Influence of loading method on curcumin bioaccessibility and stability

After the small intestinal phase, the curcumin concentration in the raw digest and mixed micelle phases were measured to determine the impact of loading method on the bioaccessibility and stability of the curcumin in the nanoemulsions. The level of curcumin in the raw digest represents the amount of curcumin remaining in the small intestine after digestion, *i.e.*, the fraction that has passed through the mouth, stomach, and small intestine without chemically degrading. The concentration of curcumin in the mixed micelle phase represents the curcumin molecules that were chemically stable and solubilized within the mixed micelles. The amount of curcumin in the mixed micelle phase and in the raw digest were affected by the loading method used: pH-driven > heat-driven > conventional method (Fig. 7a). This effect can be attributed to differences in the initial encapsulation efficiency of the three nanoemulsions, which decreased in the same order (Fig. 1a). As would be expected, a higher level of curcumin in the initial nanoemulsions led to a higher level of curcumin in the small intestine. These results suggest that the pH-driven method is the most effective at delivering a higher absolute amount of curcumin to the small intestine. However, when the curcumin concentrations are normalized to the total amount of curcumin in the digest, then the overall bioaccessibility was relatively independent of

the loading method used (Fig. 7b). This would also be expected because there would have been proportionally higher levels of curcumin in both the mixed micelles and digest.

Another important factor that impacts the overall bioavailability of curcumin is its stability to degradation within the gastrointestinal tract. The fraction of curcumin that remained after the small intestine phase was therefore determined relative to the initial amount in each system (Fig. 7b). The fraction of curcumin remaining decreased in the following order: conventional > heat-driven > pH-driven method. This suggests that the curcumin was more stable in the nanoemulsions prepared using the conventional method than those prepared using the pH-driven method. The effect may have occurred because some of the curcumin was in a crystalline form in the nanoemulsion prepared using the conventional method and was therefore more resistant to chemical degradation by aqueous phase components. Even so, the curcumin was relatively stable in all three systems, with > 80% remaining by the end of digestion. It should be noted that our *in vitro* GIT model did not include the Phase I and Phase II metabolic enzymes that are present in the human gastrointestinal tract, which means that changes in curcumin due to metabolism were not accounted for. Curcumin is known to undergo considerable metabolism in the GIT and therefore future studies should take this phenomenon into account [202].

Fig. 2

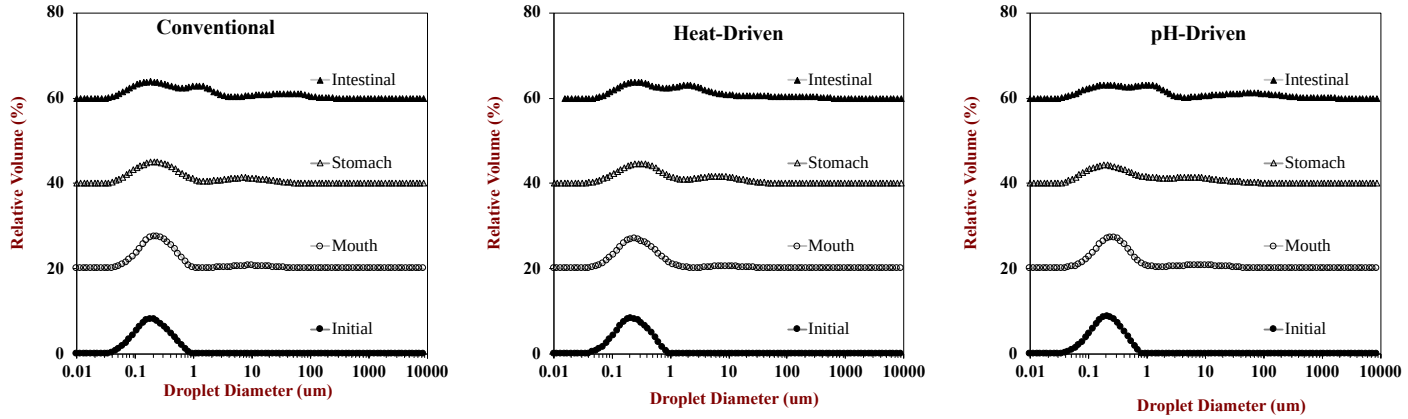

Fig. 2. Particle size distributions of curcumin-loaded nanoparticles prepared using different fabrication methods after exposure to different stages of a simulated gastrointestinal tract model.

Fig. 3

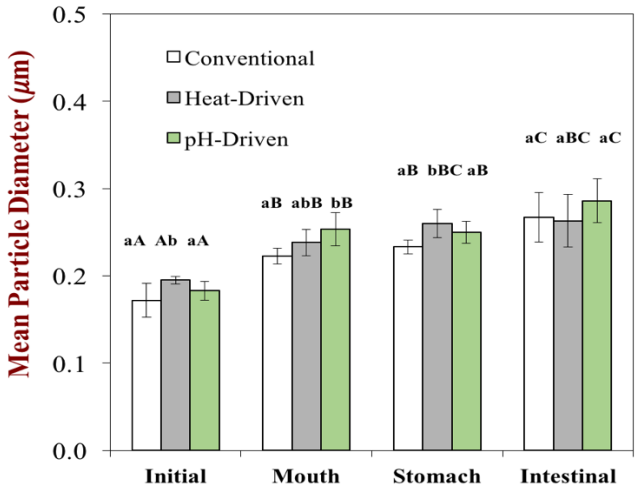

Fig. 3. Influence of simulated gastrointestinal condition on the mean particle diameter (d_{32}) of the curcumin loaded lipid nanoparticles. Different lowercase letters mean significant difference (Duncan, $p < 0.05$) of the particle charge in samples within the same digestion phases; Different capital letters mean significantly different (Duncan, $p < 0.05$) of a sample particle charge between digestion phase.

Fig. 4

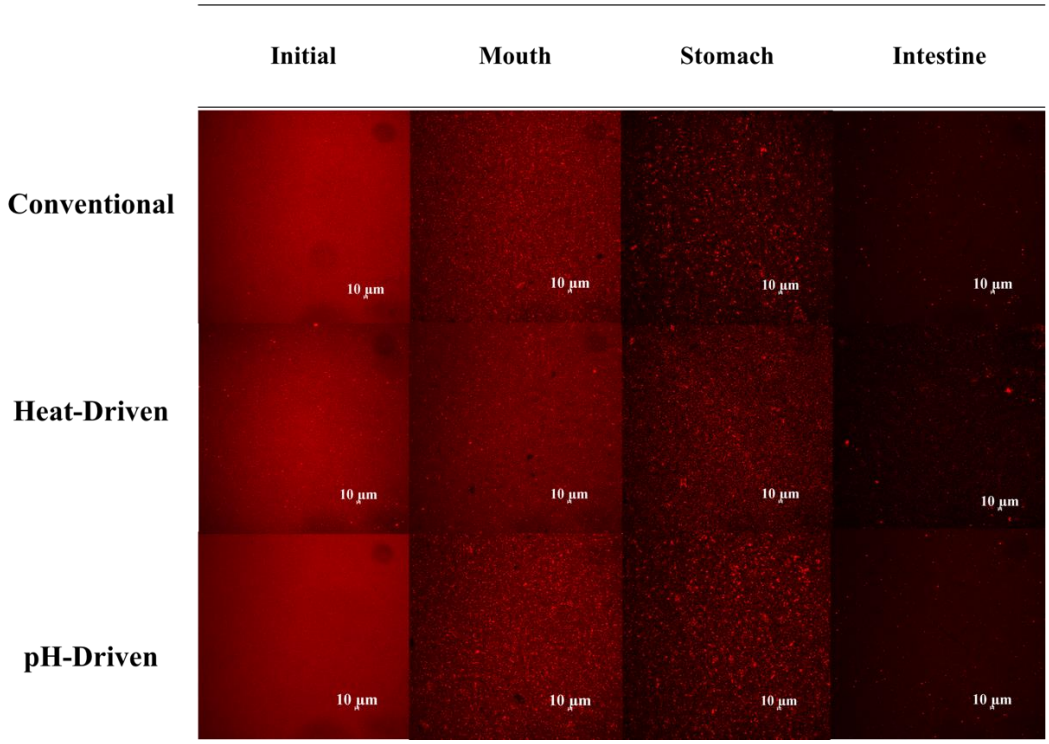

Fig. 4. Influence of simulated gastrointestinal condition on microstructure of the curcumin emulsion that prepared using different technics. The images were determined using confocal fluorescence microscopy with a scale length of 10µm, and the red regions represented the existing lipids

Fig. 5

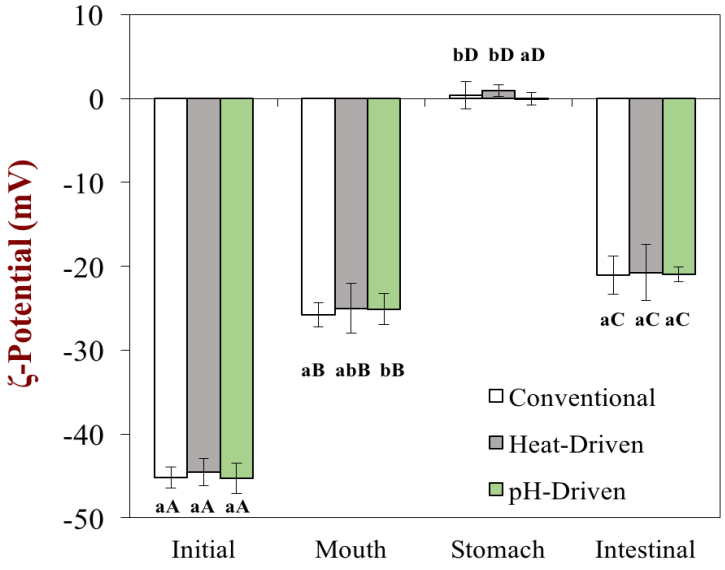

Fig. 5 Influence of simulated gastrointestinal condition on the particle charge of the curcumin loaded lipid nanoparticles. Different lowercase letters mean significant difference (Duncan, $p < 0.05$) of the particle charge in samples within the same digestion phases; Different capital letters mean significantly different (Duncan, $p < 0.05$) of a sample particle charge between digestion phase.

4.3.2 Gastrointestinal fate of commercial curcumin supplements

Curcumin supplements are already commercially available and are sold in many supermarkets, pharmacies, health food shops, and on-line retailers. These supplements come in a variety of physical forms, including capsules, pills, fluids, and powders. The precise physical form of the curcumin within a supplement has a major impact on its bioaccessibility and stability. For this reason, we measured the gastrointestinal fate of three curcumin supplements purchased from an on-line supplier: Nature Made (NM), Full Spectrum (FS) and Curcuwin (Win). The curcumin supplements from NM and Win were in a powdered form, whereas the one from FS was in a liquid form (contained inside capsules). The commercial curcumin samples

were removed from their capsules prior to testing and the capsules themselves were not used because they would interfere with the subsequent analysis.

4.3.2.1 Initial characteristics of curcumin supplements

Initially, the general properties of the three curcumin supplements used were established based on information reported on the manufacturers label and visual observations. The active ingredient in the NM supplement were reported to be a turmeric blend containing curcuminoids (47.5 mg), while the inactive ingredients were cellulose gel, gelatin, water, stearic acid, magnesium stearate, and silicon dioxide (in descending weight). These inactive ingredients have been reported to have a variety of functions in supplements, including acting as lubricants, suspending agents, stabilizers, and flow enhancers [203-206]. In addition, other functions have been reported for specific types of these inactive ingredients. Cellulose prolongs the shelf life of supplements by protecting powdered curcumin from oxygen, humidity, and enzymatic degradation [206]. Stearic acid and magnesium stearate act as emulsifying and solubilizing agents that can improve the water-dispersion and oral bioavailability of hydrophobic substances [204].

The active ingredient in the fluid FS supplement was reported to be curcuminoids, while the inactive ingredients were polysorbate 80, gelatin, and vegetable glycerin. Polysorbate 80, also known as Tween 80, is a synthetic non-ionic surfactant that can improve the water-dispersibility of curcumin by spontaneously forming nanoemulsions or microemulsions in aqueous gastrointestinal fluids [207]. Gelatin is a gel-forming protein used to form soft gel capsules that protect curcumin during storage and within the mouth, but then dissociate and release it within the stomach [208]. Glycerin acts as a cosolvent that facilitates the spontaneous formation of microemulsions and emulsions in gastrointestinal fluids [209].

The active ingredient in the Win supplement was reported to be curcuminoids, while the inactive ingredients were reported to be polyvinylpyrrolidone (PVP), cellulose, and mixed tocopherols. PVP is a synthetic water-soluble amphiphilic polymer that increases the water-dispersibility of curcumin by encapsulating it within small colloidal particles [210-212]. Cellulose functions as a stabilizer and lubricant that enhances bioactive stability and powder flowability [205, 206]. Mixed tocopherols are a natural antioxidant that inhibit the chemical degradation of active ingredients such as curcumin [7].

4.3.2.2 Digestibility on curcumin supplements

Each commercial curcumin formulation was passed through the same simulated GIT used to test the nanoemulsions and then the concentrations of curcumin in the mixed micelles and raw digest were measured. The bioaccessibility and stability of the curcumin in the commercial formulations was then calculated from this data. The initial amount of curcumin in each of the original commercial products was different: 8.8, 6.6 and 21.8% for NM, FS, and Win, respectively. For this reason, the samples were mixed with different levels of distilled water prior to being exposed to the simulated GIT so that each one contained the same final amount of curcumin (150 μg /g water) as in the nanoemulsions.

Analysis of the amount of digestible materials in the commercial supplements was carried out using the pH stat method. However, only a small volume of 0.25 M NaOH solution had to be added to maintain the samples at neutral pH throughout the small intestine phase (< 0.6 mL), which suggested that there was little or no digestible material present (data not shown). This would be expected because most of the inactive ingredients present in the supplements were indigestible. Presumably, the proteins in those samples that contained gelatin (NM and FS) had

already been digested by pepsin in the stomach phase before they reached the small intestine phase.

4.3.2.3 Properties mixed micelles and digest of commercial curcumin

The absolute amount of curcumin solubilized in the mixed micelles by the end of the small intestine phase decreased in the following order for the different supplements: Win >> FS > NM (Fig. 7). This effect can mainly be attributed to differences in the initial water-dispersibility of the products. A large amount of sediment was observed at the bottom of the test tubes containing the NM supplements throughout the *in vitro* study, whereas, no precipitate was observed for the FS and Win supplements (Fig. 8). This result suggests that the majority of curcumin from the NM supplements remained in the sediment and was not solubilized in the mixed micelles. The FS supplement had a significantly higher curcumin concentration in the mixed micelle phase than the NM supplement. This suggests that the presence of the non-ionic surfactant (polysorbate 80) increased the solubility of curcumin in the mixed micelles. The curcumin in the Win sample gave the highest curcumin concentration in the mixed micelles, which could be due to multiple reasons. First, PVP forms polymeric micelles that can encapsulate hydrophobic curcumin molecules and enhance their solubility in the mixed micelle phase [210, 212]. Second, mixed tocopherols act as an antioxidant that protects curcumin from chemical degradation within the intestinal environment [7]. Other studies have also reported that the stability and bioaccessibility of curcumin can be improved by co-encapsulating it with antioxidants in colloidal delivery systems [184, 211-213].

Interestingly, the total concentration of curcumin in the overall digest followed an opposite trend to that observed for the mixed micelles: NM > FS ≈ Win (Fig. 7). Initially, all the samples had the same initial curcumin concentration (150 μg/g), which suggests that some of the

curcumin had chemically degraded after exposure to the mouth, stomach, and small intestine phases. The relatively high concentration of curcumin in the digest for the NM sample may have been because it was insoluble and therefore more stable to chemical degradation (Fig. 8). Conversely, the curcumin in the FS and Win samples was trapped inside small colloidal particles with a relatively high specific surface area and therefore were more susceptible to chemical degradation due to the presence of reactive substances in the surrounding aqueous phase. It is known that curcumin is chemically unstable under neutral pH conditions, such as those found in the mouth and intestinal phases [3].

4.3.2.3 Bioaccessibility and Stability

The bioaccessibility and stability of the curcumin in the commercial products was calculated based on the curcumin concentrations in the initial, raw digest, and mixed micelle phases. The bioaccessibility of the curcumin from the Win (74%) sample was significantly higher than that from the FS (32%) and NM (10%) samples (Fig. 7). Again, this can be attributed to the ability of the amphiphilic polymer (PVP) used in this product to facilitate the formation of micelles that enhance the solubility of curcumin in the GIT. Conversely, the bioaccessibility of curcumin was lowest in the NM sample because it contained crystals that were difficult to solubilize. The stability of the curcumin was slightly higher in the NM product than in the FS and Win products, which can again be attributed to the fact that some of the curcumin was present in a crystalline form and was therefore more resistant to chemical degradation.

Fig. 6

a

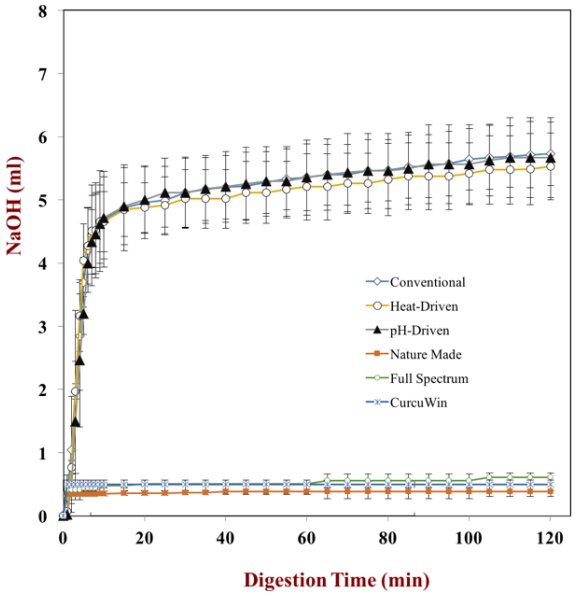

b

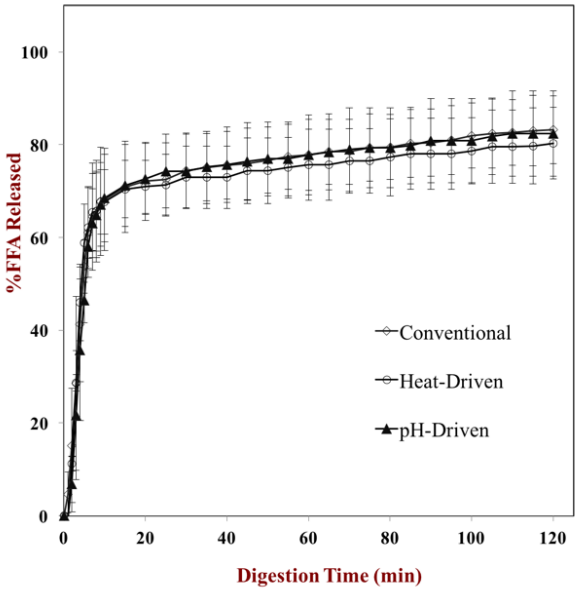

Fig.6. a. Influence of solid dispersion method on calculated free fatty acid release profile for curcumin-loaded lipid nanoparticles. **b.** Influence of lipid nanoparticle and commercial supplement on the NaOH titration profile.

Fig. 7

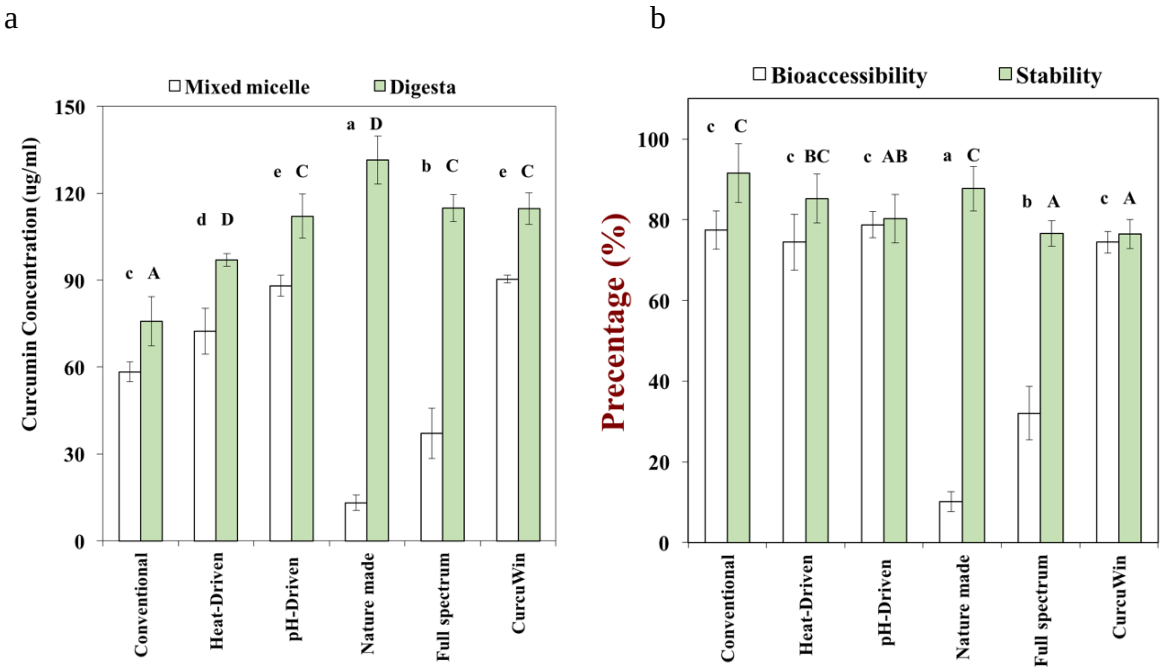

Fig 7 a. Influence of the lipid nanoparticle and commercial non-lipid contained supplements on the curcumin concentration in mixed micelles and raw digesta. b. Influence of lipid nanoparticle and commercial non-lipid contained supplements on the bioaccessibility and remnant of curcumin**.** Different lowercase letters and capital letters both mean significant difference (Duncan, $p < 0.05$) of the particle charge in samples within the same digestion phases;

4.3.4 Comparison of curcumin-loaded nanoemulsions and commercial supplements

Finally, the effectiveness of the curcumin-loaded nanoemulsions developed in this study was compared with the commercially available supplements for their ability to enhance the bioaccessibility and stability of curcumin. The absolute amount of curcumin solubilized in the mixed micelle phase decreased in the following order: Win ≈ pH-driven > heat-driven > conventional >> FS > NM. Thus, the nanoemulsions were better or similar to the commercial supplements at solubilizing the curcumin. This was probably because the triacylglycerols in the

lipid droplets were converted into monoacylglycerols and free fatty acids that increased the solubilization capacity of the mixed micelles. Conversely, the total amount of curcumin present in the digest tended to be higher for the commercial supplements: NM > Win ≈ FS ≈ pH-driven > heat-driven > conventional. This suggests that there was less chemical degradation of the curcumin in the commercial supplements, which may have been because the curcumin was in a crystalline form or because they contained antioxidants.

The bioaccessibility of curcumin calculated from this data decreased in the following order: pH-driven ≈ heat-driven ≈ conventional ≈ Win >> FS > NM. These results suggest that all the nanoemulsions gave bioaccessibilities that were as good as the best commercial formulation and better than the other two. The stability of the curcumin was fairly similar in both the nanoemulsions and the commercial supplements ranging from about 76 to 92%.

Fig. 8

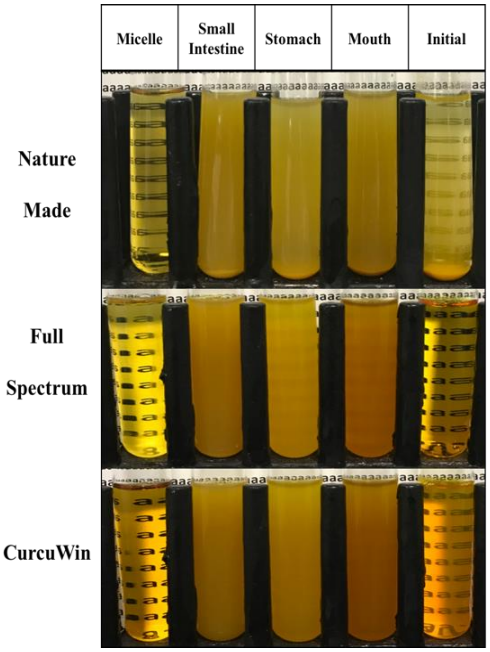

Fig. 8 Appearances of curcumin commercial products experiencing different stage of gastrointestinal tract.

4.4. Conclusion

In summary, this study demonstrated that curcumin nanoemulsions could be prepared using three different loading methods: conventional, heat-driven, or pH-driven. The pH-driven method was the simplest to implement and gave the highest encapsulation efficiency. This was because it did not involve any heating step, whereas the other two methods involved a step where the curcumin was held at an elevated temperature either in oil or an emulsion. The curcumin nanoemulsion prepared by the pH-driven method gave a significantly higher curcumin concentration in the mixed micelles phase after exposure to a simulated GIT. All the nanoemulsions developed in this study gave bioaccessibilities that were similar to those of the best commercial formulation tested. However, our nanoemulsions were formulated entirely from natural ingredients, which may be beneficial for some consumer applications.

It should be noted that the different curcumin formulations were only tested using a relatively simple static *in vitro* gastrointestinal model. This model cannot accurately simulate the complex events occurring within the human GIT, particularly metabolism carried out by Phase I and Phase II enzymes and absorption within the small intestine and colon. Future studies should therefore focus on testing the different formulations using more realistic animal or human feeding studies.

Chapter 5

5. Impact of curcumin delivery system format on bioaccessibility: nanocrystals, nanoemulsion droplets, and natural oil bodies

5.1. Introduction

Turmeric is commonly used in Asian cuisine as a natural pigment and spice due to its distinctive yellow-orange color and unique flavor profile [214]. It has also been utilized for thousands of years as a therapeutic agent in traditional Chinese and Indian medicine [215, 216]. Curcumin is one of the principal bioactive compounds found in turmeric and is claimed to exhibit a range of health benefits, including the ability to prevent or treat cancer, depression, diabetes, obesity, pain, and stroke [150, 217]. Many researchers are now using the modern techniques and approaches of science and biomedicine to determine the molecular basis of its effects and to establish the veracity of these health claims. The results of mechanistic studies, mainly carried out in laboratories, suggest that curcumin does have antioxidant, anti-inflammatory, and antimicrobial properties, as well as modulating biochemical pathways that influence our health status [150, 218]. The findings from randomized clinical trials (RCTs), however, are inconclusive, with some suggesting that consumption of curcumin has beneficial effects and others not [219].

There are numerous challenges that food formulators face when trying to incorporate curcumin into functional foods and beverages, which are associated with its strong color, low water-solubility, poor chemical stability, and low bioavailability [220]. These same factors may also contribute to the inconsistent results obtained in clinical trials of curcumin's efficacy, since the solubility, stability, and bioavailability of curcumin are rarely measured or controlled in these

studies [221]. Effective delivery systems are therefore needed to encapsulate and protect curcumin so that it can be successfully introduced into commercial foods and beverages in a bioactive form [47].

Many different kinds of curcumin delivery system have been developed, including micelles, nanoemulsions, emulsions, liposomes, biopolymer nanoparticles, microgels and dietary fibers, which have been reviewed in detail elsewhere [47, 222-224]. Each of these systems has its own benefits and limitations for specific applications, which are influenced by numerous factors, including the ease of manufacture, cost, robustness, physicochemical properties, sensory attributes, loading capacity, and bioavailability [225]. Curcumin can be loaded into the colloidal particles used in delivery systems in a variety of ways. For instance, in the case of emulsions, curcumin can be loaded into the oil phase before homogenization or incorporated into the oil droplets after homogenization. Recently, a simple low-cost method has been developed to load curcumin into preformed colloidal particles, which is based on the pH-dependence of its water-solubility [226]. Curcumin is non-charged at low pH values (< pH 8) and has a low water-solubility but it is negatively charged at higher pH values and so has a high water-solubility. The pH-shift method utilizes this phenomenon to load curcumin into the hydrophobic interiors of colloidal particles, such as casein micelles [226], biosurfactant micelles [227, 228], and emulsions [229]. Typically, the curcumin is dissolved in a strongly alkaline solution which is then mixed with an acidic colloidal dispersion. The reduction in the water-solubility of the curcumin at the lower pH drives it into the interior of the colloidal particles.

In the current study, we investigated the possibility of using the pH-shift method to create different kinds of curcumin-loaded delivery systems: curcumin nanocrystals: curcumin-loaded oil bodies (soy milk); and curcumin-loaded nanoemulsions. The formation, physicochemical

stability, and gastrointestinal fate of these delivery systems was then measured, as well as their impact on the bioaccessibility of the encapsulated curcumin. This study shows that the pH-shift approach is a simple and versatile method that can be used to load curcumin into a variety of different delivery systems, including plant-based milks and nanoemulsions.

5.2. Material & Methods

5.2.1 Materials

Corn oil (Mazola, ACH Foods, Cordova, TN) and soymilk (Dairy-free Soy Creamer, Silk, Broomfield, CO) were purchased from a local supermarket and used without further purification. Curcumin (purity 95%) was obtained from Tokyo Chemistry Industries Company (Tokyo, Japan). The following chemicals were purchased from the Sigma-Aldrich Chemical Company (St. Louis, MO): mucin from porcine stomach (M2378-100G); pepsin from porcine gastric mucosa (P7000-25G); lipase from porcine pancreas pancreatin (P8096-100G); porcine bile extract (B8831-100G); sodium hydroxide (SS266-4L); sodium chloride (S640-3); ammonium nitrate (A9642-500G); potassium phosphate (P285-500); Nile Red (N3013-100MG); potassium citrate in basic monohydrate (P1722-100G); uric acid sodium salt (U2875-5G); urea (51456-500G); lactic acid sodium salt (71718-10G); and, hydrochloric acid (A144212-2.5L). Potassium chloride (P217-500G) and calcium chloride (C1016-500G) were purchased from Fisher Scientific (Fair Lawn, NJ). Quillaja saponin (Q-Naturale® 200) was provided by Ingredion Inc. (Westchester, IL). Chloroform and other reagents were all of analytical grade.

5.2.2 Preparation protocol

The pH-driven method was used to produce three different kinds of colloidal delivery system: curcumin nanocrystals; curcumin-loaded lipid droplets; and, curcumin-loaded oil bodies. This method required the use of a stock alkaline curcumin solution (6 mg/g), which was prepared

by dissolving powdered curcumin into sodium hydroxide solution (0.1 N, pH 12.5) for 2 min in the dark at room temperature. The behavior of the delivery systems was compared to that of a control, which consisted of curcumin powder dispersed directly into water. All systems were prepared so they had the same final curcumin concentration: 0.25 mg/g.

5.2.2.1 Control

The curcumin control was prepared by dispersing 7.5 mg of curcumin powder into 30 g of double distilled water and then stirring.

5.2.2.2 Curcumin nanocrystals

Suspensions of curcumin nanocrystals in water were prepared using the pH-driven method. The stock alkaline curcumin solution (6 mg/g) was diluted with double distilled water to reach a final concentration of 0.25 mg curcumin per g liquid. The resulting mixture was then immediately adjusted to pH 6.8 and stirred for 10 min in the dark at ambient temperature, which led to the spontaneous formation of curcumin nanocrystals.

5.2.2.3 Curcumin-loaded lipid droplets

Curcumin-loaded nanoemulsions were also prepared using the pH-driven method. The nanoemulsions used consisted of 10% (w/w) corn oil and 90% (w/w) aqueous emulsifier solution (2% Q-Naturale with 5 mM phosphate buffer solution, pH 6.8). Initially, a coarse emulsion was prepared using a high-shear mixer to blend the oil and aqueous phases together for 2 min (M122.1281-0, Biospec Products, Inc., ESGC, Switzerland). These systems were then passed five times through a high-pressure homogenizer (Microfluidizer M110Y, Microfluidics, Newton, MA) with a 75-μm interaction chamber (F20Y) at an operational pressure of 12,000 psi (83 MPa). The resulting nanoemulsions were then mixed with the stock alkaline curcumin solution and the mixture was immediately adjusted to pH 6.8 and stirred for 10 min in the dark at ambient

temperature. Double distilled water was used to dilute the curcumin-loaded nanoemulsions so the final system contained 5% oil and 0.25 mg of curcumin per g emulsion.

5.2.2.4 Curcumin-loaded oil bodies

Curcumin was loaded into commercial soymilk, which consists of soy oil bodies dispersed within a compositionally complex aqueous solution, using a similar protocol as used to load the nanoemulsions. A known amount of stock curcumin alkaline solution (1.25g per 30 mL soymilk) was mixed with soymilk and then the mixture was immediately adjusted to pH 6.8. The resulting mixture was then stirred for 10 min in the dark at ambient temperature. The final system was diluted with double distilled water to reach a final concentration of 5% oil and 0.25 mg curcumin per g soymilk.

The composition of the soymilk reported on its label was: soymilk (filtered water, soybeans), cane sugar, palm oil, maltodextrin, contains 2% or less of soy lecithin, natural flavor, tapioca starch, locust bean gum, dipotassium phosphate.

5.2.3 Optical properties

The optical properties of the different systems were characterized using a colorimeter and digital camara. The instrumental colorimeter (ColorFlex EZ 45/0-LAV, Hunter Associates Laboratory Inc., Virginia, USA) was used to determine the color coordinates: L^* (darkness / lightness); a* (redness / greenness); and b^* (yellowness / blueness). A test sample (10 mL) was placed in a petri dish and illuminated with a D65-artificial daylight (10° standard angle) with a black background. The final values were obtained by averaging three replicate measurements per sample.

5.2.4 Simulated gastrointestinal tract model

A stimulated gastrointestinal tract (GIT), designed to mimic mouth, stomach, and small intestine stages of the human gut, was used to analyze the potential gastrointestinal fate of the curcumin-loaded delivery systems. An equal amount of each sample (30 mL), which contained 0.25 mg of curcumin per gram of sample, was transferred into a glass beaker for analysis. The nanoemulsion and soymilk contained the same level of oil (5% w/w). This method was slightly modified from previous study [87, 192, 230]

5.2.4.1 Solution preparation

For the oral phase, the artificial saliva stock solution (ASSS) and the stock simulated saliva fluid (SSF) were prepared two days and one day before the study, respectively. The ASSS was produced by dispersing sodium chloride (1.594 g/L), ammonium nitrate (0.328 g/L), potassium phosphate (0.636 g/L), potassium chloride (0.202 g/L), potassium citrate (0.308 g/L), uric acid sodium salt (0.021 g/L), urea (0.198 g/L), and lactic acid sodium salt (0.146 g/L) into double distilled water (1 L) at 4°C overnight. A stock simulated saliva fluid (SSF) was prepared by mixing 90 mg of mucin into 30 g of ASSS and storing the mixture at 4°C overnight before carrying out the digestions.

For the gastric phase, a simulated gastric fluid (SGF) and simulated gastric fluid work solution (SGFWS) were prepared. The SGF was prepared by fully dissolving sodium chloride (2 g/L) and hydrochloric acid (83.3 mM/L) into double distilled water at ambient temperature and then stored at 4°C overnight before being used. The SGF was warmed to room temperature and then the SGFWS was prepared by adding pepsin (3.2 mg/g) into the SGF with continuous stirring for 30 min.

For the small intestinal phase, stock simulated intestinal fluids (SIF), bile salt solution, and pancreatic lipase solution were prepared. The stock SIF was produced by dissolving calcium chloride (5.5 g) and sodium chloride (32.87 g) in 150 ml in the double distilled water. The bile salt solution was prepared by continuously stirring porcine bile extract (53.57 mg/mL) with phosphate buffer (5 mM, pH 7) overnight at room temperature. Both stock solutions were stored at room temperature before being used. The lipase solution was prepared by mixing 0.9 mg of pancreatic lipase into 5 ml phosphate buffer (pH 7) immediately before adding to the sample.

5.2.4.2. GIT study

Curcumin-loaded samples were passed through stimulated mouth, stomach, and small intestine phases. To stimulate the mouth phase, the initial sample (30 mL) and SSF (30 mL) were preheated to 37 °C and transferred into a glass beaker. The mixture was adjusted to pH 6.8 and placed into a shaking incubator (Innova Incubator Shaker, Model 4080, New Brunswick Scientific, New Jersey, USA) with an operation of 100 rpm and 37 °C for 2 min. 40 ml of the "bolus" sample collected from the mouth phase was then mixed with preheated SGFWS (40 mL) and adjusted the pH to 2.5. The resulting mixture was agitated for 2 hours using the same incubator shaker. Finally, the "chyme" (60 mL) samples collected from the stomach phase were transferred to a fresh beaker and incubated in a water bath set at 37 °C. The pH of the sample was adjusted to neutral (pH 7.0) to create a small intestinal environment. Preheated SIF (3 mL) and bile salt solution (7 mL) were then added into the sample. The pH was adjusted back to neutral. Freshly prepared pancreatic lipase (5 mL) was then added to the mixture and the pH was again altered back to neutral. An automatic titration unit (Metrohm, USA Inc.) was used to monitor and maintain the sample at pH 7.0 by addition of sodium hydroxide solution (0.25 M).

The volume of NaOH (V_{NaOH}) required to neutralize the solution was used to calculate the percentage of free fatty acids released:

$$FFA(\%) = 100 \times \frac{V_{NaOH} m_{NaOH} M_{lipid}}{2\ W_{liquid}}$$

Here, m_{NaOH} is the molarity of sodium hydroxide solution (0.25 M); M_{lipid} is the molecular weight of the oil used; and, W_{lipid} is the weight of the oil used in the digestion system (gram). This equation assumes that two fatty acids are released per triglyceride molecule if the reaction goes to completion.

5.2.5 Particle characterization

Two light scattering instruments were used to determine the particle characteristics during digestion. The mean particle diameter and particle size distribution were analyzed using a laser light scattering instrument (Mastersizer 2000, Malvern Instruments Ltd., Malvern, Worcestershire, U.K.). The ζ-potential values were determined using a particle electrophoresis device (Zetasizer Nano, Malvern Instruments, Worcestershire, U.K.). pH-adjusted double distilled water was used to dilute the samples collected from the mouth, stomach, and small intestinal phases, which had the same pH as the sample.

5.2.6 Microstructure analysis

The microstructure of the samples was characterized using light and confocal scanning fluorescence microscopy (Nikon D-Eclipse C1 80i, Nikon, Melville, NY, USA). The properties of the crystalline curcumin in the initial samples was determined using light microscopy with a cross-polarized lens (C1 Digital Eclipse, Nikon, Tokyo, Japan). Confocal scanning laser microscopy with a 200-fold magnification (20 × objective lens, 10× eyepiece lens) was used to determine the location of the oils and proteins in the samples. Nile red (1 mg/mL ethanol) and

FITC (1mg/mL DMSO) dye solutions were used to stain the oils (red) and proteins (green) in the samples, respectively. The microstructure images were taken and analyzed using analysis software (NIS-Elements, Nikon, Melville, NY).

5.2.7 Determination of curcumin concentration

A UV-visible spectrophotometer (Cary 100 UV−Vis, Agilent Technologies, Santa Clara, CA, USA) was used to determine the curcumin concentration in the initial samples, mixed micelle fraction, and total digest fraction. An organic solvent, chloroform, was used to extract curcumin from each sample by centrifuging at 3000 rpm for 10 min. The hydrophobic curcumin was transferred into the chloroform layer. The curcumin concentration was then determined using the UV-Vis spectrophotometer at a wavelength of 419 nm, and calculated based on a standard curve prepared by measuring the absorbance of the known curcumin amounts (Supplementary information Fig. 1).

5.2.7.1. Encapsulation Efficiency

The encapsulation efficiency of each delivery systems was determined using the following expression:

$$\textit{Encapsulation Efficiency} = 100 \times C_{encapsulated} / C_{initial}$$

Here $C_{initial}$ and $C_{encapsulated}$ are the concentrations of curcumin initially added to the system and that was encapsulated within the delivery system.

5.2.7.2. Bioaccessibility and Stability

After the small intestine phase, the samples were divided into two fractions: a micelle sample and a total digest sample. The micelle sample was transferred into a centrifuge tube and centrifuged (18,000 rpm, 25 °C) for 50 min (Thermo Scientific, Waltham, MA). The resulting mixed micelle fraction was then collected as the clear supernatant of the samples. The total

digest sample and the initial sample were analyzed without any further processing. The concentration of curcumin in the mixed micelle ($C_{micelle}$) and total digest (C_{digest}) samples then calculated using the spectrometry that described on 2.7 and were used to calculate the *bioaccessibility* and *stability* of the curcumin-loaded samples. Here, the concentration of curcumin within the mixed micelle phase was represents the amount of curcumin that has been solubilized with in the micelle vesicle and potential available for absorption. The concentration of curcumin within the digest phase means the total amount of curcumin remained after digestion. The *bioaccessibility* was taken to be the percentage of curcumin solubilized in the small intestine that was solubilized within the mixed micelle phase, whereas the *stability* was taken to be the percentage of total curcumin that remained in the small intestine:

$$Bioaccessibility\ (\%) = 100\ \times \frac{C_{micelle}}{C_{digest}}$$

$$Stability(\%) = 100\ \times \frac{C_{digest}}{C_{initial}}$$

The stability therefore provides information about the potential degradation of curcumin within the simulated GIT.

5.2.8 Statistical analysis

Each experiment was repeated on at least three freshly prepared samples and the mean and standard deviation were calculated from these values. Statistical differences among samples were determined using statistical analysis software (SPSS, IBM Corporation, Armonk, NY, USA), and significant difference was considered to be $p < 0.05$.

5.3. Results & Discussion

5.3.1 properties of initial curcumin-containing food matrices

Initially, the pH-driven method was used to form curcumin nanocrystals, curcumin-loaded oil droplets, and curcumin-loaded oil bodies.

5.3.1.1 Encapsulation efficiency

The initial concentrations (C_I) of curcumin in the three samples produced using the pH-driven method were fairly similar to each other (Table 1), being around 230 μg/mL sample. The fact that the curcumin level in the samples was slightly less than the starting value (250 μg/mL) can be attributed to some curcumin degradation during sample preparation. Previous studies have reported that a small amount of curcumin is lost when it is solubilized in the strong alkaline solutions used in the pH-driven method [92, 93]. These values correspond to an encapsulation efficiency (EE) of around 93%, which is relatively high for colloidal delivery systems. In addition, the commercial soy milk contains lecithin and palm oil that also helped to encapsulate curcumin within the soymilk. Therefore, Further study could force on using pure soy oil bodies to investigate their encapsulation efficiency. Overall, the pH-driven method was successfully loaded curcumin within the oil-based emulsion system and complex-formulated commercial soymilk with a high encapsulation efficiency.

Table 1

	Control	**Nanocrystals**	**Nanoemulsions**	**Oil Bodies**
CI (μg/mL)	250.00 ± 0 [a]	233.00± 7.16 [b]	233.28± 11.10 [b]	234.58± 9.01[b]
L*	6.64 ±0.80 [a]	25.81 ± 0.24 [b]	84.41 ±0.17 [c]	82.41± 0.10 [c]
a*	2.96 ± 0.74 [c]	-2.62 ± 0.13 [c]	-6.85 ± 0.06 [b]	-8.01 ± 0.09 [a]
b*	7.15 ± 1.29 [a]	38.80 ± 0.75 [b]	80.48 ± 1.12 [c]	80.62 ± 0.48 [c]
ζ- potential (mV)	-	-	-55.75 ± 1.46 [a]	-30.28 ± 1.87 [b]
D32 (μm)	-	-	0.18 ± 0.02 [b]	0.41 ± 0.01 [a]

Table 1. The initial curcumin concentration (C_I), loading capacity, tristimulus color coordinates (*L*, a*, b**), mean particle diameter (D_{32}) and electrical characteristics (ζ- potential) of curcumin-loaded samples. Samples designated with different letters are significantly different (Duncan, $p < 0.05$).

5.3.1.2 Curcumin structure and physical stability

The structure and location of the curcumin within the different samples were investigated using optical microscopy and digital photography (Fig. 1). The microscopy images showed that the control sample contained relatively large curcumin crystals (Fig. 1b), while the photographs showed that these crystals rapidly sediment to the bottom of the test tubes (Fig. 1a). Presumably, this phenomenon occurred because the curcumin crystals were relatively large and denser than water. Consequently, they were particularly prone to gravitational separation in the form of sedimentation.

As expected, the curcumin nanocrystals formed by mixing the alkaline curcumin solution with water were much smaller than the curcumin crystals in the control (Fig. 1b), highlighting the ability of the pH-driven method to generate minute nutraceutical crystals. The nanocrystals appeared to have thin needle-like structures that tended to associate with each other, probably because of hydrophobic attraction. The curcumin nanoparticle suspensions were relatively stable to gravitational separation immediately after fabrication (Fig 1a), forming a cloudy dispersion with a relatively uniform appearance. Even so, when they were allowed to stand for 2 hours an orange sediment was observed at the bottom of the test tubes (Fig. 1a), suggesting that sedimentation still occurred, albeit at a slower rate than for the control. This phenomenon can be attributed to the weaker gravitational forces acting on the nanocrystals.

Both the curcumin-loaded nanoemulsion and soymilk formed creamy yellow-orange dispersions with a uniform appearance, indicating that the oil droplets and oil bodies were stable to gravitational separation. No curcumin crystals were seen at the bottom of the test tubes or in the optical microscopy images when these samples were observed by visual inspection and optical microscopy (Figs. 1a and 1b). These results suggest that the pH-driven method was

successful in loading the curcumin into the hydrophobic interiors of the lipid droplets and oil bodies.

5.3.1.3 Color coordinates

The color of the samples was quantified against a black background using an instrumental colorimetry (Table 1). Here, L^* is the light/dark axis, which varies from pure black (0) to pure white (100); a^* is the red-green axis, which varies from strongly red (positive) to strongly green (negative); and, b^* is the yellow-blue axis, which varies from strongly yellow (positive) to strongly blue (negative).

After stirring, the control, which consisted of curcumin powder dispersed in water, had a low lightness (L^*= +6.64), a moderate yellowness (b^*= +7.2) and a slight redness (a^*= +2.96) (Table 1). These color parameters can be attributed to the yellow-orange color brought by the curcumin crystals. The suspension of curcumin nanocrystals had a higher lightness (L^*= +25.81) and yellowness (b^*= +38.80) than the control, and had a slight greenness (a^*= -2.62) rather than redness (Table 1). This effect can be attributed to the fact that the curcumin crystals were much smaller in this sample and so they scattered light more strongly and at different wavelengths [231]. As a result, more light was reflected from the surface of the samples, leading to a higher lightness. Moreover, the scattered light encountered a higher number of curcumin crystals and so there was a greater degree of selective absorption of the light waves, leading to a more intense yellow color and a change from reddish to greenish.

Interestingly, the curcumin-loaded nanoemulsions and oil bodies prepared using the pH-driven method had very similar color coordinates (Table 1). They both had relatively high L^* values, strongly positive b^* values, and slightly negative a^* values, which suggests they had a bright yellow color with a tinge of green. These effects can be attributed to the ability of the lipid

droplets and oil bodies to scatter light waves strongly, as well as to the ability of the dissolved curcumin molecules to selectively absorb light waves [231, 232].

5.3.1.4 Particle characteristics

It was not possible to determine the characteristics of the particles in the samples containing curcumin crystals using light scattering because they were highly non-spherical, having a needle-like structure. One of the assumptions in the analysis of the data for both static and dynamic light scattering instruments is that the particles are spherical. For this reason, only the particle characteristics of the curcumin-loaded lipid droplets and oil bodies were measured.

The static light scattering measurements indicated that the nanoemulsions had a monomodal particle size distribution (PSD) and contained small lipid droplets, *i.e.*, $d_{32} < 200$ nm (Table 1 and Fig. 2). This indicates that the combination of emulsifier and microfluidizer used to prepare the nanoemulsions was effective at generating small lipid droplets. The oil bodies in the soymilk had a bimodal PSD and contained somewhat larger particles ($d_{32} > 400$ nm) than those found in the nanoemulsions. The relatively large particles found in this commercial product are probably because the size of the oil bodies is determined by their natural origin, rather than homogenization. The broad particle size distribution may also have been because the soymilk contains a range of different types of colloidal particles and biopolymers, which could all have contributed to the light scattering signal.

As mentioned earlier, both the lipid droplets and oil bodies exhibited good stability against gravitational separation during storage. According to Stokes's Law, the velocity that a spherical particle moves through a fluid decreases as the particle size decreases, the fluid viscosity increases, and the density contrast decreases [128, 233]. The primary reason that the curcumin-loaded nanoemulsions were stable to creaming is the small size of the lipid droplets

then contain. Conversely, the good stability of the curcumin-loaded the soymilk may have been because of the fairly small size of the oil bodies, as well as the increase in viscosity associated with the tapioca starch and locust bean gum used as thickening agents in this product.

The surface potential of the lipid droplets in the nanoemulsions (ζ = -55.8 mV) and the oil bodies in the soymilk (ζ = -30 mV) were both strongly negative (Table 1). A high surface potential is important for inhibiting particle aggregation in colloidal dispersions since it leads to a strong electrostatic repulsion [128, 233]. The high negative charge on the lipid droplets in the nanoemulsions was attributed to the fact that they were coated with a layer of quillaja saponins, which are known to be strongly anionic due to the presence of carboxylic acid groups on their surfaces. The high negative charge on the oil bodies in the soymilk may have been due to the fact that they are naturally coated by a layer of phospholipids and proteins that are anionic at neutral pH [234, 235].

The microstructure images of the nanoemulsion and soymilk further demonstrated the good aggregation stability of the lipid droplets and oil bodies (Figs.1 b and 5). Both confocal fluorescence and light microscopy images of the curcumin-loaded colloidal systems indicated that no aggregation occurred. However, the soymilk was seen to contain particles that had a broad range of sizes (Fig 1.b), which agrees with the PSD measurements. The wide range of particles in the soymilk may have been because of the natural variation in oil body dimensions [236] or because it contained a range of other types of colloidal particles and biopolymers, such as starch and locust bean gum.

Fig.1

a

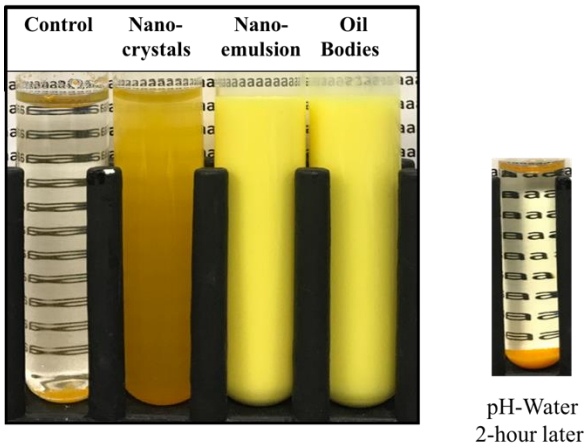

b

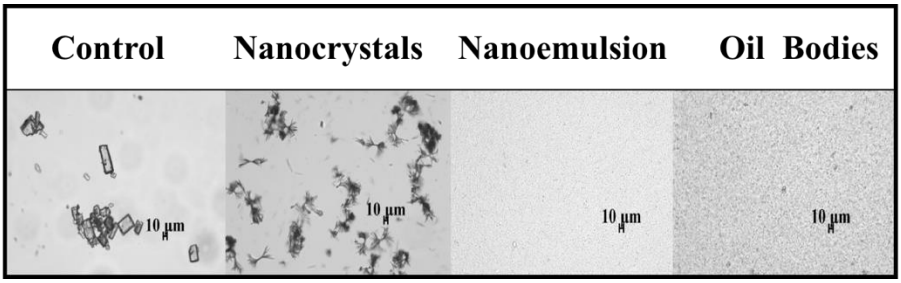

Fig. 1. (a) Appearances and (b) light microscopy images of curcumin-containing samples. The small bars in the images represent a length of 10 μm.

Fig. 2

a

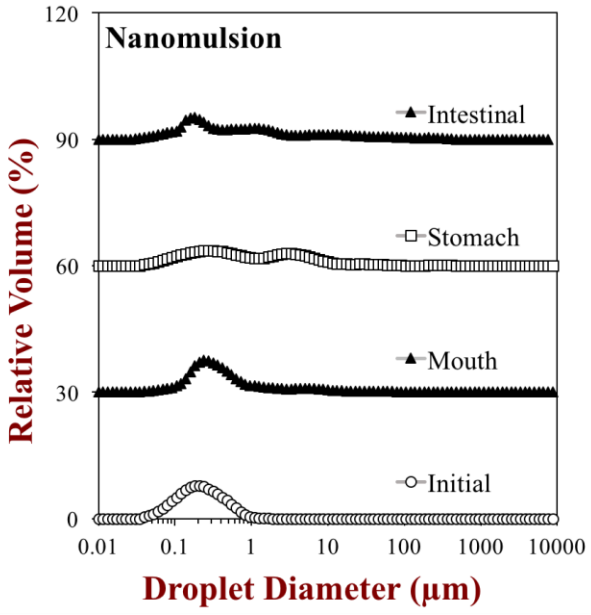

b

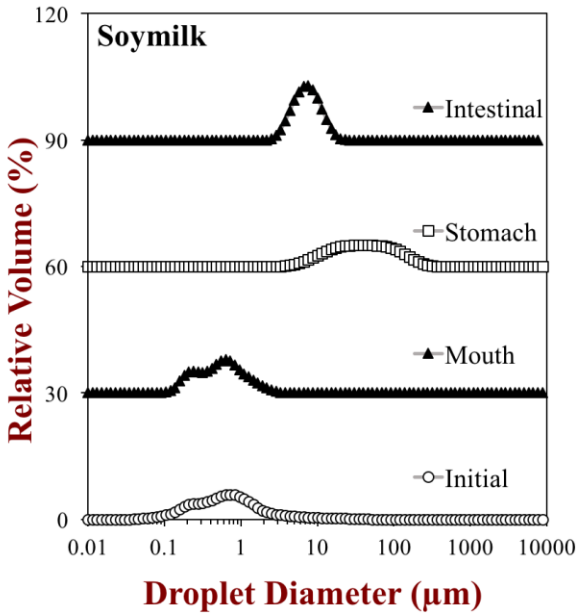

Fig. 2 Particle size distribution of curcumin-loaded emulsion and oil-bodies prepared using pH-driven method after undergo the different stages of a simulated gastrointestinal tract conditions.

5.3 Gastrointestinal fate of delivery systems

The curcumin-loaded nanoemulsion and soymilk samples were sequentially passed through artificial mouth, stomach, and small intestinal fluids to simulate passage through the human gut. Changes in the structural and physical properties of the samples were measured after exposure to each gastrointestinal stage. The two samples containing curcumin crystals dispersed in water, namely the control and nanocrystal samples, were not analyzed in these experiments because of difficulties in reliably characterizing their properties using light scattering techniques.

5.3.1. Influence of the GIT on particle properties

Oral phase: After exposure to the oral phase, there was a small but significant increase in the mean diameter of the particles in the nanoemulsions (Figs. 2 and 3). In addition, the

magnitude of their negative charged decreased appreciably (Fig. 4). On the other hand, there appeared to be little change in the structural organization of the lipid droplets in the confocal microscopy images (Fig. 5). These results suggest that there was a small amount of lipid droplet aggregation under simulated oral conditions, which can be attributed to depletion or bridging flocculation caused by the mucin in the artificial saliva [197, 198]. In addition, there may have been some electrostatic screening of the surface charge by electrolytes in the artificial saliva. In contrast, there was little change in the mean particle size or surface potential of the oil bodies in the soymilk after exposure to the simulated oral phase (Figs. 2 to 4). This suggests that the oil bodies may have been more resistant to aggregation in the artificial saliva, possibly because the mucin interacted with their surfaces less strongly [198, 237, 238]. The confocal fluorescence microscopy images suggest that there may have been a small amount of clumping of the oil bodies in the oral phase (Fig. 5), but presumably the flocs formed were so weak that they were easily disrupted when the samples were diluted for the light scattering measurements.

Stomach phase: The nanoemulsions and soymilk behaved very differently under simulated gastric conditions. There was no significant change in the mean particle diameter of the nanoemulsions when they moved from the oral to stomach phase but a huge increase in the size of the particles in the soymilk (Fig. 3). The PSD measurements and confocal fluorescence images indicated that there was only a small amount of lipid droplet aggregation in the nanoemulsions but extensive clumping of the oil bodies in the soymilk (Figs. 2 and 5).

The surface potential of the particles in both the nanoemulsions and soymilk were close to zero after exposure to the small intestine conditions (Fig. 4). This effect can be attributed to a number of physicochemical phenomena occurring in the stomach phase. First, any carboxylic acid and amino groups on the saponins, phospholipids, and proteins would have become

protonated in the highly acidic environment of the gastric fluids, leading to a reduction in negative charge and increase in positive charge. Second, the electrolytes in the gastric fluids would have reduced the magnitude of the surface potential by screening the electrostatic interactions. Third, the anionic mucin molecules arising from the artificial saliva may have bound to cationic patches on the surfaces of the particles.

The extensive aggregation of the oil bodies in the soymilk observed under gastric conditions may have been because the soy proteins on their surfaces became positively charged, thereby promoting bridging flocculation by anionic mucin molecules in the surrounding aqueous fluids. Moreover, there would have been little electrostatic repulsion between the oil bodies because of their very low surface charge. Hence, the oil bodies may also have aggregated due to the van der Waals and hydrophobic attraction between them [239, 240]. In addition, the proteases (pepsin) in the gastric fluids may have hydrolyzed the proteins at the surfaces of the oil bodies, thereby reducing their aggregation stability [87]. Interestingly, the saponin-coated lipid droplets in the nanoemulsions were relatively stable to aggregation in the gastric fluids (Figs. 2, 3 and 5) even though they only had a very low surface potential (Fig. 4). This suggests that the saponin molecules formed a coating around the lipid droplets that was resistant to disruption in the gastric fluids. Furthermore, this coating may have inhibited extensive aggregation because it generated a strong steric repulsion between the droplets. The good gastric stability of saponin-coated lipid droplets has also been reported in previous studies [241, 242].

Small intestine phase: After incubation in the artificial intestinal fluids, the particles in the nanoemulsions remained relatively small (Figs. 2, 3 and 5). On the other hand, most of the large aggregates observed in the stomach phase broke down when the soymilk was incubated in the intestinal fluids. After exposure to lipase, there is likely to be many different kinds of

colloidal particles present in the digest, including micelles, vesicles, calcium soaps, and undigested macronutrients, which all contribute to the light scattering signals used to measure the particle size and charge. The confocal microscopy images also showed that both samples contained a wide range of different sized particles.

The particles in the digests arising from the nanoemulsions (-68 mV) and the soymilk (-49 mV) had a strong negative charge. This effect can be attributed to the fact that many of the constituents in the digestion are anionic at neutral pH, including the bile acids, free fatty acids, saponins, and peptides.

Fig. 3

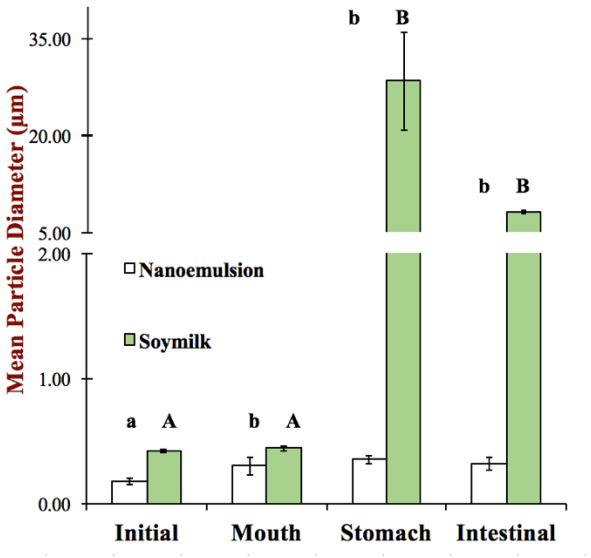

Fig.3 The Mean particle diameter (d_{32}) of the curcumin-loaded emulsion and oil-bodies under exposure to the simulated gastrointestinal tract model. Both Different lowercase and capital letters represent significant different (Duncan, $p < 0.05$) of the particle diameter between the same digestion phases

Fig. 4

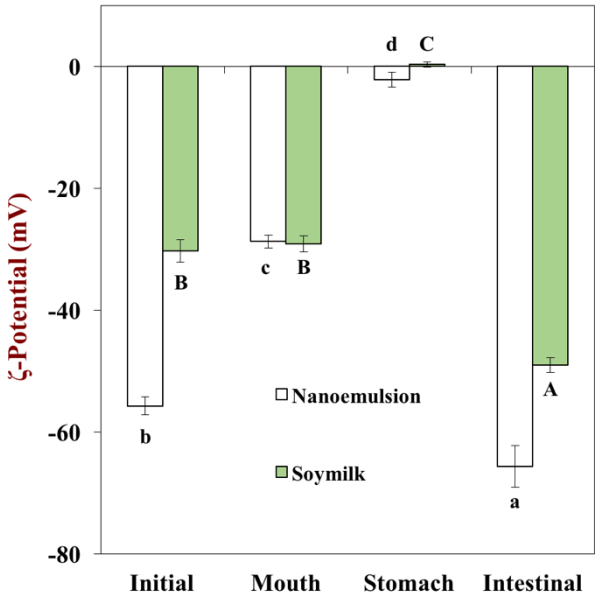

Fig. 4 influence of stimulated gastrointestinal tract models on the surface charge of the curcumin loaded nanoemulsion and oil-bodies. Both Different capital and lowercase letters mean significant difference (Duncan, $p < 0.05$) of the particle charge in samples between the same digestion phase;

Fig. 5

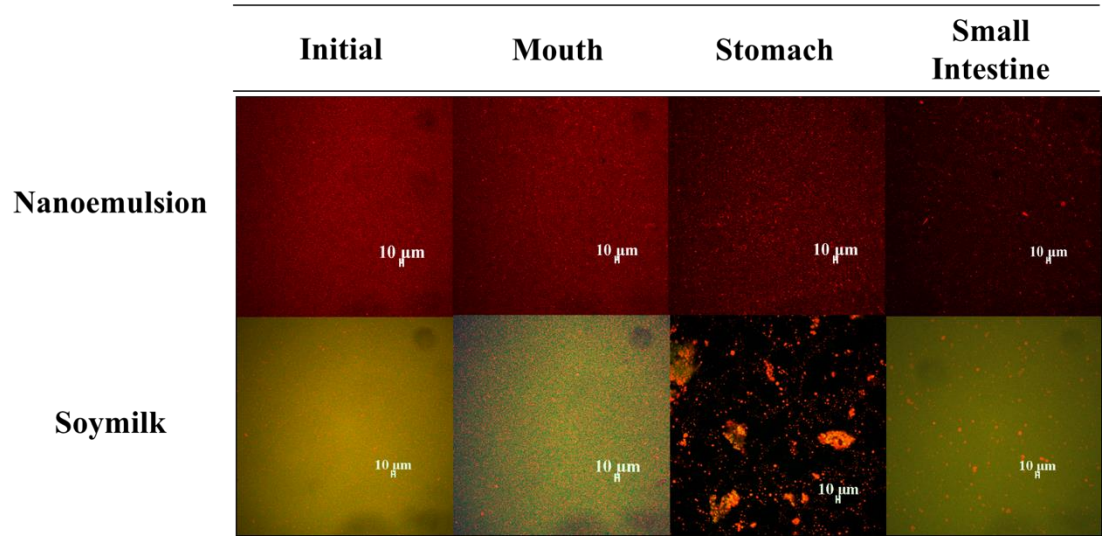

Fig. 5. The microstructure of the curcumin-loaded nanoemulsion and oil bodies under exposure to gastrointestinal condition. the confocal microscope was used to obtain the photo with fluorescent dye and a scale length of 10 μm. The red regions represent lipid and green means the protein

5.3.2. Lipid digestion profiles

The digestion of the components in the different delivery systems was measured during incubation in the small intestine phase using a pH-stat automatic titration unit (Fig. 6). The volume of NaOH solution that had to be added to maintain a neutral pH within the reaction chamber was highly dependent on sample type. There was little change for both samples containing only curcumin crystals dispersed in water (control and nanocrystals), which should be expected because they did not contain any digestible materials. Conversely, there was a rapid increase in the volume of NaOH solution added to the nanoemulsion and soymilk samples during digestion, which suggests that the lipids in these samples had been easily digested by the lipase. Presumably, the lipase molecules adsorbed to the surfaces of the lipids droplets or oil bodies and hydrolyzed the triglycerides inside.

The percentage of free fatty acids (FFAs) released from these systems was calculated from the titration data (Fig. 6). These results show that the lipid phase was rapidly digested within the first 20 minutes of incubation in the small intestine phase, with slower digestion occurring at later times. By the end of the small intestine phase, most of the lipids in the nanoemulsions (> 86%) and soymilk (> 84%) had been digested. This fact can be contributed on the relatively small particle diameter increased the surface area for the digest enzymes to approach [201, 243]. These results suggest that the small triglyceride particles in both the nanoemulsions and soymilk were easily accessible to the lipase and effectively hydrolyzed.

Fig. 6

a b

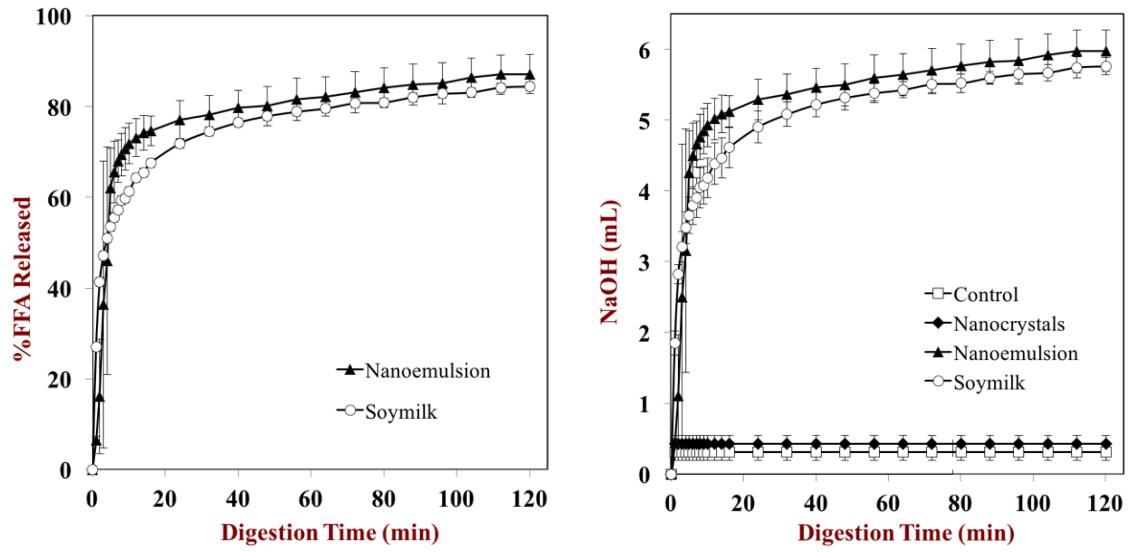

Fig. 6 a. The Calculated free fatty acid release profile for curcumin-loaded emulsion and oil bodies; b. influence of curcumin-loaded sample with and without lipid on NaOH profile

5.3.3. Properties mixed micelles and digest of curcumin delivery systems

Finally, the curcumin concentration in the mixed micelles and in the total digest collected at the end of the small intestine phase was measured for the various samples, and then the stability and bioaccessibility of the curcumin was determined (Fig. 7). This information is important because curcumin in a hydrophobic nutraceutical with a low water-solubility and poor chemical stability. The concentration of curcumin in the total digest represents the fraction that survived throughout the entire simulated GIT model. The concentration of curcumin in the mixed micelles provides an indication of the fraction available for uptake by the epithelium cells.

The level of curcumin in the total digest was significantly lower for the control samples than for any of the other samples (Fig 7a). This was probably because some of the large crystals in the curcumin did not make it to the reaction chamber because they stuck to the side of the containers or remained at the bottom of the samples. One would have expected the curcumin to be most chemically stable in the large crystals in the control sample because they have the lowest surface area exposed to water. There was no significant difference in the levels of curcumin in the total digest for the nanocrystals, nanoemulsions, or soymilk (Fig. 7a), suggesting they all had a similar effectiveness at protecting curcumin from chemical degradation. Nevertheless, there was still a reduction in the total level of curcumin present in these samples compared to the amount added initially, with only about 71%-75% remaining (Fig. 7b). This suggests that there may have been some chemical degradation of the curcumin during its passage through the simulated human gut. Curcumin is known to be highly unstable to degradation under neutral and basic conditions, so it is possible that some transformation of the curcumin molecules occurred during incubation in the simulated mouth and small intestine conditions.

The bioaccessibility was calculated from the ratio of curcumin in the mixed micelle phase to the total digest (Fig. 7b). The bioaccessibility of the curcumin was much higher in the nanoemulsions and soymilk than in the nanocrystal dispersions. This effect can be partly attributed to the fact that the free fatty acids and monoglycerides generated during lipid digestion combined with the phospholipids and bile salts in the small intestinal fluids to form mixed micelles with a higher solubilization capacity for curcumin. Moreover, the transfer of curcumin molecules from the colloidal particles into the micelles may have been easier when they were solubilized in the hydrophobic interiors of the lipid droplets and oil bodies than when they were present in a crystalline form. Interestingly, the bioaccessibility of the curcumin was slightly

higher in the soymilk than in the nanoemulsions (Fig. 7b). This suggests that the transfer of the curcumin molecules from the oil bodies to the mixed micelles may have been easier than from the saponin-coated oil droplets. It can be contributed on the additional lecithin and protein content within the soymilk product that helped to solubilize more curcumin.

Fig. 7

a b

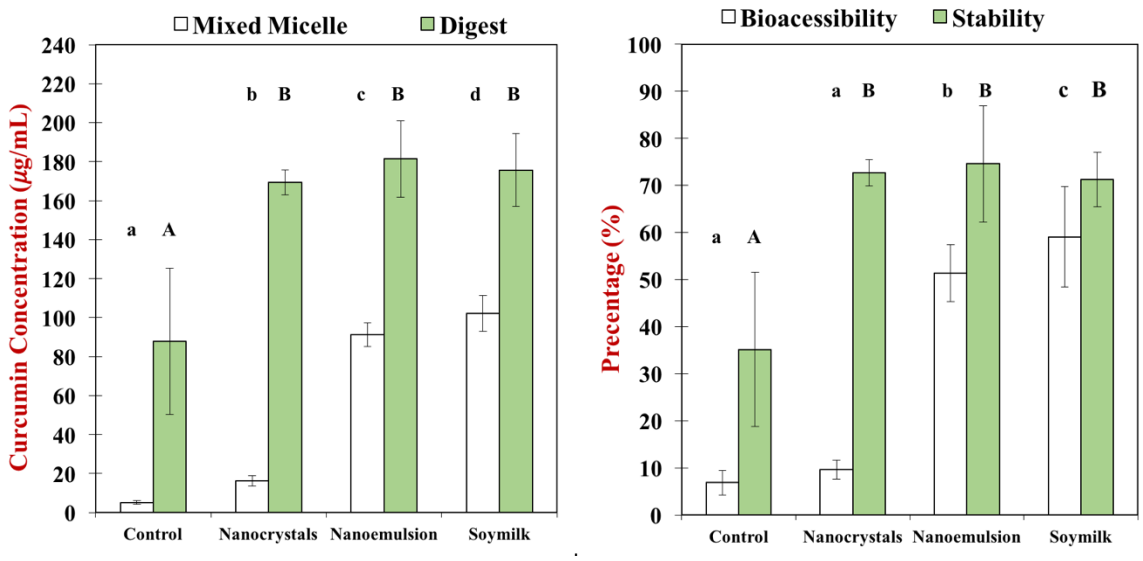

Fig 7 a. influence of curcumin-loaded water, emulsion and oil bodies on curcumin concentration in mixed micelles and raw digest; b. and bioaccessibility and stability of curcumin. Different lowercase letters and capital letters both mean significant difference (Duncan, $p < 0.05$) of the particle charge in samples within the same digestion phases

5.4. Conclusions

In conclusion, this study demonstrated the effectiveness of the pH-driven method to load curcumin into the lipid droplets in nanoemulsions, as well as the oil bodies in commercial soymilks. Moreover, it showed that the pH-driven method could also be used to form curcumin nanocrystals dispersed in water. The pH-driven method there appears to be a versatile tool for creating different kinds of curcumin delivery systems.

The curcumin-loaded nanoemulsion and soymilk had a homogeneous appearance and good stability to aggregation, which was attributed to the strong negative charge on the lipid droplets and oil bodies. Moreover, the curcumin appeared to remain solubilized within the hydrophobic domains of the lipid droplets and oil bodies, without any evidence of curcumin crystals being formed. There were appreciable differences in the behavior of the nanoemulsions and soymilk in the simulated GIT. In particular, the nanoemulsions appeared to be more susceptible to aggregation in the mouth phase, whereas the soymilk was much more susceptible to aggregation in the stomach phase. Nevertheless, both systems led to a relatively high stability and bioaccessibility of the curcumin at the end of the small GIT model. In contrast, the curcumin nanocrystals had a relatively low bioaccessibility because there were fewer mixed micelles to solubilize the curcumin molecules.

Overall, our results show that curcumin can be loaded into different kinds of colloidal delivery system using the pH-driven method and that these systems can have a high bioaccessibility. Consequently, the nanoemulsions and plant-based milk used in this system may be effective delivery systems for curcumin in functional food and beverage applications. It should be noted that there are a number of limitations of the current study. We did not include Phase I and II enzymes in our simulated gastrointestinal model, yet these are known to cause extensive metabolism of curcumin within the human gut. In future studies, it will be important to test the curcumin-loaded delivery systems using more realistic in vitro models or, better still, using in vivo animal or human feeding studies. It will also be important to ensure that the delivery systems can survive the harsh conditions that commercial foods and beverages experience throughout their lifetime.

Chapter 6

6. Loading natural emulsions with nutraceuticals using the pH-driven method: Formation & stability of curcumin-loaded soybean oils bodies

6.1 Introduction

Recently, there has been increasing interest in replacing animal-based and artificial ingredients in foods and beverages with plant-based alternatives [144]. This movement has largely been driven by the perceived benefits of plant-based foods on the health of both humans and the environment [244-246]. For this reason, the food industry is reformulating many of its existing products, as well as developing innovative new products, using plant-based components. One category of product that has been particularly successful is plant-based milks and creams, such as those based on soybean, cashew, coconut, almond, hemp, and oat [247]. These products are often designed to have a similar appearance, texture, and flavor as their dairy-based counterparts.

Many plant-based milks and creams are formed by breaking down plant structures to release oil storage bodies, such as soybeans, almonds or cashews [247]. These oil bodies are a natural form of colloidal particle that consists of a triglyceride core surrounded by a layer of phospholipids and proteins [235, 248]. These oil bodies contribute many of the desirable physicochemical attributes to plant-based milks, including their opacity, mouthfeel, and flavor profile. Like other types of colloidal particles, the aggregation stability of oil bodies is determined by the nature of the attractive and repulsive interactions acting between them, which depends on their surface chemistry and the prevailing environmental conditions, such as pH, ionic strength, and temperature [249, 250]. The formulation of stable plant-based milks and creams, therefore, depends on understanding the nature of the colloidal interactions acting between the

oil bodies. In principle, the hydrophobic core of oil bodies can be used to solubilize and transport non-polar bioactive agents, such as oil-soluble vitamins and nutraceuticals, which could be used to fortify plant-based milks and creams with health promoting-components. The challenge, however, is to load the hydrophobic bioactive into pre-existing oil bodies.

Previous researchers have loaded curcumin into artificial seed oil bodies formed by homogenization of an oil and aqueous phase together in the presence of seed proteins and phospholipids [251]. In the present study, however, we focused on loading curcumin into the natural oil bodies present in soymilk. Our method, therefore, has the advantage that it leaves the oil bodies in natural plant-based sources intact. Curcumin is the main bioactive component found in turmeric, which is used as a coloring and flavoring agent in foods, as well as a nutraceutical [47, 222, 252]. Previous studies have shown that curcumin can be loaded into pre-existing colloidal particles, such as lipid droplets, using a variety of strategies. Crystalline curcumin in powdered form has been mixed with an oil-in-water emulsion and then the resulting mixture has been heated, which causes the curcumin to dissolve and move into the hydrophobic interior of the lipid droplets [105, 253]. However, holding the emulsions at elevated temperatures can promote droplet aggregation and curcumin degradation. Alternatively, curcumin can be dissolved within an organic solvent (such as ethanol) and then mixed with pre-existing colloidal particles, which should also cause the curcumin to move into the particles. But the utilization of organic solvents in the fabrication process is often undesirable because of the additional costs associated with removing them, as well as their potential to damage the environment [88, 89].

Recently, a simple, inexpensive, organic solvent-free method has been developed to load curcumin into various types of colloidal delivery system, including micelles, liposomes, nanoemulsions, and protein nanoparticles [51, 92-94, 190]. This pH-driven method is based on changes

in the hydrophobicity, and therefore water-solubility, of curcumin when the pH is changed. At relatively low pH values (< pH 8), curcumin is a neutral non-polar molecule with a high oil-water partition coefficient and low water-solubility [225]. As the pH is raised above this value, a number of the hydroxyl groups on curcumin become progressively deprotonated, resulting in an increase in negative charge, increase in hydrophilicity, decrease in oil-water partition coefficient, and rise in water-solubility. This phenomenon can be used to load pre-existing colloidal particles using a two-step process: (i) curcumin crystals are dissolved in a strongly alkaline solution; (ii) this solution is mixed with an acidified colloidal suspension. The final pH of the mixed system is around neutral or less, which causes the curcumin in the aqueous phase to become non-polar and move into the hydrophobic interior of the colloidal particles.

The objective of the current study was, therefore, to establish whether the pH-driven method could be used to successfully load curcumin into the soybean oil bodies within a commercial soymilk product. Moreover, we examined the impact of environmental stresses, such as storage pH and temperature, on the physical and chemical study of the curcumin-loaded soymilks. Furthermore, the gastrointestinal fate of the soymilk before and after storage also investigated using an *in-vitro* model. The results of this study should aid the design and formulation of more efficacious nutraceutical-enriched functional foods and beverages.

6.2. Materials & Methods

6.2.1 Materials

A commercial soy creamer, which contained 10% w/v fat, was purchased from a local supermarket (Silk, Whitewave Foods, Broomfield, Colorado). Curcumin powder (C2302, purity 95%) was produced by TCI Chemicals (Portland, OR). Sodium Hydroxide (SS266), hydrochloric acid (83.3 mM) and dimethyl sulfoxide (BP231) were obtained from Fisher Chemicals (Fair

Lawn, NJ). Nile Red (N3013), fluorescein isothiocyanate isomer I (FITC, F1250), and sodium azide (S2002) were purchased from the Sigma-Aldrich Chemical Company (St. Louis, MO).

The *Nutrition Facts* label on the soymilk used in this study reported that the product had the following attributes: serving size (15 mL); calories per serving, 20 kCal; total fat, 1.5 g; total carbohydrate, 2 g (1g sugar); and, protein, 0 g. The ingredients reported on the product label were: soymilk (filtered water and soybean), cane sugar, palm oil maltodextrin, contains 2% or less of: soy lecithin, natural flavor, tapioca starch, locust bean gum, and dipotassium phosphate. It should be noted that soybeans do contain some protein, which was presumably below the threshold required to appear on the nutrition facts label.

6.2.2 Preparation protocol

Blank commercial soymilk

Initially, the effect of pH on the physiochemical properties of curcumin-free soymilks was examined by adjusting the pH from 2 to 10 using acid and base solutions. The particle characteristics of the soymilks were then measured using the methods described later.

Curcumin-loaded soymilk

The effect of particle characteristics on the properties of curcumin-loaded soymilks prepared using the pH-driven method was then examined. A stock curcumin solution (10 mg/g) was prepared by dissolving a weighed amount of curcumin powder into a sodium hydroxide solution (0.2 N NaOH). The alkaline curcumin stock solution was then added to a commercial soymilk (1:10 w/w) and the final system was rapidly adjusted to pH 6.5, 7.0 or 8.0 using the hydrochloric acid solution. The curcumin-loaded soymilks were then diluted with double distilled water to produce a final system containing 5 % oil, then stirred for 10 min at room temperature to ensure homogeneity. Finally, sodium azide (0.02%), which is a non-food grade

preservative, was added to the system to inhibit any microbial growth. It should be noted that the pH-shift method would lead to the formation of some NaCl in the final samples due to the addition of NaOH to create an alkaline solution and then HCl to neutralize it.

6.2.3 Storage study

The effect of pH on the chemical stability of curcumin within the soymilk was investigated when it was stored at 4 ºC for 36 days. Curcumin-loaded soymilks with three different pH values were prepared (pH 6.5, 7, and 8), poured into a series of glass test tubes (10 mL), and then sealed with a cap and parafilm to avoid evaporation and contamination. All samples were then incubated in the dark at 4 ºC to avoid photodegradation. Sealed samples were then taken and analyzed for each measurement throughout the storage period.

The impact of storage temperature (4, 20, 37 and 55 ºC) on the stability of the curcumin-loaded soymilk was then investigated at pH 7. A known volume of curcumin-loaded soymilk (10 mL) was placed within the glass test tubes and then stored in the dark. Again, samples were selected periodically for analysis to determine the impact of storage temperature on product stability.

6.2.3.1 Optical properties

The appearance and optical properties of the soymilks were determined using a digital camera and instrumental colorimeter (ColorFlex EZ 45/0-LAV, Hunter Associates Laboratory Inc., Virginia, USA), respectively. The colorimeter represented the optical properties of the samples using tristimulus color coordinates: L^*, a^* and b^* values. Here, L^* represents lightness (0) to darkness (100); a^* represents red (+) to green (-); and, b^* represents yellow (+) to blue (-). Samples (10 mL) were poured into a Petri dish and then illuminated using D65-artificial daylight using a 10^o standard angle and a black background.

6.2.3.2 Particle characterization

The particle size distribution (PSD) and mean particle diameter (D_{32}) of each sample was measured using a laser diffraction particle size analyzer (Mastersizer 2000; Malvern Instruments, Worcestershire, UK). The electrical characteristics (ζ -potential) of the particles in each sample were determined by measuring their electrophoretic mobility using a light scattering device (Nano-ZS, Malvern Instruments, Worcestershire, UK). Each sample was diluted with double distilled water with the same pH as their aqueous phase prior to measurement.

Microstructure analysis

A confocal scanning fluorescence microscopy (Nikon D-Eclipse C1 80i, Nikon, Melville, NY) was used to investigate the microstructure of the samples. Each sample was stained with Nile red (1 mg/ mL ethanol) and FITC (1 mg/mL DMSO) to highlight the lipid (stained red) and protein (stained green) regions, respectively. All images were acquired using 200× magnification (20× objective lens and 10× eyepiece lens).

6.2.4 *In-vitro* study

A simulated gastrointestinal tract (GIT) was used to measure the bioaccessibility of the curcumin in the soymilks (pH 7) both before and after storage. This GIT model is based on one previously developed in our laboratory, which consists of simulated mouth, stomach and small intestinal conditions [243]. The curcumin-loaded soymilk was passed through the full GIT model and then the amount of curcumin solubilized within the mixed micelle phase was measured.

To simulate the mouth phase, a fixed volume of pre-warmed (37 ºC) curcumin-loaded soymilk (15 mL) was transferred into a pre-warmed (37 ºC) simulated artificial saliva fluid (15 mL), which was prepared by adding mucin (3mg/mL) to artificial saliva solution. This mixture was then adjusted to pH 6.8 and placed within a temperature-controlled shaking incubator

operating at 100 rpm and 37 ºC for 30 seconds (Innova Incubator Shaker, Model 4080, New Brunswick Scientific, New Jersey, USA). The resulting sample was then incubated under simulated gastric conditions. Pre-heated (37 ºC) simulated gastric fluid (30 mL), which contained 3.2 mg/ mL pepsin, was added to the same volume of the sample from the mouth phase (30 mL). The resulting mixture was then adjusted to pH 2.5 and incubated at 37 ºC for 2 hours with 100 rpm shaking. After that, the sample (60 mL) arising from the stomach phase was transferred into the small intestinal phase. Pre-heated simulated intestinal fluid (3 mL) and bile salt solution (7 mL) was added to the mixture and the pH was adjusted to neutral. Then, a freshly prepared pancreatic lipase solution (5 mL) was added to the mixture and the pH was adjusted back to neutral. The bile salt solution was prepared by dissolving porcine bile extract (53.57 mg/mL) into phosphate buffer (5 mM, pH 7.0), and the pancreatic lipase solution was prepared by adding pancreatic lipase (0.16 mg/mL) into phosphate buffer (5 mM, pH 7.0). Throughout the 2-hour small intestinal phase, an automatic titration unit (Metrohm, USA Inc.) was used to monitor and maintain the sample at pH 7.0.

6.2.5 Curcumin concertation determination

The concentration of the curcumin within the soymilk was determined using a UV/visible spectrophotometry method. First, the curcumin was extracted from the samples using acidified dimethyl sulfoxide (0.1% v/v 6N HCl) solution. Acidification was used to enhance the chemical stability of the curcumin. The absorbance of the curcumin solutions was measured using a UV-visible-spectrometer (Genesys 150, Thermos Fisher Scientific, Madison, WI) at a wavelength of 420 nm. The curcumin concentrations were then calculated from the measured absorbance values using a standard curve prepared using a series of samples of known curcumin level.

6.2.5.1 Encapsulation Efficiency

The encapsulation efficiency of the curcumin-loaded soymilks was calculated using the following equation:

$$\textit{Encapsulation Efficiency} = 100 \times C_{encapsulated} / C_{initial} \quad (1)$$

Here, $C_{initial}$ is the total concentration of curcumin initially added to the soymilk and $C_{encapsulated}$ is the concertation of curcumin present within the curcumin-loaded soymilk after preparation using the pH-driven method.

6.2.6 Stability and Bioaccessibility

After passing through the full GIT model, the resulting fluid was collected and divided into two fractions. One fraction, which was used without any further treatment, was taken to be the total digested phase. The other fraction, which was the supernatant collected after centrifugation, was taken to be the mixed micelle phase. The mixed micelle phase was prepared by centrifugation of the total digest at 18,000 rpm at 25 ºC for 50 min (Thermo Scientific, Waltham, MA) and then collecting the clear supernatant from the samples. The curcumin concentrations within the total digested phase (C_{digest}) and with the mixed micelle phase ($C_{micelle}$) were then determined using UV/visible spectrophotometry as described earlier.

The *bioaccessibility and stability* of the curcumin-loaded soymilk were then calculated using the $C_{micelle}$, C_{digest} and $C_{initial}$ values using the following expressions:

$$Bioaccessibility\ (\%) = 100\ \times \frac{C_{micelle}}{C_{digest}} \quad (2)$$

$$Stability(\%) = 100\ \times \frac{C_{digest}}{C_{initial}} \quad (3)$$

Here, the $C_{micelle}$ is the concentration of curcumin within the mixed micelle phase; the C_{digest} is the concentration of curcumin within the digest phase; the $C_{initial}$ is the concertation of curcumin within the soymilk system before digestion. The *Bioaccessibility* represents the

fraction of curcumin solubilized in the mixed micelle phase, which is potentially available for absorption. The *Stability* represents the total amount of curcumin that survived after the soymilks were passed through the simulated GIT.

6.2.7 Kinetic study

The kinetics of curcumin degradation within the soymilk samples during storage was calculated using the Arrhenius equation:

$$k = A\, e^{-Ea/RT} \quad (4)$$

Here, k is the rate coefficient, A is the Arrhenius constant; E_a is the activation energy, R is the universal gas constant (8.314×10^{-3} kJ mol^{-1} K^{-1}); and T is the temperature in Kelvin.

6.2.8 Statistical analysis

All the data from this experimental study are displayed as the mean ± the standard deviation determined from measurements made on three freshly prepared samples. Statistical comparisons were carried out using dedicated mathematical software (SPSS version 6.0) and a significant difference was considered to occur when the *p*-value was lower than 0.05.

6.3. Results and discussions

6.3.1 Soymilk characteristics

The commercial soymilk used in this study consists of soybean oil bodies dispersed in an aqueous solution that contains various other ingredients, such as cane sugar, maltodextrin, soy lecithin, starch, locust bean gum, and dipotassium phosphate. Visually, the soymilk had a homogenous appearance with a bright milky color (Fig. 1a). Measurement of the pH of the soymilk showed that it was slightly basic (pH 7.5). The mean particle diameter (D_{32}) of the soymilk determined by laser diffraction analysis was 367 ± 2 nm. Particle size distribution analysis showed that the majority of particles had diameters between about 0.1 and 4 □m, but

that there was a small population of particles with larger dimensions (Fig 1b). The original soymilk had a relatively high negative surface potential ($\zeta = -39.8 \pm 2.6$ mV), which can be attributed to the presence of anionic phospholipids and proteins at the oil body surfaces [235]. The magnitude of the negative charge on the oil bodies should be high enough to generate a strong electrostatic repulsion that prevents them from aggregating with each other [233, 254].

Influence of pH on particle characteristics in soymilk

The impact of pH on the physicochemical properties and stability of the curcumin-free (blank) soymilk was characterized to establish whether it would remain stable during the pH-driven method and to determine the range of pH conditions where it would remain stable in commercial applications. The particle characteristics of these soymilks were measured after their aqueous phases had been adjusted to pH values ranging from 2 to 10 and then stored for several hours (Fig.1a). From pH 6 to 10, the soymilks remained visibly stable, with no evidence of phase separation. From pH 2 to 5, however, there was clear evidence of phase separation, with a curd-like whitish upper phase and a clear watery lower phase. These results show that the soymilks were highly unstable to aggregation and creaming under moderately acidic conditions.

The impact of pH on the mean particle diameter and ζ-potential of the particles in the soymilks were investigated using laser diffraction and electrophoresis analysis, respectively (Figs. 1c & 1d). From pH 10 to 7, the soybean oil bodies had a relatively high and constant negative surface potential ($\zeta \approx -42$ mV) and had relatively small and constant particle dimensions ($D_{32} < 380$ nm). When the pH was reduced to 6, the surface potential became slightly less negative ($\zeta \approx -35$ mV) and the particle dimensions increased somewhat ($D_{32} \approx 578$ nm), which suggested that a limited amount of oil body aggregation had occurred. When the pH was further reduced into the range from 5 to 2, there was a pronounced increase in the mean particle

diameter (D_{32} > 12 um), which indicated that extensive oil body aggregation occurred under these conditions. The laser diffraction measurements were therefore consistent with the visual observations of phase separation in the samples over this pH range (Fig. 1a). The origin of this effect can be attributed to the decrease in the magnitude of the surface potential on the oil bodies at lower pH values (Fig. 1c), which would have reduced the electrostatic repulsion between them. Indeed, the ζ-potential went from negative at high pH values to positive at low pH values, with a net charge of zero around pH 3.6. This effect can be attributed to progressive protonation of the carboxyl groups ($-COO^- \rightarrow -COOH$) and amino groups ($-NH_2 \rightarrow -NH_3^+$) on the adsorbed proteins and phospholipids as the pH was reduced. It should be noted, however, that the commercial soymilk contained other components that could also have attributed to its electrical characteristics, such as soy lecithin. Presumably, this ingredient was added to improve the aggregation stability of the oil bodies, probably by adsorbing to any hydrophobic patches on their surfaces.

Fig.1

a.

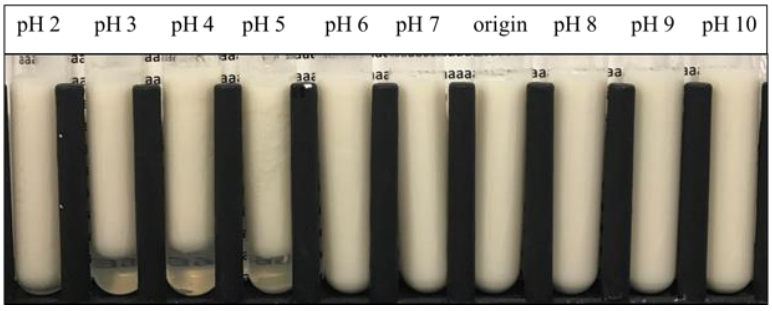

b.

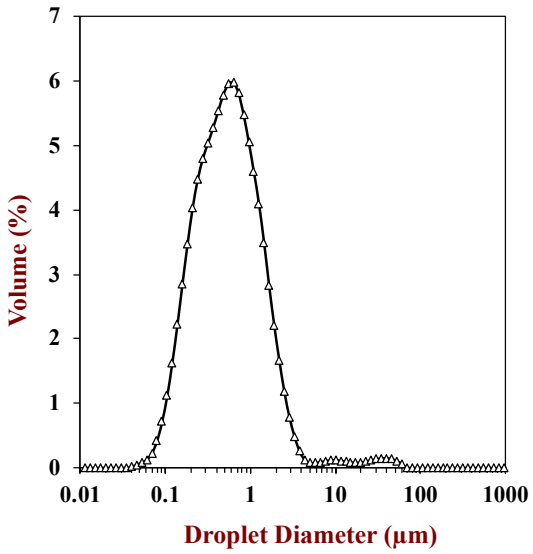

c.

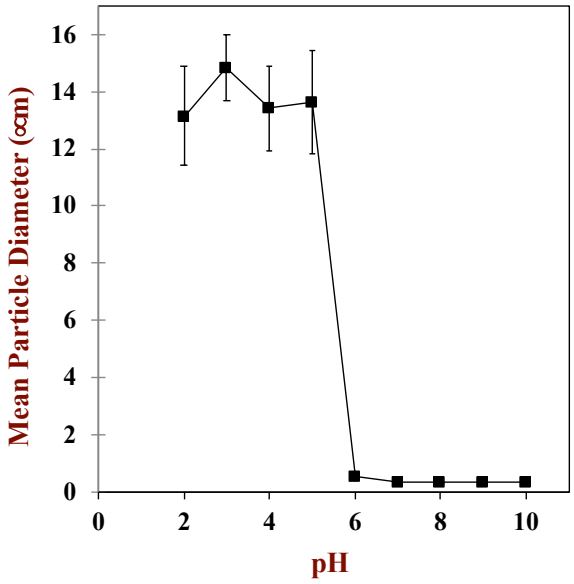

d.

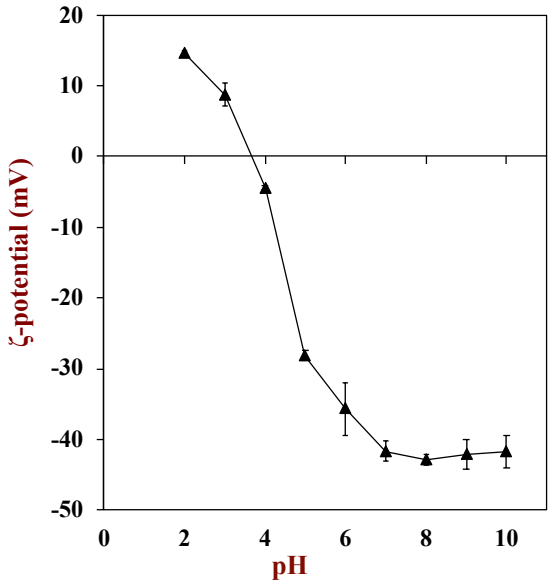

Fig. 1. a) Impact of pH on appearance of blank soymilk; b) particle size distribution of blank soymilk (pH 7.5); c) Impact of pH on electrical characteristics (ζ-potential) of blank soymilk; and d) Impact of pH on mean particle diameter (D_{32}) of blank soymilk.

6.3.2 Influence of pH-driven method on soymilk properties

The experiments described previously indicated that the soymilk remains physically stable at relatively high pH values. In commercial products, the pH may vary somewhat depending on the ingredients used to formulate them, as well as any chemical changes that occur during storage. For this reason, we carried out the following experiments using soymilk samples with three different final pH values: pH 6.5, 7.0 and 8.0. Soymilk samples above pH 8 were not evaluated because food and beverage products rarely have such highly alkaline conditions.

6.3.2.1 Appearance

Digital photography images and instrumental colorimetry measurements were used to characterize the appearance of the curcumin-loaded soymilks at the three different pH values (Figs. 3a and 4). The photography images showed that the soymilk samples had a homogenous cloudy yellow appearance at pH 6.5 and 7, but were slightly more orange-colored at pH 8 (Fig 3a). The tristimulus coordinates of the soymilks also indicated that there were appreciable differences in their color depending on pH (Table 1). At pH 6.5 and 7, the soymilks had fairly similar color characteristics indicative of a creamy yellow appearance: L^* (≈ 82), a^* (≈ -8), and b^* (≈ 81). But, at pH 8, the soymilk had significantly lower L^* (≈ 77) and b^* (≈ 75) values and higher a^* (≈ 0.6) values (Table 1). This suggests that the soymilk at the highest pH was less light, less green, and less yellow than the ones at the lower pH values. This effect can be attributed to the pH-dependent color of the curcumin molecule. When the pH is increased to around the first pK_a value of curcumin (around pH 7.5 to 8.5), one of its hydroxyl groups becomes deprotonated, which leads to a change in color from yellow to orange [1, 13, 255]. This phenomenon may be important when formulating curcumin-loaded soymilk products with specific visual characteristics.

Table 1

	pH 6.5	pH 7	pH 8
Initial curcumin concentration (μg/mL)	231.6 ± 8.8 [a]	228.3 ± 7.4 [a]	235.4 ± 3.7 [a]
Loading capacity (%)	92.6 ± 3.2 [a]	91.3 ± 2.7 [a]	94.2 ± 1.4 [c]
L*	82.2 ± 0.2 [b]	82.4± 0.1 [b]	77.3 ± 0.5 [a]
a*	-8.44 ± 0.15 [a]	-8.01 ± 0.09 [a]	0.64 ± 0.68 [b]
b*	82.2 ± 0.5 [c]	80.3 ± 0.4 [b]	75.2 ± 0.7 [a]
D_{32} (μm)	0.47 ± 0.02 [b]	0.39 ± 0.01 [a]	0.38 ± 0.01 [a]
ζ- potential (mV)	-40.8 ± 1.3 [b]	-42.1 ± 2.0 [a]	-42.8 ± 0.9 [a]

Table 1. Influence of pH on curcumin-loaded soymilk: initial curcumin concentration, loading capacity, tristimulus color value (*L**, *a**, and *b**), mean particle diameter (D_{32}) and electrical characteristics (ζ-potential). Different letters represent significant differences (Duncan, $p < 0.05$).

6.3.2.2 Curcumin concentration

The impact of the pH-driven method on the encapsulation efficiency of the curcumin within the soymilks was determined. A fixed amount of curcumin (250 μg/mL) was utilized to prepare all the nutraceutical-loaded soymilks using the pH-driven method. After loading, the encapsulation efficiencies of the curcumin in the soymilks were determined. At all three pH values, a relatively high and fairly similar encapsulation efficiency was obtained, *i.e.*, 91-94% (Table 1). These results indicate that the pH-driven method was a successful approach for incorporating curcumin into pre-existing oil bodies.

6.3.2.3 Particle characteristics

The impact of using the pH-driven method for loading curcumin into the soybean oil bodies on the structural properties of the soymilk was also investigated. The loading of the curcumin into the oil bodies had no significant impact on their surface potential (Fig. 2a) or mean particle diameter (Fig. 2b) at any of the pH values used. There was little change in the surface potential and only a slight decrease in the mean particle diameter when the pH was increased from 6.5 to 8, which is consistent with the earlier experiments (Figs. 1a, c & d). Immediately after preparation, all the curcumin-loaded soymilks had a homogenous creamy yellow appearance (Fig. 3a), which suggests that they initially had good stability to aggregation and creaming. This was confirmed by measuring the microstructures of the soymilk using confocal microscopy (Fig. 3b), which showed that at all three pH values the soymilks contained relatively small oil bodies that were distributed evenly throughout the system. Fluorescent staining indicated that the oil bodies (stained red) were dispersed in an aqueous medium that contained proteins (stained green).

Fig.2

a

b

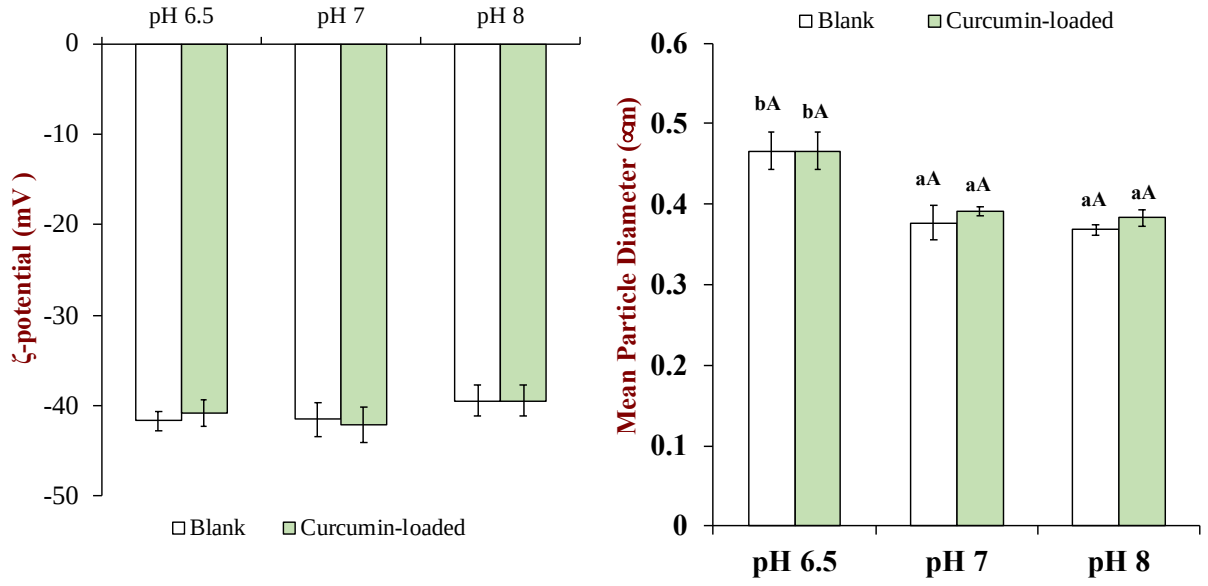

Fig. 2. The a) electrical characteristics (ζ-potential) and b) mean particle diameter (D_{32}) of the blank and curcumin-loaded soymilks at various pH values. Different lowercase letters indicate significant differences (Duncan, $p< 0.05$) within the same type of soymilk; different capital letters indicate significant differences between two types of sample (Duncan, $p< 0.05$).

Fig. 3

a.

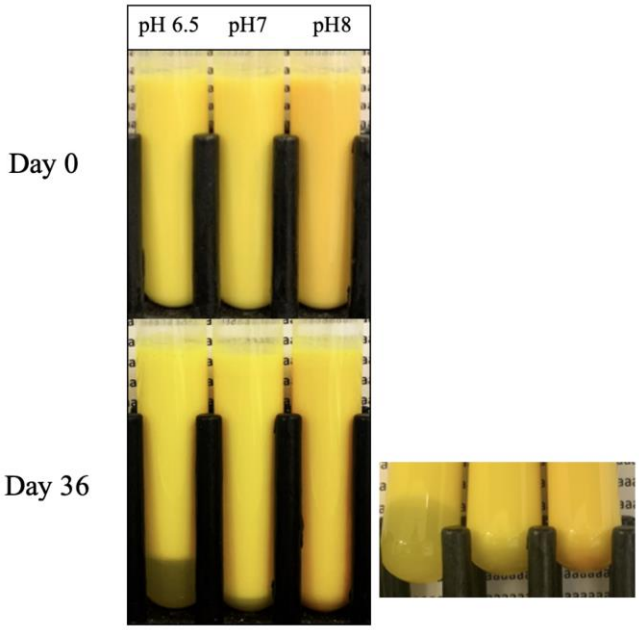

b.

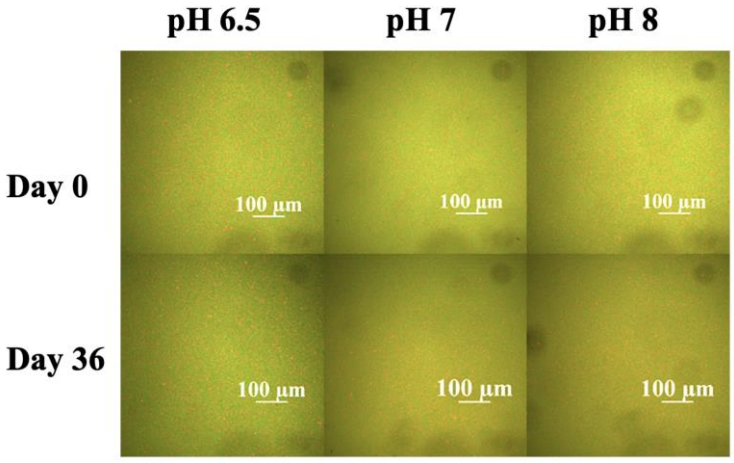

Fig 3. a) The appearances and b) microstructures of curcumin-loaded soymilks before and after storage at various pH values at 4 ºC for 36 days. The microstructure images were obtained using confocal fluorescence microscopy and the scale bars are 100 um.

6.3.3 Effect of pH on storage stability of curcumin-loaded soymilk

For commercial applications, it is important that plant-based milks have a sufficiently long shelf life. For this reason, we measured the physiochemical stability of curcumin-loaded soymilks (pH 6.5, 7, and 8) during storage at 4 ºC in the dark. This temperature was selected because the milks would be expected to be stored in the refrigerator prior to utilization.

6.3.3.1 Appearance

After 36 days storage, all of the soymilks still had a creamy yellow/orange color, but some phase separation was observed, with a watery serum layer being visible at the bottom of the test tubes (Fig 3a). This effect was attributed to the upward movement of the oil bodies due to gravity. The thickness of the serum layer was greatest for the soymilk at pH 6.5, which was probably because it contained the largest particles (Fig. 2b), presumably because some of the oil bodies had aggregated. Conversely, the soymilk at pH 8 was the most stable to gravitational separation, maintaining a uniform creamy yellow/orange appearance after storage. There did, however, appear to be a slight reduction in the intensity of the color in this sample after storage, as well as the formation of thin orange sediment at the bottom of the test tube (Fig. 3a). This orange sediment was assumed to be due to the formation and sedimentation of curcumin crystals within the soymilks. The decrease in the color-intensity of the soymilk at pH 8 may, therefore, have been because some of the curcumin had moved to the bottom of the samples and therefore did not contribute to their overall appearance. In addition, some of the curcumin may have chemically degraded during storage (see later).

Fig. 4

a. b.

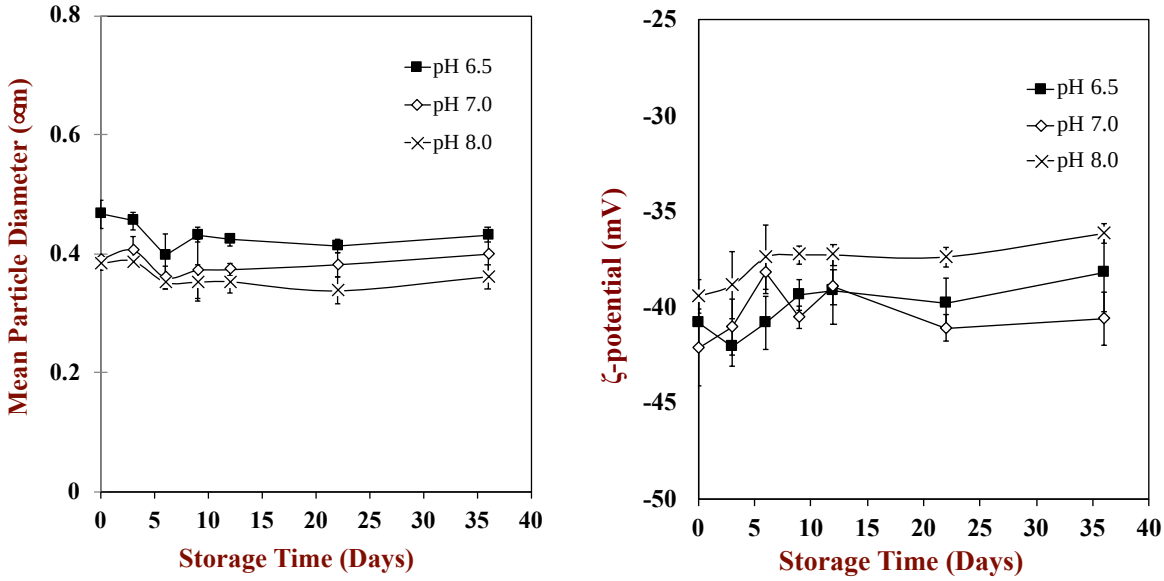

Fig. 4. Influence of pH on the a) mean particle diameters (D_{32}) and b) electrical characteristics (ζ- potential) of curcumin-loaded soymilk during 4 ºC storage for 36 days.

Fig. 5

a b

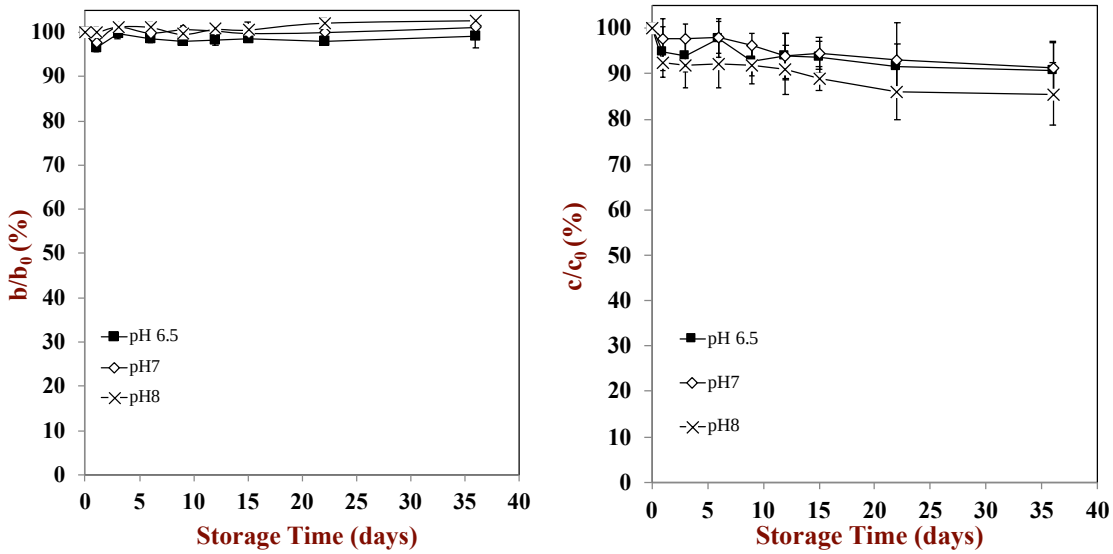

Fig. 5 Influence of pH on a) the yellow color (*b**) and b) curcumin concentration within the soymilks during 4 ºC storage for 36 days.

The instrumental color coordinates of the curcumin-loaded soymilk were measured before and after storage (Fig. 5a, Table 1). The kinetics of color fading during storage is highlighted by plotting the normalized yellowness *versus* time because this was the dominant color coordinate: b^*/b_0^*, where b_0^* is the color coordinate at zero time. This value changed by less than 2% during storage, which suggests that there was little alteration in yellow color. There was also little change in the *a**-value of the soymilks (Table 1). Indeed, *a** increased from -8 to -6 for the soymilks at pH 6.5 and 7, which indicates a slight decrease in their greenish hue. Conversely, the *a** of the soymilk at pH 8 decreased slightly from 0 to -1, which indicates that it became slightly more greenish.

6.3.3.2 Curcumin concentration

The concertation of curcumin remaining in the soymilk was also measured during storage to investigate the impact of pH on its chemical stability (Fig. 5b). After 36 days storage at 4 ^{o}C, the majority of curcumin was still present, with the precise amount depending on solution conditions (Table 1): pH 6.5 (91%), pH 7 (90%), and pH 8 (87%). Overall, these results suggest that curcumin was relatively stable to degradation under these storage conditions, but that the rate of degradation increased as the pH was raised, which is consistent with previous results [256].

6.3.3.3 Particle characteristics

Changes in the characteristics of the particles in the curcumin-loaded soymilks stored at different pH values were also determined (Fig. 4). The mean particle diameter of all the soymilks remained relatively constant during storage (Fig. 4a), suggesting that the oil bodies were stable to aggregation. The ζ-potentials of the particles in all the soymilks became slightly less negative (from around -40 to -35 mV) during storage (Fig. 4b), which suggests that there were some changes in the interfacial composition of the oil bodies during storage. Even so, the negative surface potential should still have been large enough to generate a strong electrostatic repulsion that inhibited the aggregation of the oil bodies. As mentioned earlier, we did see some phase separation (creaming) of the oil bodies after 36 days storage, particularly at the lower pH values. This result suggests that there may have been some weak flocs formed in the soymilk samples that promoted creaming due to the increase in particle size, but which were disrupted when the samples were diluted for the particle size measurements.

Effect temperature on the soymilk containing curcumin

Many commercial food and beverage products experience changes in their temperature during their manufacture, storage, and utilization. Consequently, it is important to establish the

impact of temperature on the physicochemical properties and stability of the curcumin-loaded soymilk samples. For this reason, changes in the properties of the soymilk were measured when they were stored at 4, 20, 37, and 55 ºC for 14 days. The soymilk at pH 7 was selected for these studies because it was more stable to creaming than the pH 6.5 sample and more stable to curcumin crystallization than the pH 8 sample.

Fig. 6

a.

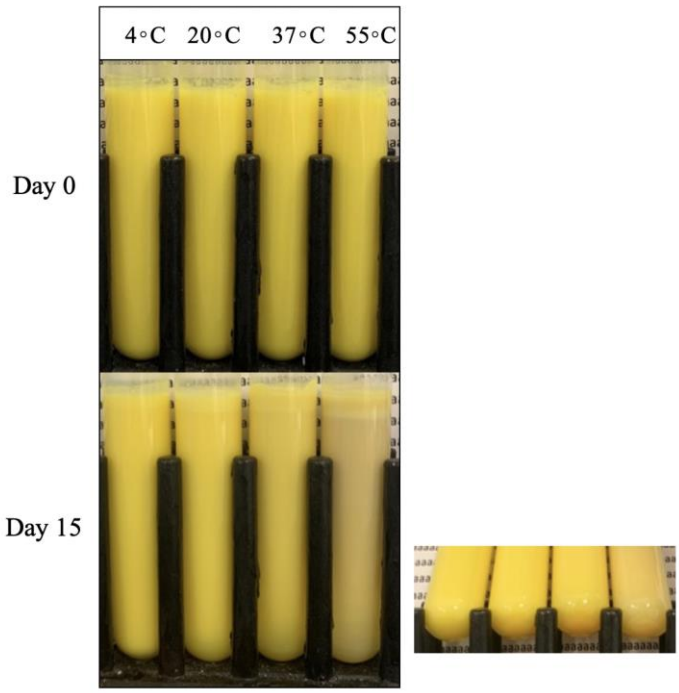

b.

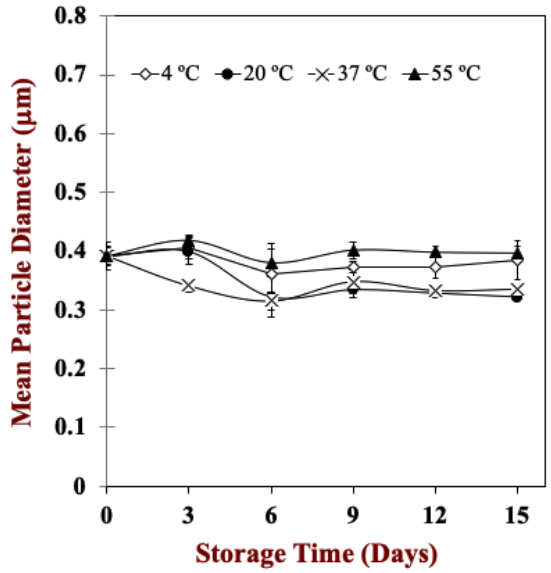

c.

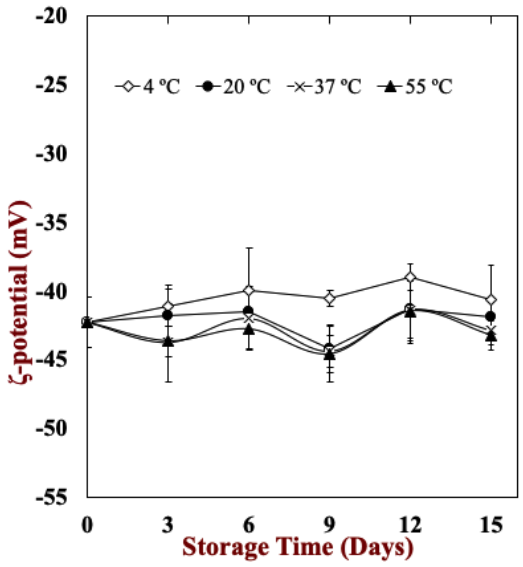

d.

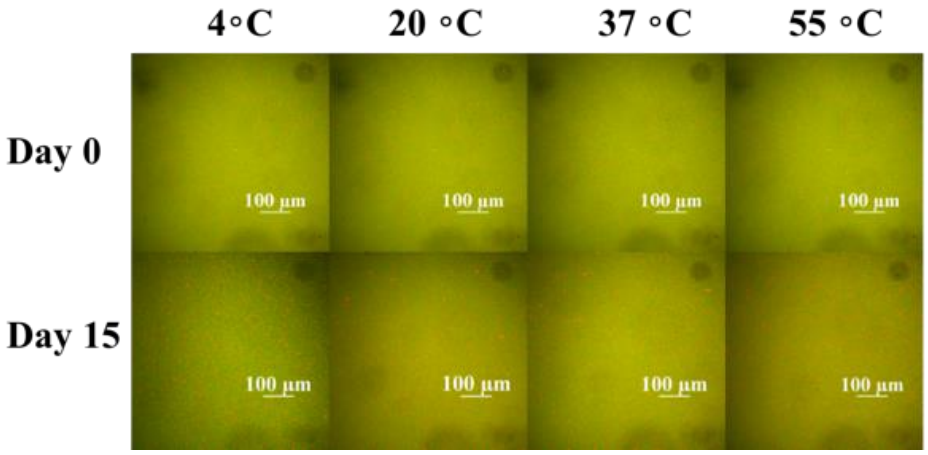

Fig. 6 Influence of temperatures on the a) appearances of curcumin-loaded soymilk before and after 15-days storage. The impact of temperature on b) mean particle diameters (D_{32}) and c) electrical characteristics (ζ- potential) of curcumin-loaded soymilks during 15-days storage. d) the microstructure of curcumin-loaded soymilks before and after incubated under four different temperatures and a length of 100 um scale bars were applied.

6.3.4 Effect of temperature on storage stability of curcumin-loaded soymilk

6.3.4.1 Appearance

The storage temperature had a pronounced impact on the overall appearance of the curcumin-loaded soymilks (Fig. 6a). The extent of color fading increased as the storage temperature increased. At 4 and 20 ºC, the curcumin was relatively stable to fading, with the soymilks maintaining a strong yellowish color, but at 37 and 55 ºC there was clear evidence of color fading. In addition, the soymilks exhibited a greater degree of gravitational separation as the storage temperature was raised. The samples stored at 4 and 20 ºC were relatively stable to creaming during storage, but those stored at 37 and 55 ºC had a thick cream layer at their surfaces after storage, which was attributed to the upward movement of the oil bodies due to the gravitational forces acting upon them.

Instrumental colorimetry analysis of the curcumin-loaded soymilk during storage also showed that the rate of color fading increased with storage temperature. The color stability of the soymilk samples was represented by plotting the relative change in their yellowness (b^*/b_0^*) over time (Fig. 7a). The L^*, a^* and b^* values of the soymilks before and after storage is shown in Table 2. Overall, color fading increased in the following order: 4 ºC ≈ 20 ºC < 37 ºC < 55 ºC (Fig. 7a). The lightness (L^*) of all the soymilks remained greater than 90 % even after 15-days storage. The greenness (a^*) of the soymilks decreased by about 20% at 4 and 20 ºC, 30% at 37 ºC, and 50% at 55 ºC after 15-days storage. The yellowness (b^*) of the soymilks did not change appreciably (< 2%) at 4 and 20 ºC, but decreased by about 10% at 37 ºC, and 30% at 55 ºC. These results suggest that the curcumin should be stored at a relatively low temperature in order to minimize color fading.

Fig. 7

a. b.

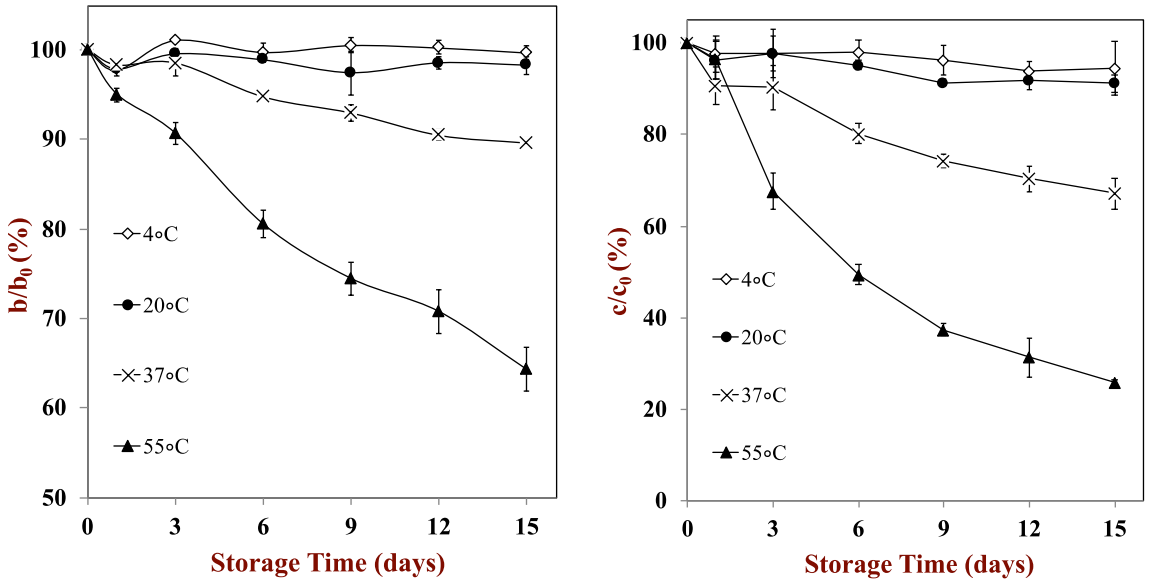

Fig. 7 Influence of temperature on a) yellow color (*b**) and b) curcumin concentration within soymilks during 15-days storage.

Table 2

		4 °C	20 °C	37 °C	55 °C
Before Storage	*L**	82.41± 0.1 [a]	82.41± 0.1 [a]	82.41± 0.1 [a]	82.41± 0.1[a]
	*a**	-8.01 ± 0.09 [a]	-8.01 ± 0.09 [a]	-8.01 ± 0.09 [a]	-8.01 ± 0.09 [a]
	*b**	80.32 ± 0.40 [a]	80.32 ± 0.40 [a]	80.32 ± 0.40 [a]	80.32 ± 0.40 [a]
After Storage	*L**	80.86 ± 0.08 [c]	80.82 ± 0.64 [c]	78.70 ± 0.12	76.30 ± 1.00
	*a**	-6.58 ± 0.03 [c]	-6.53 ± 0.04 [c]	-5.40 ± 0.16 [b]	-3.74 ± 0.30 [a]
	*b**	80.10 ± 0.27 [d]	78.94 ± 0.53 [c]	72.02 ± 0.26 [b]	51.66 ± 1.86 [a]

Table 2. Influence of temperature on the tristimulus color coordinates (*L**, *a**, and *b**) of samples before and after 15-day incubation. Different letters represent significant differences (Duncan, $p < 0.05$).

6.3.4.2 Curcumin concentration

The fading of the curcumin-loaded soymilks was most likely due to the chemical instability of the curcumin molecule at elevated temperatures. We therefore measured the impact of temperature on the change in curcumin concentration during storage (Fig. 7b). The rate of curcumin degradation clearly increased with increasing temperature. After 15 days storage, less than 10% of the curcumin degraded at 4 and 20 ºC, around 35% at 37 ºC, and around 75 % at 55 ºC. The chemical transformation of the curcumin during storage would therefore account for the faster color fading observed at the higher temperatures.

A more detailed analysis of the reaction kinetics of curcumin degradation in the soymilks was obtained by applying the Arrhenius equation (Equation 4). This equation can be rearranged to give:

$$\ln(k) = \ln(A) - \frac{E_A}{RT} \qquad (5)$$

Thus, the activation energy can be determined by plotting the logarithm of the reaction rate (k) versus the reciprocal of the absolute temperature ($1/T$) (Fig. 8). The reaction rate was determined at each temperature from plots of curcumin concentration *versus* time, assuming a first order reaction, *i.e.*, $C/C_0 = A \exp(-kt)$. This analysis indicated that the activation energy for curcumin degradation was around 48.4 KJ/mol.

Fig. 8.

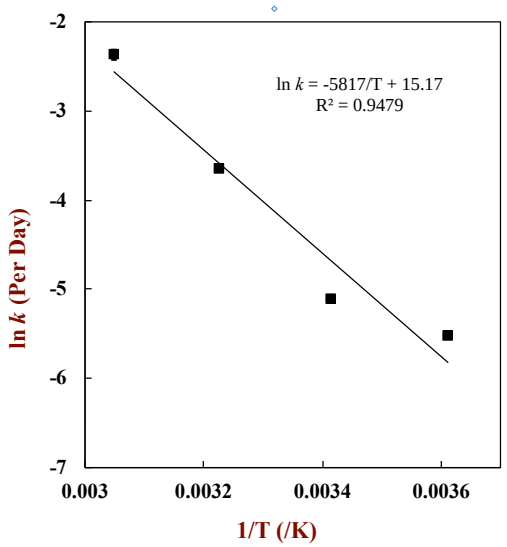

Fig. 8 Arrhenius equation graph of curcumin within soymilks, which represents the temperature dependence of the chemical reaction rate.

6.3.4.5 Particle characteristics

The size and electrical characteristics of the particles in the soymilk samples were also measured during storage at the four different temperatures (Figs. 6b & 6c). Overall, the mean particle diameter remained relatively small (< 400 nm) and the ζ-potential remained highly negative (≈ –40 mV) throughout storage. These results suggest that the soymilk samples were relatively stable to coalescence or strong flocculation at all temperatures. Conversely, the fact that we did observe appreciable creaming at the higher storage temperatures suggests that some weak flocculation of the oil bodies may have occurred. However, the confocal microscopy images of the samples did not indicate that extensive oil body aggregation had occurred (Fig. 6d). An alternative explanation is that more rapid oil body creaming occurred at the higher storage temperatures because of the reduction in aqueous phase viscosity. The dynamic shear viscosity of water has been reported to be 1.6, 1.0, 0.69, and 0.50 mPa s at 4, 20, 37, and 55 ^{o}C,

respectively (www.vaxasoftware.com). Thus, there is more than a 3-fold decrease in the aqueous phase viscosity from the lowest to highest storage temperatures used. According to Stoke's law, the creaming velocity of a spherical particle due to gravity is inversely related to the viscosity of the surrounding fluid, so a decrease in aqueous phase viscosity should promote faster creaming [128]. Overall, these results suggest that the physical stability of the soymilks is also improved by storing them at relatively low temperatures.

6.3.5 Bioaccessibility and stability

Finally, we examined the impact of encapsulation of curcumin within the soymilks on two of the main factors affecting nutraceutical bioavailability after ingestion: bioaccessibility and stability in the gastrointestinal tract (GIT) [257, 258]. The curcumin-loaded soymilk stored at pH 7 and 4 ºC was used for these experiments because it had the best physical and chemical stability. The potential bioavailability of the curcumin was determined using a simulated GIT before and after storage of the soymilks (Table 3). As expected, the total fraction of curcumin within both the total digest and the mixed micelle phases were slightly (but significantly) higher before storage than after storage, which can be attributed to some curcumin degradation. The gastrointestinal stability and bioaccessibility of the curcumin were fairly similar before and after storage. About 82-85% of the curcumin survived passage through the simulated mouth, stomach, and small intestine phases, but only about 55-59% of the curcumin was solubilized within the mixed micelle phase and therefore available for absorption. It is possible that the remainder of the curcumin either formed crystals that precipitated or bound to insoluble protein complexes and was therefore not present in the mixed micelle phase. Nevertheless, these measurements show that a substantial fraction of the ingested curcumin should still be in a from that would be bioavailable. Having said this, it is important to note that the human gut contains

many types of metabolic enzymes that can transform curcumin into different forms [4, 68], which was not considered in the current study. In future studies, it would therefore be useful to test the curcumin-loaded soymilks using animal or human feeding trials.

Table 3.

	C_{Digest} (ug/mL)	$C_{Micelle}$ (ug/mL)	Stability (%)	Bioaccessibility (%)
Before Storage	186.80 ± 2.56	109.63 ± 18.13	81.87± 1.82	58.60 ± 9.08
After Storage	177.67 ± 1.43	97.23 ± 10.06	85.39 ± 3.14	54.76 ± 6.04

Table 3. Impact of storage at pH 7 on the gastrointestinal stability and bioaccessibility of curcumin in soymilks determined using a simulated gastrointestinal tract

6.4 Conclusions

In summary, this study has shown that the pH-driven method can be successfully used to load curcumin into commercial soymilks and that the storage stability of the resulting systems depends on pH and temperature. The soymilks had good chemical stability when stored at refrigerator temperatures at pH 6.5, 7 and 8 for 36 days, but there was some change in the color of the curcumin-loaded soymilks at the highest pH. The soymilks were susceptible to phase separation due to creaming when stored at pH 6.5, which was attributed to oil body aggregation. They also showed evidence of phase separation due to the formation and sedimentation of curcumin crystals when stored at pH 8. The physical and chemical stability of the curcumin-loaded soymilks (pH 7) was relatively high at 4 and 20 ºC, but decreased at higher temperatures of 37 and 55 ºC. Overall, our results suggest that curcumin-loaded soymilks prepared using the pH driven method should be stored at neutral pH at relatively low temperatures. We also showed that these samples had relatively good bioavailability in a simulated GIT model.

Nevertheless, further studies are needed to test their bioavailability using *in vivo* animal or human feed studies, as well as to test their stability under the conditions found in real food products.

Chapter 7

7. Fabrication of curcumin-loaded dairy milks using the pH-shift method: Formation, stability, and bioaccessibility

7.1.1 Introduction

The creation of functional foods and beverages, which are products specifically designed to enhance human health and performance, is a rapidly growing area within the food and nutrition industry due to its potential economic and health benefits [259, 260]. Ideally, these products should contain bioactive substances that provide demonstrated health benefits beyond basic nutrition [261, 262], such as the prevention and treatment of specific diseases [262, 263], without posing a health risk to those consuming them [264]. It has been reported that the global functional food market generated around $300 billion dollars of revenue in 2017, which has been predicted to rise to more than $440 billion by 2022 [265]. There is also a growing market for dietary supplements (such as pills and capsules) that may help prevent or treat certain kinds of chronic diseases [266]. In this case, there is interest in developing alternative delivery formats that are more acceptable to consumers and that ensure a high bioavailability and bioactivity of the encapsulated bioactive substances.

Nutraceuticals are commonly used for their potential health benefits in functional food and supplement products [267]. These bioactive molecules are typically natural food components derived from edible plants, animal, or microbial sources, including: phytochemicals from fruits, vegetables, cereals, and nuts; collagen, conjugated linolenic acid (CLA), and omega-3 fatty acids from meat and fish; and, probiotics from microbial cultures [2, 263]. Many of these nutraceutical ingredients play multiple roles in foods. For instance, in addition to their potential health

benefits, they may also function as natural colors, flavors, antioxidants, preservatives, stabilizers, and texture modifiers [268, 269].

In this article, we focus on the incorporation of a model hydrophobic nutraceutical (curcumin) into functional food products. This nutraceutical is claimed to exhibit a broad spectrum of biological activities [270-272], but there are some challenges that have to be overcome before it can be successfully incorporated into functional foods [47, 63]. Curcumin is a bioactive polyphenol from turmeric that has strong antioxidant and anti-inflammatory activities [63, 272]. It naturally has a bright yellow-orange appearance and a distinctive flavor, which means that it can be used as a natural colorant and flavoring in certain foods [1, 2]. However, it is prone to chemical degradation during storage, has poor water-solubility, and has a low oral bioavailability [47, 273]. It is, therefore, important to design functional food products with good storage stability and bioavailability [47, 63].

Previously, it has been shown that encapsulating curcumin within colloidal delivery systems that contain oily domains, such as micelles, liposomes, emulsions, and nanoemulsions, can improve its stability and bioavailability [92, 93, 96, 132]. This effect has mainly been attributed to the higher chemical stability of curcumin in oily environments than in aqueous environments [256]. Usually, curcumin has to be dissolved within the oil phase of an emulsion or nanoemulsion before homogenization is carried out [63]. Nevertheless, there are situations where it would be advantageous to load curcumin into the oil phase of pre-existing colloidal particles. For instance, if one wanted to load curcumin into a naturally occurring colloidal dispersion (such as oil bodies from plants or animals) or if wanted to avoid chemical degradation during the homogenization process. A number of studies have shown that this can be achieved using the pH-shift method [51, 92, 93, 96]. This method uses pH to control the water-solubility of curcumin[92, 93]. At relatively low

pH values (pH < 8), curcumin is a neutral hydrophobic molecule that has a relatively low water-solubility. Conversely, at relatively high pH values, the hydroxide groups on curcumin become deprotonated, which leads to an increase in its negative charge, polarity, and water-solubility. In the presence of a colloidal dispersion containing oily domains, curcumin can therefore be driven from the water phase to the oil phase by adjusting the pH from highly alkaline to slightly acidic. Previous studies have shown that this process is simple and rapid to carry out and does not lead to appreciable degradation of the curcumin [51, 94, 96].

The purpose of the current study was to determine whether the pH-shift method could be used to successfully load curcumin into dairy milk products, and then to establish the physicochemical stability and *in vitro* bioaccessibility of the resulting systems. Our motivation was that cow's milk is already a widely and routinely consumed beverage and would therefore be a highly suitable delivery vehicle for incorporating beneficial nutraceuticals into consumers' regular diets.

7.2. Materials & Methods

7.2.1 Materials

Powdered curcumin (C2302, purity 95%) was purchased from the TCI chemical company (Portland, OR). Ultra-pasteurized dairy creamer (10% w/v fat) was obtained from a local supermarket (HP Hood LLC, Lynnfield, MA). The following chemicals were purchased from Fisher Chemicals (Fair Lawn, NJ): sodium hydroxide (SS266), hydrochloric acid (83.3 mM) and dimethyl sulfoxide (BP231). Fluorescein isothiocyanate isomer I (FITC, F1250), Nile Red (N3013), and sodium azide (S2002) were purchased from the Sigma-Aldrich Chemical Company (St. Louis, MO).

The *Nutrition Facts* label of the dairy creamer reported a serving size to be 30 mL, which contained: 30 kCal; 3 g total fat; 1 g total carbohydrate (1g sugar); < 1g protein, 2%DV for vitamin A; and 4% DV for calcium. The ingredients listed on the product label were: milk and cream with disodium phosphate.

7.2.2 Preparation protocol

Blank dairy milk

Initially, the original dairy milk sample was adjusted to a range of pH values (2 to 10) using HCl or NaOH solutions to examine its suitability for carrying out curcumin loading using the pH-shift method. After 3 hours, the particle characteristics of the milks were measured using the techniques described later.

Curcumin-loaded dairy milk

Curcumin-loaded dairy milk was prepared using the pH-shift method, and the particle characteristics were measured before and after loading. Initially, curcumin powder was dissolved in an alkaline solution (0.2N NaOH) at room temperature for 1 min. This curcumin stock solution was then added into the dairy milk and the pH was quickly adjusted back to the target value (pH 6.5, 7 and 8). Double-distilled water was then added to the curcumin-loaded milks to reach a final oil content of 5% oil. A non-food grade preservative, sodium azide (0.02%), was added to the final samples to inhibit microbial growth. The curcumin-loaded milks were then stirred for 10 min at room temperature in the dark to ensure their homogeneity.

7.2.3 Storage study

The impact of storage pH and temperature on the stability of the curcumin-loaded milk was investigated. The influence of pH (6.5, 7 and 8) on particle characteristics and curcumin stability within the milk was determined by storing the samples at 4 ºC for 60 days. This pH

range was selected to represent those typically found in commercial dairy milks. The sample with the best stability was selected to determine the influence of storage temperature on the stability of the curcumin-loaded milk (4, 20, 37 and 55 ºC). To avoid evaporation, contamination, and photodegradation, an aliquot of each sample (10 mL) was transferred into a glass test tube, sealed with a cap and parafilm, and then stored in the dark. Finally, samples were collected and analyzed at selected periods throughout the storage period.

7.2.3.1 Optical properties

The appearance of the curcumin-loaded milks was characterized using both a digital camera and an instrumental colorimeter (ColorFlex EZ 45/0-LAV, Hunter Associates Laboratory Inc., Virginia, USA). The colorimeter measures the color of the samples under standardized light conditions and then reports it using the CIE tristimulus system: L*, a*, and b*. Here, *L** represents lightness (0) to darkness (100), *a** represents red (+) to green (-), and, *b** represents yellow (+) to blue (-). An aliquot of each sample (10 mL) was transferred into a medium-size disposable petri dish, and then analyzed using D65 artificial daylight (10 standard angles) against a black background.

7.2.3.2 Particle characterization

The particle characteristics of the samples were determined using a laser diffraction particle size analyzer (Mastersizer 2000; Malvern Instruments, Worcestershire, UK) and a particle electrophoresis device (Nano-ZS, Malvern Instruments, Worcestershire, UK). The laser diffraction instrument was used to measure the mean particle diameter (D_{32}) of the samples, while the particle electrophoresis device was used to measure the surface potential (ζ-potential) of the samples. All samples were diluted with double-distilled water (adjusted to the same pH as

the sample) prior to measurement to ensure light waves could pass through them and avoid multiple scattering.

7.2.3.3 Microstructure analysis

The microstructures of the samples were investigated using confocal scanning fluorescence microscopy (Nikon D-Eclipse C1 80i, Nikon, Melville, NY). Samples were stained with Nile red (1mg / mL ethanol) and FITC (1 mg / mL DMSO) to highlight the location of lipids (red region) and proteins (green region). All images were obtained with a 10× eyepiece and a 20× objective lens, giving an overall 200× magnification.

7.2.4 Simulated gastrointestinal study

A simulated gastrointestinal tract (GIT) model was used to evaluate the gastrointestinal fate (stability and bioaccessibility) of the curcumin within the milk samples. The GIT model consisted of simulated mouth, stomach, and small intestine phases, and was slightly modified from our previous study [243].

Initially, the curcumin-loaded milk entered the simulated mouth phase. Here, the sample (15 mL) was pre-warmed (37 ºC) and mixed with pre-warmed (37 ºC) simulated artificial saliva fluid (15 mL), which contained 3 mg/mL mucin. The mixture was then adjusted to pH 6.8 and incubated in a temperature-controlled shaking incubator (100 rpm, 37 ºC) for 30 seconds (Innova Incubator Shaker, Model 4080, New Brunswick Scientific, New Jersey, USA). The bolus sample resulting from the mouth phase was then exposed to simulated gastric conditions. A pre-heated (37 ºC) simulated gastric fluid (30 mL), which contained 3.2 mg/ mL pepsin, was added to the bolus sample and then the pH was adjusted to 2.5. The resulting mixture was placed back into the same shaking incubator at the same settings for 2 hours. The chyme sample resulting from the stomach phase (60 mL) was then exposed to the small intestinal phase. Pre-heated (37 ºC)

simulated intestinal fluid (3 mL) and bile salt solution (7 mL) were added to the chyme sample with continuous stirring, and then the pH was adjusted to 7.0. Finally, freshly prepared pancreatic lipase solution (5 mL) was transferred into the sample and the pH was quickly adjusted back to 7.0. The bile salt solution was prepared by dissolving porcine bile extract (53.57 mg/mL) into the phosphate buffer solution (5 mM, pH 7.0). The pancreatic lipase solution was prepared by adding pancreatic lipase (0.16 mg/mL) into phosphate buffer solution (5 mM, pH 7.0). An automatic titration unit (Metrohm, USA Inc.) was used to monitor and maintain the sample at pH 7.0 by titrating NaOH (0.25 N) solution for 2 hours at 37 ºC.

7.2.5 Curcumin concentration determination

The concentration of curcumin within the milk samples was determined using UV/visible spectrophotometry. An acidified dimethyl sulfoxide solution (0.1% v/v 6N HCl) was used to extract curcumin from the milk samples. A UV/Vis-spectrometer (Genesys 150, Thermos Fisher Scientific, Madison, WI) was utilized to measure the absorbance of the extracted curcumin solution at a wavelength of 420 nm. Finally, the curcumin concentration was determined by using the measured absorbance value and a standard curve prepared using curcumin solutions of known concentration.

7.2.6 Encapsulation efficiency

The encapsulation efficiency of the curcumin-loaded milks was calculated using the following expression:

$$\textit{Encapsulation Efficiency} = 100 \times C_E / C_I \quad (1)$$

Here, C_I is the total curcumin concentration initially added to the milk and C_E is the curcumin concentration remaining after preparation using the pH-shift method.

7.2.7 Stability and bioaccessibility

The stability and bioaccessibility of the curcumin in the milk samples was measured after they had been passed through the simulated GIT model. After the small intestine stage, the digest was collected and divided into two portions: (i) *Digest portion*: the curcumin concentration (C_D) in one portion was measured directly using the UV/Vis spectrophotometry method; (ii) *Micelle portion*: the curcumin in the supernatant of the other portion (C_M) was measured after it had been centrifuged at 18,000 rpm at 25 ºC for 50 min (Thermo Scientific, Waltham, MA). This latter portion was considered to represent the amount of curcumin that had been solubilized within the mixed micelles generated during digestion. The bioaccessibility and stability of the curcumin-loaded milk samples were then calculated using the following expressions:

$$Bioaccessibility\ (\%) = 100\ \times \frac{C_M}{C_D} \quad (2)$$

$$Stability(\%) = 100\ \times \frac{C_D}{C_I} \quad (3)$$

The *Bioaccessibility* represents the fraction of curcumin solubilized in the mixed micelle phase, which is potentially available for absorption. The *Stability* represents the total amount of curcumin that survived after the milk was passed through the simulated GIT[274].

7.2.8 Kinetics of curcumin degradation

The kinetics of curcumin degradation within the milk samples during storage were modelled using the Arrhenius equation:

$$k = A\ e^{-Ea/RT} \quad (4)$$

Here, k is the rate coefficient, A is the Arrhenius constant, E_a is the activation energy, R is the universal gas constant (8.314×10^{-3} kJ mol^{-1} K^{-1}); and T is the absolute temperature (K).

7.2.9 Statistical analysis

The mean ± standard deviation was calculated from measurements made on at least three freshly prepared samples. Mathematical software (SPSS version 6.0) was used to calculate the statistical differences and considered as significantly different when the p-value was lower than 0.05.

7.3. Results and discussions

7.3.1 Influence of pH on particle characteristics of blank dairy milk

Initially, the characteristics of the original dairy milk were analyzed. Visually, the milk had a light milky appearance, which can be attributed to light scattering by the milk fat globules and casein micelles it contained. The milk had a pH value of 6.8. The particles in the milk had a relatively small mean diameter (D_{32} =396 ± 5 nm) and high negative surface potential (ζ = -40.1 ± 1.3 mV). This high negative charge can be attributed to the adsorption of anionic surface-active species, such as milk phospholipids and proteins above their isoelectric point (such as casein and whey proteins).

The influence of pH on the physical stability of the milk was evaluated to determine whether it was suitable for preparing curcumin-loaded milks using the pH-shift method, since this method requires that the fat globules remain stable to aggregation under both neutral and highly alkaline conditions. Samples of the milk were adjusted to different pH values (pH 3 to 10), and then their physical stability was determined after they were stored at room temperature for several hours (Fig. 1). The digital photography images showed that the milk samples exposed to different pH values all had a homogenously white appearance. At pH 3 to 5, however,

the milk samples were more likely to stick to the sides of the test tube walls than at higher pH values (Fig. 1a). This phenomenon can be attributed to changes in the aggregation state of the particles as the pH was varied. The laser diffraction measurements show that the mean particle diameter of the milk samples were relatively small from pH 10 to 6 (D_{32} < 1 □m), but relatively large at lower pH values (D_{32} > 15 nm) (Fig. 1b). These results indicate that extensive fat globule aggregation occurred in the milk particles under acidic conditions. The surface potential (ζ-potential) of the milk fat globules was relatively high and negative from pH 10 to 5 but then became positive when the pH was reduced further, with a point of zero charge around pH 4.3 (Fig.1c). This effect can be attributed to the presence of milk proteins (mainly casein and whey) at the surfaces of the fat globules, which have an isoelectric point between 4 and 5. The high negative charge observed from pH 6 to 10 should be sufficient to generate a strong electrostatic repulsion, which inhibits droplet aggregation. Presumably, the milk fat globules irreversibly aggregate when the pH is around the isoelectric point of the adsorbed protein layer because the electrostatic repulsion between the droplets is weakened.

Overall, these results show that the dairy milk should remain physically stable from pH 6 to 10, which is suitable for application of the pH-shift method.

Fig.1

a.

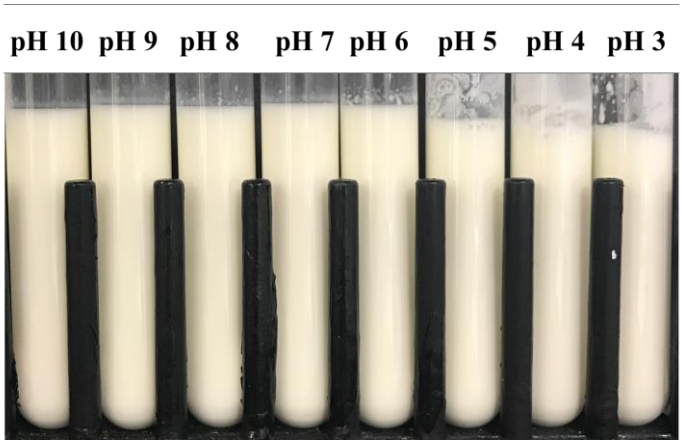

b.

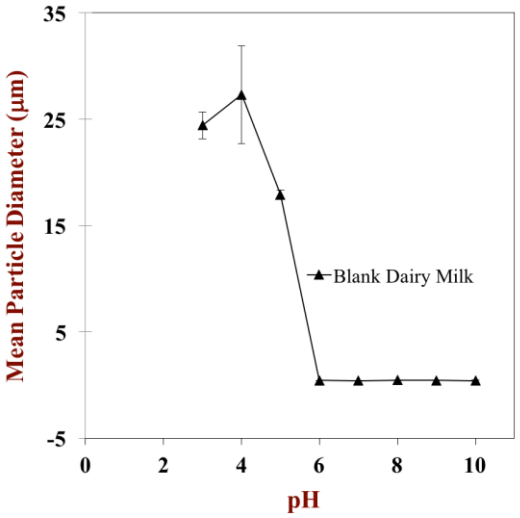

c.

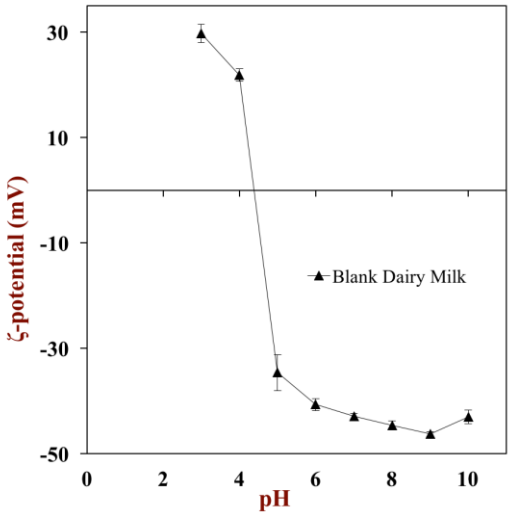

Fig. 1 a) Impact of pH on appearance of blank dairy milks; b) Impact of pH on electrical characteristics (ζ-potential) of blank dairy milks; and c) Impact of pH on mean particle diameter (D_{32}) of blank dairy milks.

Fig.2

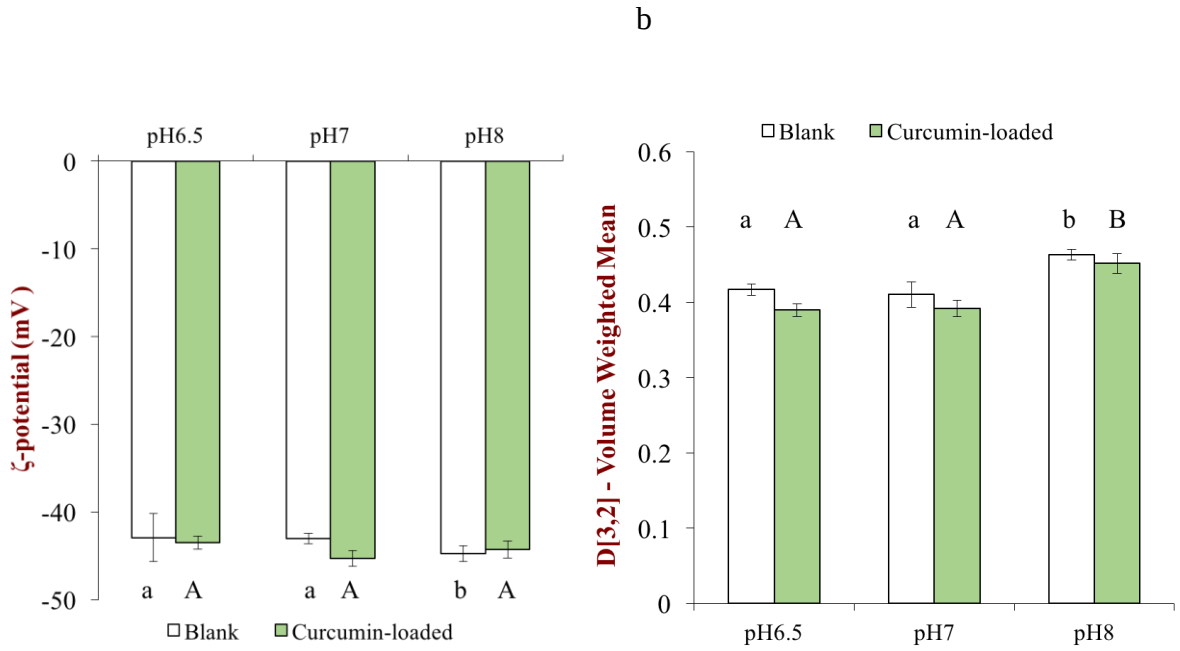

Fig. 2 the a) electrical characteristic (ζ- potential) and b) mean particle diameter (D_{32}) of the blank dairy milk with curcumin-loaded dairy milks under pH 6.5, 7 and 8. Different lowercase letters mean significant different (Duncan, $p< 0.05$) within the same type of dairy milks; different capital letter represents the significantly different between two types of sample (Duncan, $p< 0.05$).

7.3.2 Influence of pH-shift method on milk properties

In this section, the suitability of the pH-shift method for loading curcumin into the milk samples was investigated. Moreover, the impact of a limited range of pH values (pH 6.5, 7, and 8) on the appearance, physical stability, and encapsulation efficiency of the milks was examined because commercial products may have aqueous phases that fall within this range.

7.3.2.1 Appearance

Digital photography and instrumental colorimetry measurements were used to characterize the general appearance and overall color of the curcumin-loaded milk (Fig. 3a & Table 1). The photography images showed that the milk fat globules in all the curcumin-loaded

milk samples were homogenously distributed throughout the tubes, without any evidence of phase separation (Fig. 3a). The milks had a cloudy yellow color at pH 6.5 and 7, but a more orangey color at pH 8. The instrumental colorimeter measurements also indicated that the color of the emulsions depended their pH (Table 1). At pH 6.5 and 7, the curcumin-loaded milks had similar color coordinates, which were indicative of a creamy yellow appearance: L^* (≈ 87), a^* (≈ -11), and b^* (≈ +79). At pH 8, the milks had a lower whiteness (L^* ≈ 83), greenness (a^* ≈ -4), and yellowness (b^* ≈ 74) than at lower pH values. This color change can be attributed to pH-dependent changes in the structural arrangement (and therefore absorption spectrum) of the curcumin molecules. When the pH of curcumin reaches its first pK_a value (around 7.5 to 8.5), the color of the curcumin changes from yellow to orange due to deprotonation of one of the curcumin hydroxyl groups[1, 13, 255]. Our results show that it is important to carefully control the pH of a milk sample to obtain a consistent color. Alternatively, this phenomenon could be used to create curcumin-loaded milks with different colors.

Table 1

	pH 6.5	**pH 7**	**pH 8**
Initial curcumin concentration (μg/mL)	230.8 ± 6.5[a]	233.0± 6.2 [a]	232 ± 11 [a]
Loading capacity (%)	92.3 ± 2.4 [a]	93.2 ± 2.2 [a]	92.7 ± 4.0 [a]
D_{32} (μm)	0.39 ± 0.01 [a]	0.39 ± 0.01 [a]	0.45 ± 0.01 [b]
ζ- potential (mV)	-43.5 ± 1.3 [b]	-45.30 ± 0.91 [a]	-44.3 ± 1.0 [ab]

Table 1. Influence of pH on the physical and chemical properties of curcumin-loaded dairy milk: the initial curcumin concentration, loading capacity, mean particle diameter (D_{32}), and electrical characteristics (ζ- potential). The different letters represent significant differences between the samples (Duncan, $p < 0.05$).

7.3.2.2 Curcumin concentration

The encapsulation efficiency (EE) of curcumin within the milk after using the pH-shift method was also investigated using a fixed amount of curcumin (250 μg/mL). All the curcumin-loaded milk samples had a relatively high and fairly similar amount of curcumin trapped within them, *i.e.,* 92 to 93 % (Table 1). This result indicates that the pH-shift method can be used to successfully load curcumin into samples containing milk fat globules.

7.3.2.3 Particle characteristics

The impact of loading the curcumin into the milk samples on their particle characteristics was also investigated. The pH-shift method did not have a significant impact on the surface potential of the milks (Fig. 2a). Surprisingly, the mean particle diameters of the curcumin-loaded milks were slightly smaller than the blank milks (Fig. 2b), which may have been because the pH-shift method reduced the interfacial thickness or degree of aggregation of the milk fat globules. Photography images of the curcumin-loaded milks showed they all had a homogenous creamy yellow appearance, regardless of the pH value (Fig. 3a). These results indicate that the pH-shift method does not promote aggregation or phase separation of the milk fat globules during the curcumin loading process. The microstructure images of the curcumin-loaded milks also confirmed this (Fig. 3b). All the milk samples contained relatively small milk fat globules (stained red) that were uniformly distributed throughout an aqueous medium containing protein (stained green).

7.3.3 Effect of pH on storage stability of curcumin-loaded milk

Commercially, it is important that milk-based products have a shelf life that is sufficiently long. The physicochemical stability of the curcumin-loaded milks was therefore monitored during storage for 60 days at 4 ºC in the dark (pH 6.5, 7.0 and 8.0). This relatively low

temperature was selected because the milks would be expected to be stored in a commercial or domestic refrigerator prior to utilization.

7.3.3.1 Appearance

Digital photography images were used to monitor changes in the appearance of the milk samples after storage (Fig. 3a). These images showed that the milks all remained evenly distributed through the test tubes after storage, indicating that aggregation and phase separation of the milk fat globules had not occurred during storage. At pH 6.5 and 7.0, the milks had creamy yellow colors that were very similar to the initial samples. At pH 8.0, the orange color of the milk samples was slightly less intense, which is indicative of some curcumin degradation during storage.

Table 2

		pH 6.5	pH 7	pH 8	4 °C	20 °C	37 °C	55 °C
Before Storage	*L**	87.42 ± 0.34^{cA}	86.98 ± 0.12^{bA}	83.0 ± 0.5^{aA}	87.0 ± 0.1^{aB}	87.0 ± 0.1^{aB}	87.0 ± 0.1^{aB}	87.0 ± 0.1^{aB}
	*a**	-11.6 ± 1.2^{aA}	-11.10 ± 0.21^{aA}	-4.27 ± 0.20^{bA}	-11.1 ± 0.2^{aA}	-11.1 ± 0.2^{aA}	-11.1 ± 0.2^{aA}	-11.1 ± 0.2^{aA}
	*b**	79.2 ± 1.7^{cA}	78.71 ± 0.37^{bA}	74.6 ± 0.7^{aA}	78.7 ± 0.4^{aA}	78.7 ± 0.4^{aA}	78.7 ± 0.4^{aB}	78.7 ± 0.4^{aB}
After Storage	*L**	87.4 ± 0.1^{bA}	87.27 ± 0.12^{bB}	83.8 ± 0.1^{cA}	86.4 ± 0.2^{dA}	86.0 ± 0.2^{cA}	85.6 ± 0.2^{bA}	84.6 ± 0.1^{aA}
	*a**	-10.3 ± 0.1^{aA}	-8.68 ± 0.26^{bB}	-3.87 ± 0.15^{cB}	-9.70 ± 0.23^{bcB}	-9.53 ± 0.06^{cB}	-10.3 ± 0.4^{aB}	-9.84 ± 0.20^{bB}
	*b**	79.6 ± 0.2^{bA}	80.07 ± 0.22^{a}	76.7 ± 0.2^{cB}	78.6 ± 0.3^{cA}	78.26 ± 0.09^{cA}	76.1 ± 0.4^{bA}	65.3 ± 1.0^{aA}

Table 2. influence of pH and temperature on the tristimulus color value (*L**, *a**, and *b**). Left hand part of table: impact of pH on color values before and after 60 days' incubation at 4 ºC; Right hand part of table: impact of temperature on color values before and after 15-day incubation at pH 7. The different lower-case letters represent significant differences between samples (between pHs or temperature) (Duncan, $p < 0.05$). The different capital-case letter represent significant difference before and after storage (Independent-Sample T-test, $p < 0.05$).

The instrumental color coordinates of the curcumin-loaded milks were also measured to detect any changes in the appearance of the samples before and after storage (Table 2). The lightness (L^*) values of the stored samples were similar to those of the fresh samples, which suggests there was little change in light scattering by the milk fat globules. The a*-values of all the milk samples became slightly less negative (less green) after storage, whereas the b*-values became slightly more positive (more yellow). Overall, our results suggest that the milk samples remained relatively stable to color fading during storage for two months under refrigeration conditions, which would be important for their commercial application.

Fig. 3

a

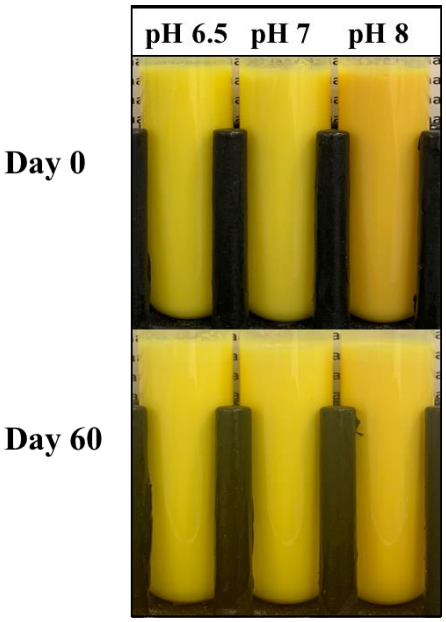

b

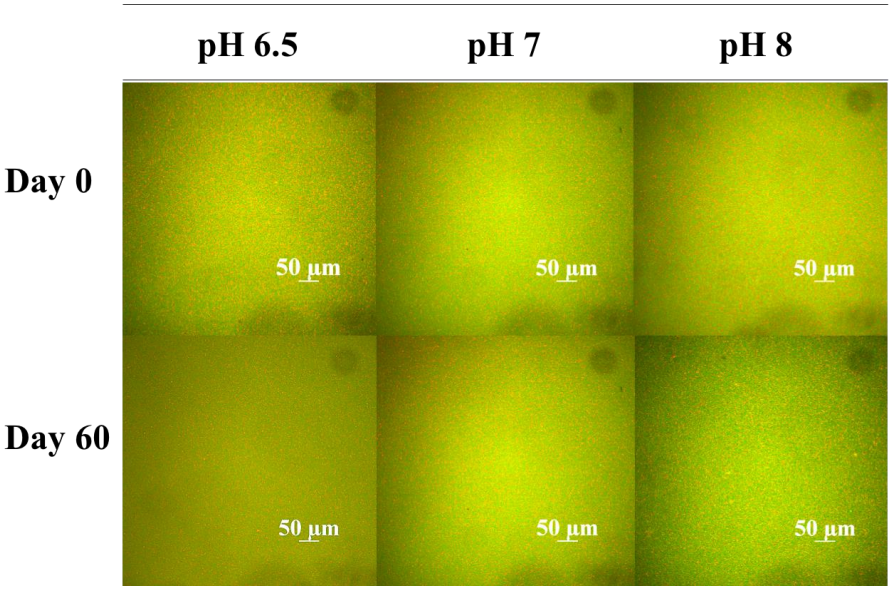

Fig 3. a) The appearances and b) microstructures of curcumin-loaded dairy milks before and after storage at various pH values at 4 ºC for 60 days. The microstructure images were obtained using confocal fluorescence microscopy and the scale bars are 100 um.

7.3.3.2 Curcumin concentration

The chemical stability of the curcumin in the milks was also investigated throughout storage under refrigeration conditions (Fig. 4b). After 60-day incubation at 4 ºC, the majority of the curcumin was still present in all the milk samples, regardless of storage pH: 88 ± 3% at pH 6.5; 88 ± 2% at pH 7; and, 87 ± 2% at pH 8. This result suggests that the encapsulated curcumin was relatively stable to chemical degradation at all pH values studied under refrigeration conditions.

7.3.3.3 Particle characteristics

For commercial products, it is important that the milk fat globules do not aggregate and cream during storage. For this reason, the influence of pH on the particle characteristics of the milks was also evaluated throughout refrigerated storage (Fig. 5). These results showed that the curcumin-loaded milks remained physically stable during storage, with little change in mean

particle diameter (Fig. 5a) or ζ-potential (Fig. 5b). These results therefore support the visual observations discussed earlier (Fig. 3). Presumably, the high negative charge on the milk fat globules generated a strong electrostatic repulsion that inhibited their aggregation. As a result, the particles in the milk remained relatively small, which also inhibited their gravitational separation.

Fig. 4

a b

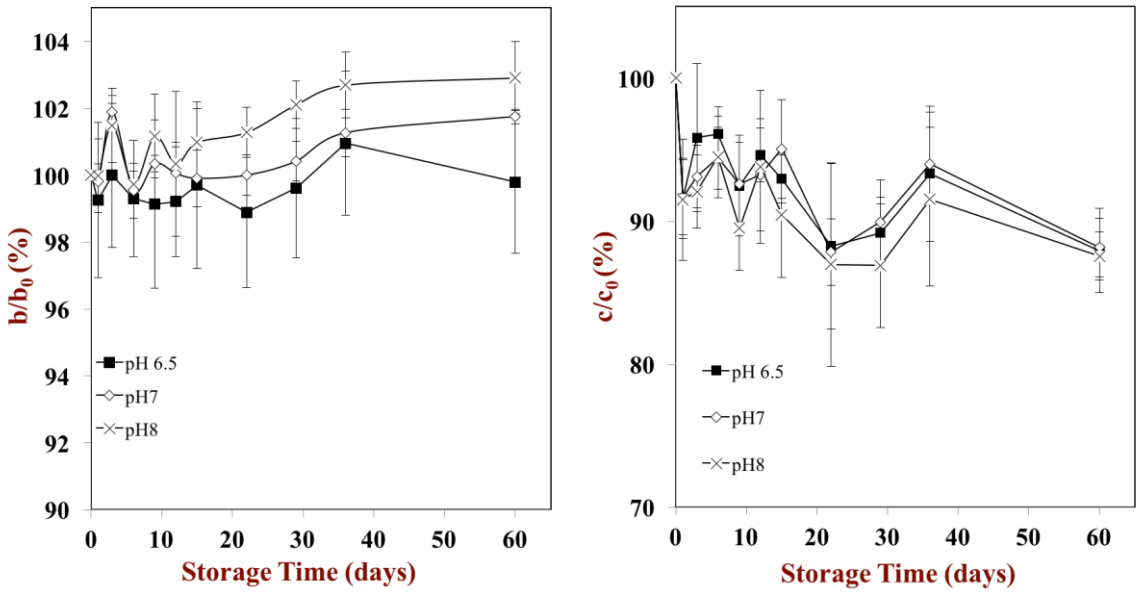

Fig. 4. Influence of pH on a) the yellow color (*b**) and b) curcumin degradation of curcumin within the dairy milks during 4 ºC storage for 60 days.

Fig. 5

a. b

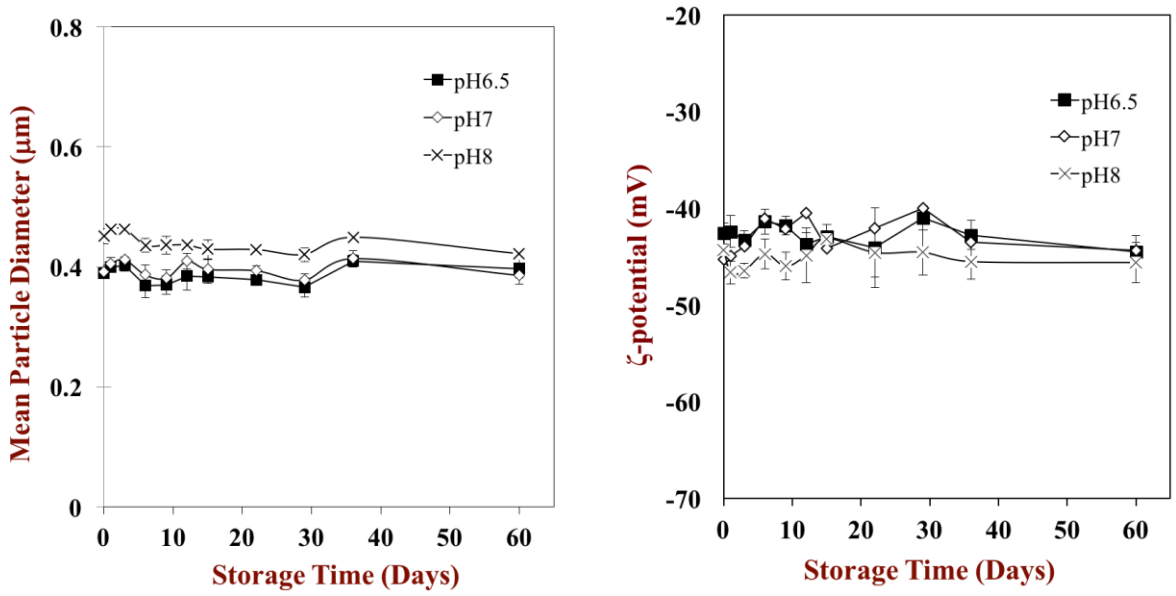

Fig. 5. Influence of pH on the a) mean particle diameters (D_{32}) and b) electrical characteristics (ζ- potential) of curcumin-loaded dairy milk during 4 ºC storage for 36 day

7.3.4 Effect of storage temperature on the stability of curcumin-loaded milk

In principle, milk products may experience a range of different temperatures during their production, storage, and utilization. For this reason, we examined the impact of storage temperature on the physical and chemical stability of the curcumin-loaded milk. The milk samples (pH 7.0) were poured into sealed containers and then stored at 4, 20, 37, and 55 ºC for 15-days in the dark.

7.3.4.1 Appearance

There were noticeable changes in the appearance of the curcumin-loaded milks after storage, which depended on the storage temperature employed (Fig. 6a). In particular, there was evidence of color fading and gravitational separation in some of the samples. The extent of color

fading increased as the storage temperature was raised, with the greatest degree of color fading being observed at 55 ºC. The extent of gravitational separation also increased with increasing storage temperature. There was no visible evidence of phase separation during storage at 4 and 20 ºC, but a thick cream layer was observed at the surface of the samples stored at 37 and 55 ºC. This effect was attributed to the upward movement of aggregated milk fat globules due to the gravitational forces acting upon them.

Instrumental colorimetry measurements also indicated that there were temperature-dependent differences in the color stability of the curcumin-loaded milks during storage. The L^*, a^* and b^* values of the milks before and after storage are given in Table 2. The lightness (L^*) and greenness (a^*) of the milks remained fairly constant throughout storage at all temperatures, with only slight decreases being observed (Table 2). On the other hand, the yellowness (b^*) of some of the milks decreased appreciably during storage, suggesting that there was some chemical degradation of the curcumin that led to color fading. For this reason, the change in the relative yellowness (b^*/b_0^*) of the samples was plotted over time to provide an indication of the kinetics of color fading (Fig.7a). The rate of color fading increased with increasing storage temperature: 4 ºC ≈ 20 ºC > 37 ºC >> 55 ºC (Fig. 7a). After 15 days storage, there was no color fading in the milk samples stored at 4 and 20 ºC, about 4% in the samples stored at 37 ºC, and about 16% in the samples stored at 55 ºC. These results suggest that the curcumin-loaded milks will remain stable to color fading provided that they are stored at sufficiently low temperatures (≤ 20 ºC), which is important for commercial applications.

Fig. 6

a.

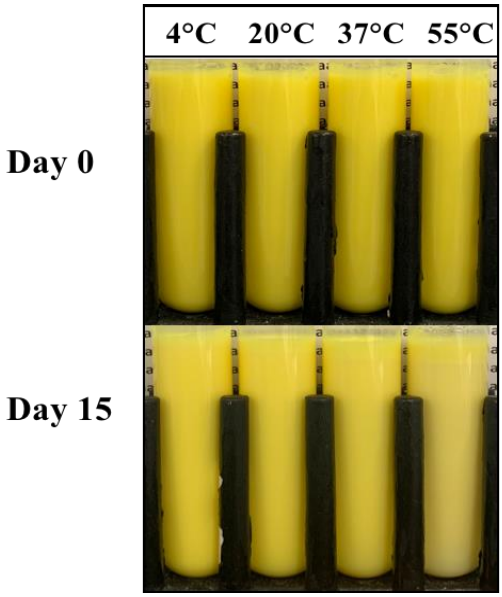
4°C
20°C
37°C
55°C
Day 0
Day 15

b.

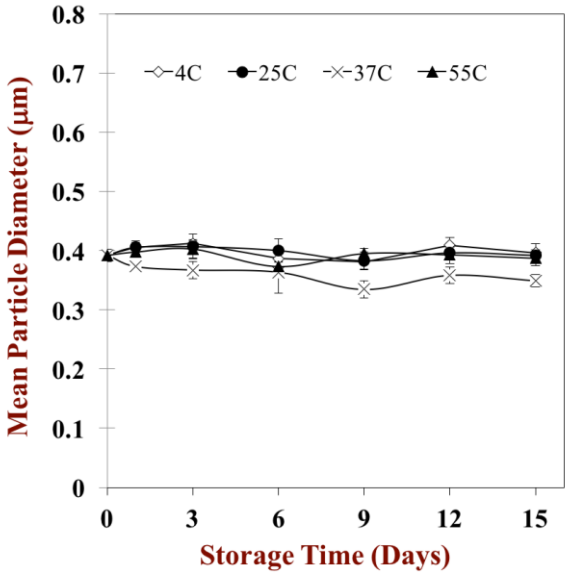
Mean Particle Diameter (µm)
0.8
0.7
0.6
0.5
0.4
0.3
0.2
0.1
0
4C
25C
37C
55C
0
3
6
9
12
15
Storage Time (Days)

c.

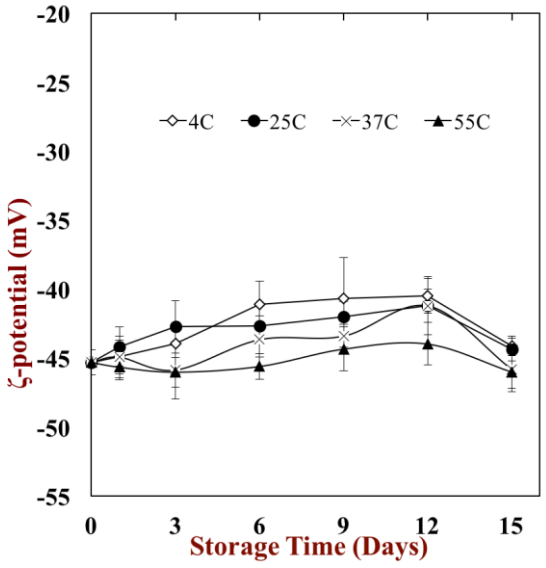
ζ-potential (mV)
-20
-25
-30
-35
-40
-45
-50
-55
4C
25C
37C
55C
0
3
6
9
12
15
Storage Time (Days)

d.

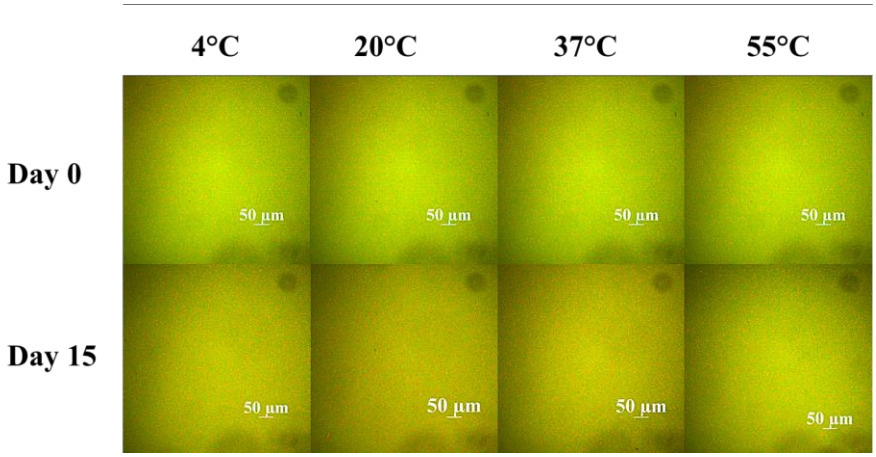

Fig. 6 Influence of temperatures on the a) appearances of curcumin-loaded dairy milk before and after 15-days storage. The impact of temperature on b) mean particle diameters (D_{32}) and c) electrical characteristics (ζ- potential) of curcumin-loaded dairy milks during 15-days storage. d) the microstructure of curcumin-loaded dairy milks before and after incubated under four different temperatures and a length of 100 um scale bars were applied.

7.3.4.2 Curcumin concentration

Changes in the curcumin concentration of the milks during storage were also measured to investigate the impact of storage temperature on curcumin stability (Fig. 7b). The observed rate of curcumin degradation increased with increasing storage temperature. For instance, after 15-days storage, about 4%, 10%, 22% and 47% of the curcumin had degraded at 4, 20, 37, and 55 ºC, respectively. These results suggest that elevated storage temperatures accelerate the chemical degradation of curcumin, which is obviously undesirable for commercial applications of functional food products.

Fig. 7

a. b.

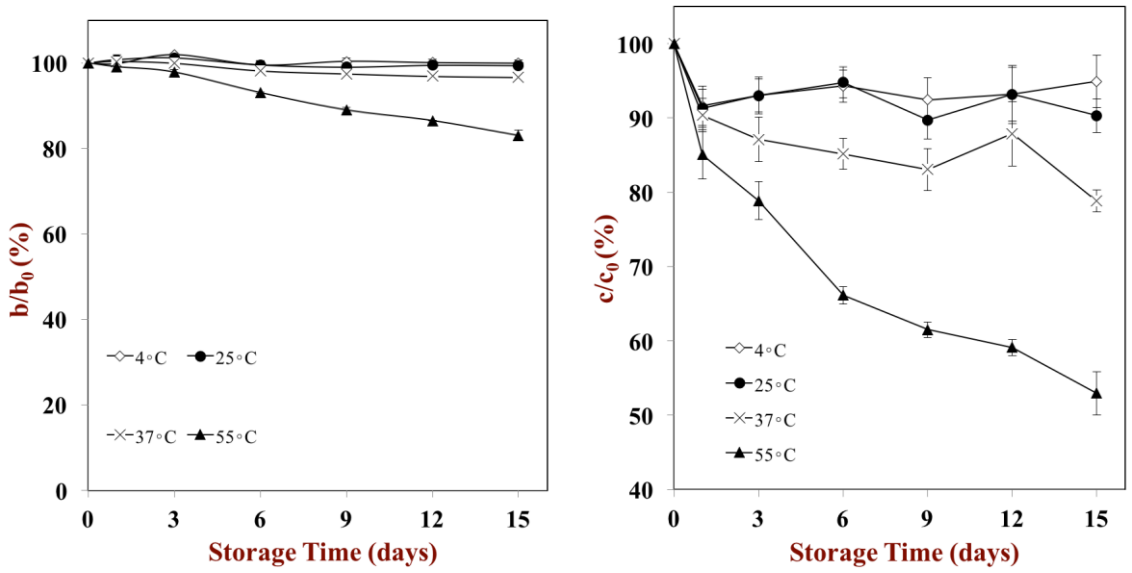

Fig. 7 Influence of temperature on the a) yellow color (b^*) and b) curcumin content of curcumin within the dairy milk system were determined during 15-days storage.

More quantitative information about the kinetics of curcumin degradation in the milk samples were obtained by fitting the experimental data with the re-arranged Arrhenius equation:

$$\ln(k) = \ln(A) - \frac{E_A}{RT} \qquad (5)$$

The activation energy (E_A) was calculated by plotting the logarithm of the reaction rate constant (k) against the reciprocal of the absolute temperature (1/T) (Fig. 8). The reaction rate was determined at each temperature from plots of curcumin concentration *versus* time, assuming a first-order reaction, *i.e.*, $C/C_0 = \exp(-kt)$. This analysis indicated that the activation energy for curcumin degradation was around +51.6 kJ/mol and the ln(A) value was around 15.6 (when time

expressed in days). The half-time was defined as the time required for the curcumin to degrade by 50%, which is given by the following expression:

$$t_{1/2} = -\frac{\ln(0.5)}{k} \quad (6)$$

Assuming the data can be extrapolated to higher temperatures, which needs to be verified experimentally, the calculated half-times for curcumin degradation are 184, 47, 14, 5.0 and 1.9 days for 20, 40, 60, 80, and 100 ^{o}C, respectively. This information may be useful for predicting the stability of the curcumin under different thermal processing and storage conditions.

Fig. 8

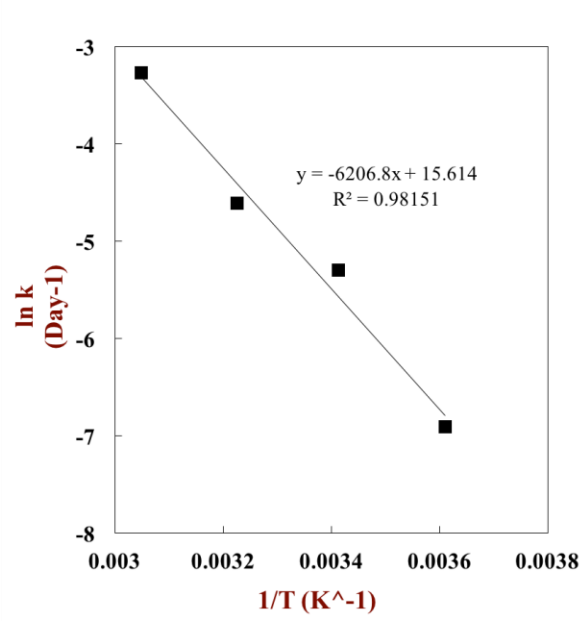

Fig. 8 the Arrhenius equation graph of curcumin within the dairy milks system, which represents the temperature dependence on chemical reaction rate of curcumin

7.3.4.3 Particle characteristics

The impact of storage temperature on the characteristics of the particles in the milk samples were also evaluated (Fig. 6b & 6c). The measured mean particle diameter of the particles remained relatively small throughout storage ($D_{32} \approx 400$ nm) while the ζ-potential remained relatively high and negative ($\zeta \approx -45$ mV). The confocal microscopy images suggested that the fat globules remained evenly spread throughout the samples at all temperatures (Fig. 6d). Taken together these results suggest that storage temperature did not have a major impact on the surface chemistry or aggregation stability of the milk samples. However, this is somewhat inconsistent with the appearance of the milk samples held at the higher storage temperatures, which exhibited some creaming after storage (Fig. 6a). This may have been an experimental artefact associated with sample preparation. For the laser diffraction and confocal microscopy measurements, the samples were inverted a few times to ensure they were homogeneous prior to collecting an aliquot for analysis. This process may have disrupted any weak flocs in the milk samples, thereby releasing the individual milk fat globules.

7.3.5 Curcumin bioaccessibility and stability during simulated digestion

Finally, two of the main factors expected to impact curcumin bioavailability in the milk samples, namely bioaccessibility and stability, were investigated using a well-established simulated gastrointestinal tract (GIT) model [257, 258]. The bioaccessibility and stability of the curcumin-loaded milk (pH 7.0) samples were measured before and after they were stored at 4 ºC for 60-days (Table 3). As mentioned earlier, the total concentration of curcumin in the milk samples was reduced by about 13% (from 233 to 205 ug/mL) after storage due to some chemical degradation of the polyphenol (Fig. 4b). This phenomenon accounts for the fact that the total

curcumin concentrations in the digest and mixed micelle fractions were higher before storage than after storage (Table 3). After exposure to simulated GIT conditions, the stability of the curcumin in the samples was higher before storage (89%) than after storage (71%), but the bioaccessibility was similar (around 40 %). The stability represents the amount of curcumin that survived after exposure to simulated mouth, stomach, and small intestinal conditions. Our results suggest that the aged curcumin was more susceptible to degradation than the fresh curcumin, although the origin of this effect is currently unknown. The bioaccessibility represents the fraction of curcumin in the small intestine phase that is solubilized within the mixed micelle phase, and thus available for absorption. The chemical stability of the curcumin should not therefore impact this value because it is a ratio of two curcumin concentrations in the small intestine. Overall, our results suggest that the curcumin has a relatively high bioavailability both before and after storage. In future, it would be useful to test these systems using animal and human feeding studies to establish the overall bioavailability, which also depends on the metabolism, absorption, and excretion of the curcumin [63].

Table 3

	C_{Digest} (ug/mL)	$C_{Micelle}$ (ug/mL)	Stability (%)	Bioaccessibility (%)
Before Storage	217 ± 19^{B}	89 ± 28^{A}	89.6 ± 3.0^{B}	41 ± 11^{A}
After Storage	160 ± 4^{A}	61 ± 11^{A}	71.0 ± 1.9^{A}	38.0 ± 8.1^{A}

Table 3. The curcumin concentration within the digest phase (C_{Digest}), the curcumin concentration within the mixed micelle phase, the stability and bioaccessibility of curcumin-loaded dairy milk at pH7 that determined before and after storage using a stimulated gastrointestinal tract. The different letters represent significant differences before and after storage (Independent-Sample T-test, $p < 0.05$).

7.3.6 Conclusions

In conclusion, we have shown that curcumin can be successfully loaded into pre-existing milk fat globules using the pH-shift method, and that the resulting curcumin-loaded milks have good chemical and physical stability under various storage conditions. For instance, around 88 % of the curcumin remained in the milk samples after storage under refrigerator temperatures for 60 days. Moreover, there was no evidence of aggregation or creaming of the milk fat globules when they were stored under these conditions. A study of the impact of storage temperature on the stability of the curcumin-loaded milk samples showed that they were both chemically and physically stable at 4 and 20 ºC, but unstable at 37 and 55 ºC. We also showed that the curcumin-loaded milks had relatively good bioaccessibility (40%) under simulated gastrointestinal conditions. The information obtained in this study may be useful for the rational design of a new range of curcumin-fortified functional food products based on dairy milk. Future research, however, is still needed to establish the bioavailability of the curcumin in these products using animal or human feeding studies.

8. Conclusions and Future Directions

This research has shown that emulsion-based delivery systems can overcome the low solubility, poor chemical stability, and low bioaccessibility of curcumin in foods. It was demonstrated that a new organic solvent-free pH-driven method was particularly suitable at introducing curcumin into a variety of colloidal delivery systems, including nanoemulsions, soymilk, and dairy milk. This technique gave a high encapsulation efficiency and produced delivery systems that had a high bioaccessibility. The delivery systems developed in this study may be used by the food, supplement, and pharmaceutical industries to incorporate curcumin into a diverse range of products designed to improve human health.

Future work should focus on examining the efficacy of these delivery systems when used in real food applications such as different food matrices and storage/processing conditions. For example, the poor light stability of curcumin is a major challenge in food products with transparent packaging, such as soft drinks and other beverages. Therefore, investigations of the photostability of curcumin-loaded colloidal delivery systems would be useful. Moreover, examination of the factors affecting the bioavailability of curcumin using *in vivo* animal and human feeding studies would be advantageous. In addition, the impact of these delivery systems on the sensory attributes of curcumin-fortified foods would be important, as it is critical that nutritionally fortified foods and beverages look and taste good, otherwise consumers will not purchase them.

REFERENCES

1. Sharma, R.; Gescher, A.; Steward, W., Curcumin: the story so far. *European journal of cancer* **2005**, *41*, 1955-1968.
2. Shahidi, F.; Naczk, M., *Phenolics in food and nutraceuticals*. CRC press: 2003.
3. Heger, M.; van Golen, R. F.; Broekgaarden, M.; Michel, M. C., The molecular basis for the pharmacokinetics and pharmacodynamics of curcumin and its metabolites in relation to cancer. *Pharmacological reviews* **2014**, *66*, 222-307.
4. Priyadarsini, K. I., The chemistry of curcumin: from extraction to therapeutic agent. *Molecules* **2014**, *19*, 20091-20112.
5. Jurenka, J. S., Anti-inflammatory properties of curcumin, a major constituent of Curcuma longa: a review of preclinical and clinical research. *Alternative medicine review* **2009**, *14*.
6. Menon, V. P.; Sudheer, A. R., Antioxidant and anti-inflammatory properties of curcumin. In *The molecular targets and therapeutic uses of curcumin in health and disease*, Springer: 2007; pp 105-125.
7. Ak, T.; Gülçin, İ., Antioxidant and radical scavenging properties of curcumin. *Chemico-biological interactions* **2008**, *174*, 27-37.
8. Zorofchian Moghadamtousi, S.; Abdul Kadir, H.; Hassandarvish, P.; Tajik, H.; Abubakar, S.; Zandi, K., A review on antibacterial, antiviral, and antifungal activity of curcumin. *BioMed research international* **2014**, *2014*.
9. Martins, C.; Da Silva, D.; Neres, A.; Magalhaes, T.; Watanabe, G.; Modolo, L.; Sabino, A.; De Fátima, A.; De Resende, M., Curcumin as a promising antifungal of clinical interest. *Journal of Antimicrobial Chemotherapy* **2008**, *63*, 337-339.
10. Bar-Sela, G.; Epelbaum, R.; Schaffer, M., Curcumin as an anti-cancer agent: review of the gap between basic and clinical applications. *Current medicinal chemistry* **2010**, *17*, 190-197.
11. Naksuriya, O.; Okonogi, S.; Schiffelers, R. M.; Hennink, W. E., Curcumin nanoformulations: a review of pharmaceutical properties and preclinical studies and clinical data related to cancer treatment. *Biomaterials* **2014**, *35*, 3365-3383.
12. Anand, P.; Kunnumakkara, A. B.; Newman, R. A.; Aggarwal, B. B., Bioavailability of curcumin: problems and promises. *Molecular pharmaceutics* **2007**, *4*, 807-818.
13. Tønnesen, H. H.; Másson, M.; Loftsson, T., Studies of curcumin and curcuminoids. XXVII. Cyclodextrin complexation: solubility, chemical and photochemical stability. *International Journal of Pharmaceutics* **2002**, *244*, 127-135.
14. Kharat, M.; Du, Z.; Zhang, G.; McClements, D. J., Physical and chemical stability of curcumin in aqueous solutions and emulsions: Impact of pH, temperature, and molecular environment. *Journal of agricultural and food chemistry* **2017**, *65*, 1525-1532.

15. McClements, D. J.; Decker, E. A.; Park, Y.; Weiss, J., Structural design principles for delivery of bioactive components in nutraceuticals and functional foods. *Critical reviews in food science and nutrition* **2009**, *49*, 577-606.
16. Garti, N., *Delivery and controlled release of bioactives in foods and nutraceuticals*. Elsevier: 2008.
17. Zhang, Z.; Zhang, R.; Decker, E. A.; McClements, D. J., Development of food-grade filled hydrogels for oral delivery of lipophilic active ingredients: pH-triggered release. *Food Hydrocolloids* **2015**, *44*, 345-352.
18. McClements, D.; Decker, E.; Weiss, J., Emulsion‐based delivery systems for lipophilic bioactive components. *Journal of food science* **2007**, *72*, R109-R124.
19. Lee, W.-H.; Loo, C.-Y.; Bebawy, M.; Luk, F.; Mason, R. S.; Rohanizadeh, R., Curcumin and its derivatives: their application in neuropharmacology and neuroscience in the 21st century. *Current neuropharmacology* **2013**, *11*, 338-378.
20. Bhatia, N. K.; Kishor, S.; Katyal, N.; Gogoi, P.; Narang, P.; Deep, S., Effect of pH and temperature on conformational equilibria and aggregation behaviour of curcumin in aqueous binary mixtures of ethanol. *RSC advances* **2016**, *6*, 103275-103288.
21. Manolova, Y.; Deneva, V.; Antonov, L.; Drakalska, E.; Momekova, D.; Lambov, N., The effect of the water on the curcumin tautomerism: A quantitative approach. *Spectrochimica Acta Part A: Molecular and Biomolecular Spectroscopy* **2014**, *132*, 815-820.
22. Murugan, P.; Pari, L., Influence of tetrahydrocurcumin on hepatic and renal functional markers and protein levels in experimental type 2 diabetic rats. *Basic & clinical pharmacology & toxicology* **2007**, *101*, 241-245.
23. Willcox, J. K.; Ash, S. L.; Catignani, G. L., Antioxidants and prevention of chronic disease. *Critical reviews in food science and nutrition* **2004**, *44*, 275-295.
24. Barclay, L. R. C.; Vinqvist, M. R.; Mukai, K.; Goto, H.; Hashimoto, Y.; Tokunaga, A.; Uno, H., On the antioxidant mechanism of curcumin: classical methods are needed to determine antioxidant mechanism and activity. *Organic letters* **2000**, *2*, 2841-2843.
25. Jayaprakasha, G.; Rao, L. J.; Sakariah, K., Antioxidant activities of curcumin, demethoxycurcumin and bisdemethoxycurcumin. *Food chemistry* **2006**, *98*, 720-724.
26. Goel, A.; Kunnumakkara, A. B.; Aggarwal, B. B., Curcumin as "Curecumin": from kitchen to clinic. *Biochemical pharmacology* **2008**, *75*, 787-809.
27. Arun, N.; Nalini, N., Efficacy of turmeric on blood sugar and polyol pathway in diabetic albino rats. *Plant foods for human nutrition* **2002**, *57*, 41-52.
28. Chandran, B.; Goel, A., A randomized, pilot study to assess the efficacy and safety of curcumin in patients with active rheumatoid arthritis. *Phytotherapy research* **2012**, *26*, 1719-1725.
29. Anna, K. T.; Suhana, M.; Das, S.; Faizah, O.; Hamzaini, A., Anti-inflammatory effect of Curcuma longa (turmeric) on collagen-induced arthritis: an anatomico-radiological study. *Clin Ter* **2011**, *162*, 201-207.
30. Yang, Q. Q.; Farha, A. K.; Kim, G.; Gul, K.; Gan, R. Y.; Corke, H., Antimicrobial and anticancer applications and related mechanisms of curcumin-mediated photodynamic treatments. *Trends in Food Science & Technology* **2020**, *97*, 341-354.
31. Gupta, S. C.; Sung, B.; Kim, J. H.; Prasad, S.; Li, S. Y.; Aggarwal, B. B., Multitargeting by turmeric, the golden spice: From kitchen to clinic. *Molecular Nutrition & Food Research* **2013**, *57*, 1510-1528.

32. Vaughn, A. R.; Haas, K. N.; Burney, W.; Andersen, E.; Clark, A. K.; Crawford, R.; Sivamani, R. K., Potential role of curcumin against biofilm-producing organisms on the skin: A review. *Phytotherapy research* **2017**, *31*, 1807-1816.
33. Tyagi, P.; Singh, M.; Kumari, H.; Kumari, A.; Mukhopadhyay, K., Bactericidal activity of curcumin I is associated with damaging of bacterial membrane. *PloS one* **2015**, *10*, e0121313.
34. Tomeh, M. A.; Hadianamrei, R.; Zhao, X., A review of curcumin and its derivatives as anticancer agents. *International journal of molecular sciences* **2019**, *20*, 1033.
35. Arbiser, J. L.; Klauber, N.; Rohan, R.; van Leeuwen, R.; Huang, M.-T.; Fisher, C.; Flynn, E.; Byers, H. R., Curcumin is an in vivo inhibitor of angiogenesis. *Molecular Medicine* **1998**, *4*, 376-383.
36. Teiten, M.-H.; Gaascht, F.; Eifes, S.; Dicato, M.; Diederich, M., Chemopreventive potential of curcumin in prostate cancer. *Genes & nutrition* **2010**, *5*, 61.
37. Dorai, T.; Dutcher, J. P.; Dempster, D. W.; Wiernik, P. H., Therapeutic potential of curcumin in prostate cancer—IV: Interference with the osteomimetic properties of hormone refractory C4-2B prostate cancer cells. *The Prostate* **2004**, *60*, 1-17.
38. Liu, Q.; Loo, W. T.; Sze, S.; Tong, Y., Curcumin inhibits cell proliferation of MDA-MB-231 and BT-483 breast cancer cells mediated by down-regulation of NFκB, cyclinD and MMP-1 transcription. *Phytomedicine* **2009**, *16*, 916-922.
39. Nesson, J.; William, G., Curcumin regulates miR-21 expression and inhibits invasion and metastasis in colorectal cancer. **2013**.
40. Mudduluru, G.; George-William, J. N.; Muppala, S.; Asangani, I. A.; Kumarswamy, R.; Nelson, L. D.; Allgayer, H., Curcumin regulates miR-21 expression and inhibits invasion and metastasis in colorectal cancer. *Bioscience reports* **2011**, *31*, 185-197.
41. Cheng, A.-L.; Hsu, C.-H.; Lin, J.-K.; Hsu, M.-M.; Ho, Y.-F.; Shen, T.-S.; Ko, J.-Y.; Lin, J.-T.; Lin, B.-R.; Ming-Shiang, W., Phase I clinical trial of curcumin, a chemopreventive agent, in patients with high-risk or pre-malignant lesions. *Anticancer Res* **2001**, *21*, 2895-2900.
42. Lao, C. D.; Ruffin, M. T.; Normolle, D.; Heath, D. D.; Murray, S. I.; Bailey, J. M.; Boggs, M. E.; Crowell, J.; Rock, C. L.; Brenner, D. E., Dose escalation of a curcuminoid formulation. *BMC complementary and alternative medicine* **2006**, *6*, 10.
43. Rodriguez, J. C.; Santibanez, D.; Narayanan, S.; Dave, A., Ginger and Curcumin in Cancer Prevention and Health Promotion. *Botanical Medicine in Clinical Practice* **2008**, 321.
44. Authority, E. F. S., Refined exposure assessment for curcumin (E 100). *EFSA Journal* **2014**, *12*, 3876.
45. Hewlings, S.; Kalman, D., Curcumin: a review of its' effects on human health. *Foods* **2017**, *6*, 92.
46. DiSilvestro, R. A.; Joseph, E.; Zhao, S.; Bomser, J., Diverse effects of a low dose supplement of lipidated curcumin in healthy middle aged people. *Nutrition journal* **2012**, *11*, 79.
47. Araiza-Calahorra, A.; Akhtar, M.; Sarkar, A., Recent advances in emulsion-based delivery approaches for curcumin: From encapsulation to bioaccessibility. *Trends in Food Science & Technology* **2018**, *71*, 155-169.
48. Grynkiewicz, G.; Ślifirski, P., Curcumin and curcuminoids in quest for medicinal status. *Acta Biochimica Polonica* **2012**, *59*.
49. Schneider, C.; Gordon, O. N.; Edwards, R. L.; Luis, P. B., Degradation of curcumin: from mechanism to biological implications. *Journal of agricultural and food chemistry* **2015**, *63*, 7606-7614.

50. Wang, Y.-J.; Pan, M.-H.; Cheng, A.-L.; Lin, L.-I.; Ho, Y.-S.; Hsieh, C.-Y.; Lin, J.-K., Stability of curcumin in buffer solutions and characterization of its degradation products. *Journal of pharmaceutical and biomedical analysis* **1997**, *15*, 1867-1876.
51. Zheng, B.; Peng, S.; Zhang, X.; McClements, D. J., Impact of Delivery System Type on Curcumin Bioaccessibility: Comparison of Curcumin-Loaded Nanoemulsions with Commercial Curcumin Supplements. *Journal of agricultural and food chemistry* **2018**, *66*, 10816-10826.
52. Nelson, K. M.; Dahlin, J. L.; Bisson, J.; Graham, J.; Pauli, G. F.; Walters, M. A., The essential medicinal chemistry of curcumin: miniperspective. *Journal of medicinal chemistry* **2017**, *60*, 1620-1637.
53. Priyadarsini, K. I., Photophysics, photochemistry and photobiology of curcumin: Studies from organic solutions, bio-mimetics and living cells. *Journal of Photochemistry and Photobiology C: Photochemistry Reviews* **2009**, *10*, 81-95.
54. E Wright, L.; B Frye, J.; Gorti, B.; N Timmermann, B.; L Funk, J., Bioactivity of turmeric-derived curcuminoids and related metabolites in breast cancer. *Current pharmaceutical design* **2013**, *19*, 6218-6225.
55. Ogiwara, T.; Satoh, K.; Kadoma, Y.; Murakami, Y.; Unten, S.; Atsumi, T.; Sakagami, H.; Fujisawa, S., Radical scavenging activity and cytotoxicity of ferulic acid. *Anticancer research* **2002**, *22*, 2711-2717.
56. Tai, A.; Sawano, T.; Yazama, F.; Ito, H., Evaluation of antioxidant activity of vanillin by using multiple antioxidant assays. *Biochimica et Biophysica Acta (BBA)-General Subjects* **2011**, *1810*, 170-177.
57. Gordon, O. N.; Schneider, C., Vanillin and ferulic acid: not the major degradation products of curcumin. *Trends in molecular medicine* **2012**, *18*, 361-363.
58. Gordon, O. N.; Luis, P. B.; Sintim, H. O.; Schneider, C., Unraveling curcumin degradation autoxidation proceeds through spiroepoxide and vinylether intermediates en route to the main bicyclopentadione. *Journal of Biological Chemistry* **2015**, *290*, 4817-4828.
59. Griesser, M.; Pistis, V.; Suzuki, T.; Tejera, N.; Pratt, D. A.; Schneider, C., Autoxidative and cyclooxygenase-2 catalyzed transformation of the dietary chemopreventive agent curcumin. *Journal of Biological Chemistry* **2011**, *286*, 1114-1124.
60. Sanidad, K. Z.; Zhu, J.; Wang, W.; Du, Z.; Zhang, G., Effects of stable degradation products of curcumin on cancer cell proliferation and inflammation. *Journal of agricultural and food chemistry* **2016**, *64*, 9189-9195.
61. McClements, D. J.; Li, F.; Xiao, H., The nutraceutical bioavailability classification scheme: classifying nutraceuticals according to factors limiting their oral bioavailability. *Annual review of food science and technology* **2015**, *6*, 299-327.
62. Ravindranath, V.; Chandrasekhara, N., Absorption and tissue distribution of curcumin in rats. *Toxicology* **1980**, *16*, 259-265.
63. Sanidad, K. Z.; Sukamtoh, E.; Xiao, H.; McClements, D. J.; Zhang, G. D., Curcumin: Recent Advances in the Development of Strategies to Improve Oral Bioavailability. In *Annual Review of Food Science and Technology, Vol 10*, Doyle, M. P.; McClements, D. J., Eds. 2019; Vol. 10, pp 597-617.
64. Jain, G.; Patil, U. K., STRATEGIES FOR ENHANCEMENT OF BIOAVAILABILITY OF MEDICINAL AGENTS WITH NATURAL PRODUCTS. *International Journal of Pharmaceutical Sciences and Research* **2015**, *6*, 5315-5324.
65. Mollazadeh, S.; Sahebkar, A.; Hadizadeh, F.; Behravan, J.; Arabzadeh, S., Structural and functional aspects of P-glycoprotein and its inhibitors. *Life Sciences* **2018**, *214*, 118-123.

66. Zhou, S. F.; Lim, L. Y.; Chowbay, B., Herbal modulation of P-glycoprotein. *Drug Metabolism Reviews* **2004**, *36*, 57-104.
67. Singh, D. V.; Godbole, M. M.; Misra, K., A plausible explanation for enhanced bioavailability of P-gp substrates in presence of piperine: simulation for next generation of P-gp inhibitors. *Journal of Molecular Modeling* **2013**, *19*, 227-238.
68. Prasad, S.; Tyagi, A. K.; Aggarwal, B. B., Recent Developments in Delivery, Bioavailability, Absorption and Metabolism of Curcumin: the Golden Pigment from Golden Spice. *Cancer Research and Treatment* **2014**, *46*, 2-18.
69. Ireson, C. R.; Jones, D. J.; Orr, S.; Coughtrie, M. W.; Boocock, D. J.; Williams, M. L.; Farmer, P. B.; Steward, W. P.; Gescher, A. J., Metabolism of the cancer chemopreventive agent curcumin in human and rat intestine. *Cancer Epidemiology and Prevention Biomarkers* **2002**, *11*, 105-111.
70. Ireson, C.; Orr, S.; Jones, D. J.; Verschoyle, R.; Lim, C.-K.; Luo, J.-L.; Howells, L.; Plummer, S.; Jukes, R.; Williams, M., Characterization of metabolites of the chemopreventive agent curcumin in human and rat hepatocytes and in the rat in vivo, and evaluation of their ability to inhibit phorbol ester-induced prostaglandin E2 production. *Cancer research* **2001**, *61*, 1058-1064.
71. Asai, A.; Miyazawa, T., Occurrence of orally administered curcuminoid as glucuronide and glucuronide/sulfate conjugates in rat plasma. *Life sciences* **2000**, *67*, 2785-2793.
72. Sharma, R. A.; Euden, S. A.; Platton, S. L.; Cooke, D. N.; Shafayat, A.; Hewitt, H. R.; Marczylo, T. H.; Morgan, B.; Hemingway, D.; Plummer, S. M., Phase I clinical trial of oral curcumin: biomarkers of systemic activity and compliance. *Clinical Cancer Research* **2004**, *10*, 6847-6854.
73. Dubey, S. K.; Sharma, A. K.; Narain, U.; Misra, K.; Pati, U., Design, synthesis and characterization of some bioactive conjugates of curcumin with glycine, glutamic acid, valine and demethylenated piperic acid and study of their antimicrobial and antiproliferative properties. *European journal of medicinal chemistry* **2008**, *43*, 1837-1846.
74. Huang, Y.; Cao, S.; Zhang, Q.; Zhang, H.; Fan, Y.; Qiu, F.; Kang, N., Biological and pharmacological effects of hexahydrocurcumin, a metabolite of curcumin. *Archives of biochemistry and biophysics* **2018**, *646*, 31-37.
75. Srimuangwong, K.; Tocharus, C.; Chintana, P. Y.; Suksamrarn, A.; Tocharus, J., Hexahydrocurcumin enhances inhibitory effect of 5-fluorouracil on HT-29 human colon cancer cells. *World journal of gastroenterology: WJG* **2012**, *18*, 2383.
76. Chen, C.-Y.; Yang, W.-L.; Kuo, S.-Y., Cytotoxic activity and cell cycle analysis of hexahydrocurcumin on SW 480 human colorectal cancer cells. *Natural product communications* **2011**, *6*, 1934578X1100601126.
77. Zhang, Z.; Luo, D.; Xie, J.; Lin, G.; Zhou, J.; Liu, W.; Li, H.; Yi, T.; Su, Z.; Chen, J., Octahydrocurcumin, a final hydrogenated metabolite of curcumin, possesses superior anti-tumor activity through induction of cellular apoptosis. *Food & function* **2018**, *9*, 2005-2014.
78. Luo, D.-D.; Chen, J.-F.; Liu, J.-J.; Xie, J.-H.; Zhang, Z.-B.; Gu, J.-Y.; Zhuo, J.-Y.; Huang, S.; Su, Z.-R.; Sun, Z.-H., Tetrahydrocurcumin and octahydrocurcumin, the primary and final hydrogenated metabolites of curcumin, possess superior hepatic-protective effect against acetaminophen-induced liver injury: role of CYP2E1 and Keap1-Nrf2 pathway. *Food and chemical toxicology* **2019**, *123*, 349-362.

79. Shoji, M.; Nakagawa, K.; Watanabe, A.; Tsuduki, T.; Yamada, T.; Kuwahara, S.; Kimura, F.; Miyazawa, T., Comparison of the effects of curcumin and curcumin glucuronide in human hepatocellular carcinoma HepG2 cells. *Food chemistry* **2014**, *151*, 126-132.
80. Shen, L.; Liu, C.-C.; An, C.-Y.; Ji, H.-F., How does curcumin work with poor bioavailability? Clues from experimental and theoretical studies. *Scientific reports* **2016**, *6*, 20872.
81. Perkins, S.; Verschoyle, R. D.; Hill, K.; Parveen, I.; Threadgill, M. D.; Sharma, R. A.; Williams, M. L.; Steward, W. P.; Gescher, A. J., Chemopreventive efficacy and pharmacokinetics of curcumin in the min/+ mouse, a model of familial adenomatous polyposis. *Cancer Epidemiology and Prevention Biomarkers* **2002**, *11*, 535-540.
82. Suresh, D.; Srinivasan, K., Tissue distribution & elimination of capsaicin, piperine & curcumin following oral intake in rats. *Indian Journal of Medical Research* **2010**, *131*.
83. Ravindranath, V.; Chandrasekhara, N., Metabolism of curcumn-studies with [3H] curcumin. *Toxicology* **1981**, *22*, 337-344.
84. Pan, M.-H.; Huang, T.-M.; Lin, J.-K., Biotransformation of curcumin through reduction and glucuronidation in mice. *Drug metabolism and disposition* **1999**, *27*, 486-494.
85. Kakran, M.; Sahoo, N. G.; Tan, I.-L.; Li, L., Preparation of nanoparticles of poorly water-soluble antioxidant curcumin by antisolvent precipitation methods. *Journal of Nanoparticle Research* **2012**, *14*, 757.
86. Yadav, D.; Kumar, N., Nanonization of curcumin by antisolvent precipitation: process development, characterization, freeze drying and stability performance. *International journal of pharmaceutics* **2014**, *477*, 564-577.
87. Zou, L.; Zheng, B.; Zhang, R.; Zhang, Z.; Liu, W.; Liu, C.; Xiao, H.; McClements, D. J., Food-grade nanoparticles for encapsulation, protection and delivery of curcumin: comparison of lipid, protein, and phospholipid nanoparticles under simulated gastrointestinal conditions. *RSC Advances* **2016**, *6*, 3126-3136.
88. Khan, F. I.; Ghoshal, A. K., Removal of volatile organic compounds from polluted air. *Journal of loss prevention in the process industries* **2000**, *13*, 527-545.
89. Mozafari, M. R., Liposomes: an overview of manufacturing techniques. *Cellular and Molecular Biology Letters* **2005**, *10*, 711.
90. Lesoin, L.; Crampon, C.; Boutin, O.; Badens, E., Preparation of liposomes using the supercritical anti-solvent (SAS) process and comparison with a conventional method. *The journal of supercritical fluids* **2011**, *57*, 162-174.
91. Ginty, P. J.; Whitaker, M. J.; Shakesheff, K. M.; Howdle, S. M., Drug delivery goes supercritical. *Materials today* **2005**, *8*, 42-48.
92. Peng, S.; Li, Z.; Zou, L.; Liu, W.; Liu, C.; McClements, D. J., Enhancement of Curcumin Bioavailability by Encapsulation in Sophorolipid-Coated Nanoparticles: An in Vitro and in Vivo Study. *Journal of agricultural and food chemistry* **2018**, *66*, 1488-1497.
93. Cheng, C.; Peng, S.; Li, Z.; Zou, L.; Liu, W.; Liu, C., Improved bioavailability of curcumin in liposomes prepared using a pH-driven, organic solvent-free, easily scalable process. *RSC Advances* **2017**, *7*, 25978-25986.
94. Pan, K.; Luo, Y.; Gan, Y.; Baek, S. J.; Zhong, Q., pH-driven encapsulation of curcumin in self-assembled casein nanoparticles for enhanced dispersibility and bioactivity. *Soft Matter* **2014**, *10*, 6820-6830.
95. Zhou, M.; Wang, T.; Hu, Q.; Luo, Y., Low density lipoprotein/pectin complex nanogels as potential oral delivery vehicles for curcumin. *Food Hydrocolloids* **2016**, *57*, 20-29.

96. Zheng, B.; Zhang, X.; Peng, S.; McClements, D. J., Impact of delivery system format on curcumin bioaccessibility: Nanocrystals, nanoemulsion droplets, and natural oil bodies. *Food & function* **2019**.
97. Cabrera-Trujillo, M. A.; Sotelo-Díaz, L. I.; Quintanilla-Carvajal, M. X., Effect of amplitude and pulse in low frequency ultrasound on oil/water emulsions. *Dyna* **2016**, *83*, 63-68.
98. Kim, H. N.; Suslick, K. S., The effects of ultrasound on crystals: sonocrystallization and sonofragmentation. *Crystals* **2018**, *8*, 280.
99. Zou, L.; Zheng, B.; Zhang, R.; Zhang, Z.; Liu, W.; Liu, C.; Xiao, H.; McClements, D. J., Food matrix effects on nutraceutical bioavailability: impact of protein on curcumin bioaccessibility and transformation in nanoemulsion delivery systems and excipient nanoemulsions. *Food Biophysics* **2016**, *11*, 142-153.
100. Zou, L.; Zheng, B.; Zhang, R.; Zhang, Z.; Liu, W.; Liu, C.; Zhang, G.; Xiao, H.; McClements, D. J., Influence of lipid phase composition of excipient emulsions on curcumin solubility, stability, and bioaccessibility. *Food Biophysics* **2016**, *11*, 213-225.
101. Zhu, J. L.; Sanidad, K. Z.; Sukamtoh, E.; Zhang, G. D., Potential roles of chemical degradation in the biological activities of curcumin. *Food & Function* **2017**, *8*, 907-914.
102. Kharat, M.; Skrzynski, M.; Decker, E. A.; McClements, D. J., Enhancement of chemical stability of curcumin-enriched oil-in-water emulsions: Impact of antioxidant type and concentration. *Food Chemistry* **2020**, *320*.
103. Zou, L. Q.; Zheng, B. J.; Zhang, R. J.; Zhang, Z. P.; Liu, W.; Liu, C. M.; Xiao, H.; McClements, D. J., Food-grade nanoparticles for encapsulation, protection and delivery of curcumin: comparison of lipid, protein, and phospholipid nanoparticles under simulated gastrointestinal conditions. *Rsc Advances* **2016**, *6*, 3126-3136.
104. Dai, L.; Zhou, H. L.; Wei, Y.; Gao, Y. X.; McClements, D. J., Curcumin encapsulation in zein-rhamnolipid composite nanoparticles using a pH-driven method. *Food Hydrocolloids* **2019**, *93*, 342-350.
105. Zou, L. Q.; Zheng, B. J.; Liu, W.; Liu, C. M.; Xiao, H.; McClements, D. J., Enhancing nutraceutical bioavailability using excipient emulsions: Influence of lipid droplet size on solubility and bioaccessibility of powdered curcumin. *Journal of Functional Foods* **2015**, *15*, 72-83.
106. del Castillo, M. L. R.; Lopez-Tobar, E.; Sanchez-Cortes, S.; Flores, G.; Blanch, G. P., Stabilization of curcumin against photodegradation by encapsulation in gamma-cyclodextrin: A study based on chromatographic and spectroscopic (Raman and UV-visible) data. *Vibrational Spectroscopy* **2015**, *81*, 106-111.
107. Price, L. C.; Buescher, R. W., Decomposition of turmeric curcuminoids as affected by light, solvent and oxygen. *Journal of Food Biochemistry* **1996**, *20*, 125-133.
108. Higaki, K.; Yata, T.; Sone, M.; Ogawara, K.; Kimura, T., Estimation of absorption enhancement by medium-chain fatty acids in rat large intestine. *Research Communications in Molecular Pathology and Pharmacology* **2001**, *109*, 231-240.
109. Aungst, B. J., Intestinal permeation enhancers. *Journal of Pharmaceutical Sciences* **2000**, *89*, 429-442.
110. Patra, A. K.; Amasheh, S.; Aschenbach, J. R., Modulation of gastrointestinal barrier and nutrient transport function in farm animals by natural plant bioactive compounds - A comprehensive review. *Critical Reviews in Food Science and Nutrition* **2019**, *59*, 3237-3266.
111. McClements, D. J., Enhancing nutraceutical bioavailability through food matrix design. *Current Opinion in Food Science* **2015**, *4*, 1-6.

112. Dordevic, V.; Balanc, B.; Belscak-Cvitanovic, A.; Levic, S.; Trifkovic, K.; Kalusevic, A.; Kostic, I.; Komes, D.; Bugarski, B.; Nedovic, V., Trends in Encapsulation Technologies for Delivery of Food Bioactive Compounds. *Food Engineering Reviews* **2015**, *7*, 452-490.
113. Wang, Z. L., Bioavailability of organic compounds solubilized in nonionic surfactant micelles. *Applied Microbiology and Biotechnology* **2011**, *89*, 523-534.
114. Kimpel, F.; Schmitt, J. J., Review: Milk Proteins as Nanocarrier Systems for Hydrophobic Nutraceuticals. *Journal of Food Science* **2015**, *80*, R2361-R2366.
115. Livney, Y. D., Milk proteins as vehicles for bioactives. *Current Opinion in Colloid & Interface Science* **2010**, *15*, 73-83.
116. Torchilin, V. P., Micellar nanocarriers: pharmaceutical perspectives. *Pharmaceutical research* **2007**, *24*, 1.
117. Wang, X. Y.; Gao, Y., Effects of length and unsaturation of the alkyl chain on the hydrophobic binding of curcumin with Tween micelles. *Food Chemistry* **2018**, *246*, 242-248.
118. Pan, K.; Zhong, Q.; Baek, S. J., Enhanced dispersibility and bioactivity of curcumin by encapsulation in casein nanocapsules. *Journal of agricultural and food chemistry* **2013**, *61*, 6036-6043.
119. Schiborr, C.; Kocher, A.; Behnam, D.; Jandasek, J.; Toelstede, S.; Frank, J., The oral bioavailability of curcumin from micronized powder and liquid micelles is significantly increased in healthy humans and differs between sexes. *Molecular nutrition & food research* **2014**, *58*, 516-527.
120. Akbarzadeh, A.; Rezaei-Sadabady, R.; Davaran, S.; Joo, S. W.; Zarghami, N.; Hanifehpour, Y.; Samiei, M.; Kouhi, M.; Nejati-Koshki, K., Liposome: classification, preparation, and applications. *Nanoscale research letters* **2013**, *8*, 102.
121. Chen, X.; Zou, L.-Q.; Niu, J.; Liu, W.; Peng, S.-F.; Liu, C.-M., The stability, sustained release and cellular antioxidant activity of curcumin nanoliposomes. *Molecules* **2015**, *20*, 14293-14311.
122. Jin, H.-H.; Lu, Q.; Jiang, J.-G., Curcumin liposomes prepared with milk fat globule membrane phospholipids and soybean lecithin. *Journal of dairy science* **2016**, *99*, 1780-1790.
123. Takahashi, M.; Uechi, S.; Takara, K.; Asikin, Y.; Wada, K., Evaluation of an oral carrier system in rats: bioavailability and antioxidant properties of liposome-encapsulated curcumin. *Journal of agricultural and food chemistry* **2009**, *57*, 9141-9146.
124. Li, C.; Zhang, Y.; Su, T.; Feng, L.; Long, Y.; Chen, Z., Silica-coated flexible liposomes as a nanohybrid delivery system for enhanced oral bioavailability of curcumin. *International journal of nanomedicine* **2012**, *7*, 5995.
125. Bergonzi, M.; Hamdouch, R.; Mazzacuva, F.; Isacchi, B.; Bilia, A., Optimization, characterization and in vitro evaluation of curcumin microemulsions. *LWT-Food Science and Technology* **2014**, *59*, 148-155.
126. Setthacheewakul, S.; Mahattanadul, S.; Phadoongsombut, N.; Pichayakorn, W.; Wiwattanapatapee, R., Development and evaluation of self-microemulsifying liquid and pellet formulations of curcumin, and absorption studies in rats. *European Journal of Pharmaceutics and Biopharmaceutics* **2010**, *76*, 475-485.
127. Hu, L.; Jia, Y.; Niu, F.; Jia, Z.; Yang, X.; Jiao, K., Preparation and enhancement of oral bioavailability of curcumin using microemulsions vehicle. *Journal of agricultural and food chemistry* **2012**, *60*, 7137-7141.
128. McClements, D. J., *Food emulsions: principles, practices, and techniques*. CRC press: 2015.

129.McClements, D. J., Nanoemulsions versus microemulsions: terminology, differences, and similarities. *Soft matter* **2012**, *8*, 1719-1729.
130.Zheng, B.; Lin, H.; Zhang, X.; McClements, D. J., Fabrication of Curcumin-Loaded Dairy Milks Using the pH-Shift Method: Formation, Stability, and Bioaccessibility. *Journal of Agricultural and Food Chemistry* **2019**, *67*, 12245-12254.
131.Ma, P.; Zeng, Q.; Tai, K.; He, X.; Yao, Y.; Hong, X.; Yuan, F., Preparation of curcumin-loaded emulsion using high pressure homogenization: Impact of oil phase and concentration on physicochemical stability. *LWT* **2017**, *84*, 34-46.
132.Zou, L.; Zheng, B.; Liu, W.; Liu, C.; Xiao, H.; McClements, D. J., Enhancing nutraceutical bioavailability using excipient emulsions: Influence of lipid droplet size on solubility and bioaccessibility of powdered curcumin. *Journal of functional foods* **2015**, *15*, 72-83.
133.Onodera, T.; Kuriyama, I.; Andoh, T.; Ichikawa, H.; Sakamoto, Y.; Lee-Hiraiwa, E.; Mizushina, Y., Influence of particle size on the in vitro and in vivo anti-inflammatory and anti-allergic activities of a curcumin lipid nanoemulsion. *International journal of molecular medicine* **2015**, *35*, 1720-1728.
134.Mishra, V.; Bansal, K. K.; Verma, A.; Yadav, N.; Thakur, S.; Sudhakar, K.; Rosenholm, J. M., Solid lipid nanoparticles: Emerging colloidal nano drug delivery systems. *Pharmaceutics* **2018**, *10*, 191.
135.Müller, R. H.; Radtke, M.; Wissing, S. A., Solid lipid nanoparticles (SLN) and nanostructured lipid carriers (NLC) in cosmetic and dermatological preparations. *Advanced drug delivery reviews* **2002**, *54*, S131-S155.
136.Helgason, T.; Salminen, H.; Kristbergsson, K.; McClements, D. J.; Weiss, J., Formation of transparent solid lipid nanoparticles by microfluidization: Influence of lipid physical state on appearance. *Journal of colloid and interface science* **2015**, *448*, 114-122.
137.Xue, J.; Wang, T.; Hu, Q.; Zhou, M.; Luo, Y., Insight into natural biopolymer-emulsified solid lipid nanoparticles for encapsulation of curcumin: Effect of loading methods. *Food hydrocolloids* **2018**, *79*, 110-116.
138.Kakkar, V.; Singh, S.; Singla, D.; Kaur, I. P., Exploring solid lipid nanoparticles to enhance the oral bioavailability of curcumin. *Molecular nutrition & food research* **2011**, *55*, 495-503.
139.Sadegh Malvajerd, S.; Azadi, A.; Izadi, Z.; Kurd, M.; Dara, T.; Dibaei, M.; Sharif Zadeh, M.; Akbari Javar, H.; Hamidi, M., Brain delivery of curcumin using solid lipid nanoparticles and nanostructured lipid carriers: preparation, optimization, and pharmacokinetic evaluation. *ACS chemical neuroscience* **2018**, *10*, 728-739.
140.Gota, V. S.; Maru, G. B.; Soni, T. G.; Gandhi, T. R.; Kochar, N.; Agarwal, M. G., Safety and pharmacokinetics of a solid lipid curcumin particle formulation in osteosarcoma patients and healthy volunteers. *Journal of agricultural and food chemistry* **2010**, *58*, 2095-2099.
141.McClements, D. J., Recent progress in hydrogel delivery systems for improving nutraceutical bioavailability. *Food Hydrocolloids* **2017**, *68*, 238-245.
142.Zheng, B.; Zhang, Z.; Chen, F.; Luo, X.; McClements, D. J., Impact of delivery system type on curcumin stability: Comparison of curcumin degradation in aqueous solutions, emulsions, and hydrogel beads. *Food Hydrocolloids* **2017**, *71*, 187-197.
143.Mohammadian, M.; Salami, M.; Momen, S.; Alavi, F.; Emam-Djomeh, Z., Fabrication of curcumin-loaded whey protein microgels: Structural properties, antioxidant activity, and in vitro release behavior. *LWT* **2019**, *103*, 94-100.
144.Zhang, Z.; Zhang, R.; Zou, L.; Chen, L.; Ahmed, Y.; Al Bishri, W.; Balamash, K.; McClements, D. J., Encapsulation of curcumin in polysaccharide-based hydrogel beads: Impact

of bead type on lipid digestion and curcumin bioaccessibility. *Food Hydrocolloids* **2016**, *58*, 160-170.
145. Lee, J. Y., Pectin hydrogels of curcumin and obesity applications. *Master of Science, University of* **2015**.
146. Esmaili, M.; Ghaffari, S. M.; Moosavi-Movahedi, Z.; Atri, M. S.; Sharifizadeh, A.; Farhadi, M.; Yousefi, R.; Chobert, J.-M.; Haertlé, T.; Moosavi-Movahedi, A. A., Beta casein-micelle as a nano vehicle for solubility enhancement of curcumin; food industry application. *LWT-food science and technology* **2011**, *44*, 2166-2172.
147. Purpura, M.; Lowery, R. P.; Wilson, J. M.; Mannan, H.; Münch, G.; Razmovski-Naumovski, V., Analysis of different innovative formulations of curcumin for improved relative oral bioavailability in human subjects. *European journal of nutrition* **2018**, *57*, 929-938.
148. Zheng, B.; Zhang, X.; Lin, H.; McClements, D. J., Loading natural emulsions with nutraceuticals using the pH-driven method: Formation & stability of curcumin-loaded soybean oils bodies. *Food & function* **2019**.
149. Aggarwal, B. B.; Harikumar, K. B., Potential therapeutic effects of curcumin, the anti-inflammatory agent, against neurodegenerative, cardiovascular, pulmonary, metabolic, autoimmune and neoplastic diseases. *International Journal of Biochemistry & Cell Biology* **2009**, *41*, 40-59.
150. Epstein, J.; Sanderson, I. R.; MacDonald, T. T., Curcumin as a therapeutic agent: the evidence from in vitro, animal and human studies. *British Journal of Nutrition* **2010**, *103*, 1545-1557.
151. Singh, M.; Arseneault, M.; Sanderson, T.; Murthy, V.; Ramassamy, C., Challenges for research on polyphenols from foods in Alzheimer's disease: Bioavailability, metabolism, and cellular and molecular mechanisms. *Journal of Agricultural and Food Chemistry* **2008**, *56*, 4855-4873.
152. Yang, C. S.; Sang, S. M.; Lambert, J. D.; Lee, M. J., Bioavailability issues in studying the health effects of plant polyphenolic compounds. *Molecular Nutrition & Food Research* **2008**, *52*, S139-S151.
153. Bansal, S. S.; Goel, M.; Aqil, F.; Vadhanam, M. V.; Gupta, R. C., Advanced Drug Delivery Systems of Curcumin for Cancer Chemoprevention. *Cancer Prevention Research* **2011**, *4*, 1158-1171.
154. Patel, A. R.; Velikov, K. P., Colloidal delivery systems in foods: A general comparison with oral drug delivery. *Lwt-Food Science and Technology* **2011**, *44*, 1958-1964.
155. Sun, M.; Su, X.; Ding, B. Y.; He, X. L.; Liu, X. J.; Yu, A. H.; Lou, H. X.; Zhai, G. X., Advances in nanotechnology-based delivery systems for curcumin. *Nanomedicine* **2012**, *7*, 1085-1100.
156. Vecchione, R.; Quagliariello, V.; Calabria, D.; Calcagno, V.; De Luca, E.; Iaffaioli, R. V.; Netti, P. A., Curcumin bioavailability from oil in water nano-emulsions: In vitro and in vivo study on the dimensional, compositional and interactional dependence. *Journal of Controlled Release* **2016**, *233*, 88-100.
157. Joung, H. J.; Choi, M. J.; Kim, J. T.; Park, S. H.; Park, H. J.; Shin, G. H., Development of Food-Grade Curcumin Nanoemulsion and its Potential Application to Food Beverage System: Antioxidant Property and In Vitro Digestion. *Journal of Food Science* **2016**, *81*, N745-N753.
158. Pinheiro, A. C.; Coimbra, M. A.; Vicente, A. A., In vitro behaviour of curcumin nanoemulsions stabilized by biopolymer emulsifiers - Effect of interfacial composition. *Food Hydrocolloids* **2016**, *52*, 460-467.

159. Ahmed, K.; Li, Y.; McClements, D. J.; Xiao, H., Nanoemulsion- and emulsion-based delivery systems for curcumin: Encapsulation and release properties. *Food Chemistry* **2012**, *132*, 799-807.
160. McClements, D. J.; Li, Y., Structured emulsion-based delivery systems: Controlling the digestion and release of lipophilic food components. *Advances in colloid and interface science* **2010**, *159*, 213-228.
161. Schmitt, C.; Sanchez, C.; Desobry-Banon, S.; Hardy, J., Structure and technofunctional properties of protein-polysaccharide complexes: a review. *Critical Reviews in Food Science and Nutrition* **1998**, *38*, 689-753.
162. Jones, O. G.; McClements, D. J., Functional biopolymer particles: design, fabrication, and applications. *Comprehensive Reviews in Food Science and Food Safety* **2010**, *9*, 374-397.
163. McClements, D. J., Recent progress in hydrogel delivery systems for improving nutraceutical bioavailability. *Food Hydrocolloids* **2016**.
164. George, M.; Abraham, T. E., Polyionic hydrocolloids for the intestinal delivery of protein drugs: alginate and chitosan—a review. *Journal of controlled release* **2006**, *114*, 1-14.
165. Tønnesen, H. H.; Karlsen, J., Alginate in drug delivery systems. *Drug development and industrial pharmacy* **2002**, *28*, 621-630.
166. Gombotz, W. R.; Wee, S. F., Protein release from alginate matrices. *Advanced drug delivery reviews* **2012**, *64*, 194-205.
167. Schipper, N. G.; Olsson, S.; Hoogstraate, J. A.; Vårum, K. M.; Artursson, P., Chitosans as absorption enhancers for poorly absorbable drugs 2: mechanism of absorption enhancement. *Pharmaceutical research* **1997**, *14*, 923-929.
168. Wiącek, A.; Chibowski, E., Zeta potential, effective diameter and multimodal size distribution in oil/water emulsion. *Colloids and Surfaces A: Physicochemical and Engineering Aspects* **1999**, *159*, 253-261.
169. McClements, D. J., Theoretical prediction of emulsion color. *Advances in Colloid and Interface Science* **2002**, *97*, 63-89.
170. Bajpai, S.; Sharma, S., Investigation of swelling/degradation behaviour of alginate beads crosslinked with Ca 2+ and Ba 2+ ions. *Reactive and Functional Polymers* **2004**, *59*, 129-140.
171. Gan, Q.; Wang, T.; Cochrane, C.; McCarron, P., Modulation of surface charge, particle size and morphological properties of chitosan–TPP nanoparticles intended for gene delivery. *Colloids and Surfaces B: Biointerfaces* **2005**, *44*, 65-73.
172. Bhumkar, D. R.; Pokharkar, V. B., Studies on effect of pH on cross-linking of chitosan with sodium tripolyphosphate: a technical note. *Aaps Pharmscitech* **2006**, *7*, E138-E143.
173. Espinal-Ruiz, M.; Parada-Alfonso, F.; Restrepo-Sanchez, L. P.; Narvaez-Cuenca, C. E.; McClements, D. J., Impact of dietary fibers methyl cellulose, chitosan, and pectin on digestion of lipids under simulated gastrointestinal conditions. *Food & Function* **2014**, *5*, 3083-3095.
174. Jovanovic, S. V.; Steenken, S.; Boone, C. W.; Simic, M. G., H-atom transfer is a preferred antioxidant mechanism of curcumin. *Journal of the American Chemical Society* **1999**, *121*, 9677-9681.
175. Longo, G. S.; Szleifer, I., Adsorption and protonation of peptides and proteins in pH responsive gels. *Journal of Physics D-Applied Physics* **2016**, *49*.
176. Jain, B., A spectroscopic study on stability of curcumin as a function of pH in silica nanoformulations, liposome and serum protein. *Journal of Molecular Structure* **2017**, *1130*, 194-198.

177.Mi, F. L.; Shyu, S. S.; Lee, S. T.; Wong, T. B., Kinetic study of chitosan-tripolyphosphate complex reaction and acid-resistive properties of the chitosan-tripolyphosphate gel beads prepared by in-liquid curing method. *Journal of Polymer Science Part B: Polymer Physics* **1999**, *37*, 1551-1564.
178.Torres, O.; Murray, B.; Sarkar, A., Emulsion microgel particles: Novel encapsulation strategy for lipophilic molecules. *Trends in Food Science & Technology* **2016**, *55*, 98-108.
179.Shewan, H. M.; Stokes, J. R., Review of techniques to manufacture micro-hydrogel particles for the food industry and their applications. *Journal of Food Engineering* **2013**, *119*, 781-792.
180.Matalanis, A.; Jones, O. G.; McClements, D. J., Structured biopolymer-based delivery systems for encapsulation, protection, and release of lipophilic compounds. *Food Hydrocolloids* **2011**, *25*, 1865-1880.
181.Kunnumakkara, A. B.; Anand, P.; Aggarwal, B. B., Curcumin inhibits proliferation, invasion, angiogenesis and metastasis of different cancers through interaction with multiple cell signaling proteins. *Cancer letters* **2008**, *269*, 199-225.
182.HSIEH, C.-Y., Phase I clinical trial of curcumin, a chemopreventive agent, in patients with high-risk or pre-malignant lesions. *Anticancer research* **2001**, *21*, 2895-2900.
183.Gupta, N. K.; Dixit, V. K., Bioavailability enhancement of curcumin by complexation with phosphatidyl choline. *Journal of pharmaceutical sciences* **2011**, *100*, 1987-1995.
184.Vasconcelos, T.; Sarmento, B.; Costa, P., Solid dispersions as strategy to improve oral bioavailability of poor water soluble drugs. *Drug discovery today* **2007**, *12*, 1068-1075.
185.Shaikh, J.; Ankola, D.; Beniwal, V.; Singh, D.; Kumar, M. R., Nanoparticle encapsulation improves oral bioavailability of curcumin by at least 9-fold when compared to curcumin administered with piperine as absorption enhancer. *European Journal of Pharmaceutical Sciences* **2009**, *37*, 223-230.
186.Sun, D.; Zhuang, X.; Xiang, X.; Liu, Y.; Zhang, S.; Liu, C.; Barnes, S.; Grizzle, W.; Miller, D.; Zhang, H.-G., A novel nanoparticle drug delivery system: the anti-inflammatory activity of curcumin is enhanced when encapsulated in exosomes. *Molecular Therapy* **2010**, *18*, 1606-1614.
187.Huang, Y.; Dai, W.-G., Fundamental aspects of solid dispersion technology for poorly soluble drugs. *Acta Pharmaceutica Sinica B* **2014**, *4*, 18-25.
188.Kurien, B. T.; Singh, A.; Matsumoto, H.; Scofield, R. H., Improving the solubility and pharmacological efficacy of curcumin by heat treatment. *Assay and drug development technologies* **2007**, *5*, 567-576.
189.Shen, T. T., Industrial pollution prevention. In *Industrial Pollution Prevention*, Springer: 1995; pp 15-35.
190.Luo, Y.; Pan, K.; Zhong, Q., Casein/pectin nanocomplexes as potential oral delivery vehicles. *International journal of pharmaceutics* **2015**, *486*, 59-68.
191.Zebib, B.; Mouloungui, Z.; Noirot, V., Stabilization of curcumin by complexation with divalent cations in glycerol/water system. *Bioinorganic chemistry and applications* **2010**, *2010*.
192.Li, Y.; Hu, M.; McClements, D. J., Factors affecting lipase digestibility of emulsified lipids using an in vitro digestion model: Proposal for a standardised pH-stat method. *Food Chemistry* **2011**, *126*, 498-505.
193.Kaptay, G., A new paradigm on the chemical potentials of components in multi-component nano-phases within multi-phase systems. *Rsc Advances* **2017**, *7*, 41241-41253.
194.Yang, Y.; Leser, M. E.; Sher, A. A.; McClements, D. J., Formation and stability of emulsions using a natural small molecule surfactant: Quillaja saponin (Q-Naturale®). *Food Hydrocolloids* **2013**, *30*, 589-596.

195. Mitra, S.; Dungan, S. R., Micellar properties of Quillaja saponin. 1. Effects of temperature, salt, and pH on solution properties. *Journal of Agricultural and Food Chemistry* **1997**, *45*, 1587-1595.
196. McClements, D. J.; Decker, E. A.; Park, Y., Controlling lipid bioavailability through physicochemical and structural approaches. *Critical reviews in food science and nutrition* **2008**, *49*, 48-67.
197. Silletti, E.; Vingerhoeds, M. H.; Norde, W.; Van Aken, G. A., The role of electrostatics in saliva-induced emulsion flocculation. *Food Hydrocolloids* **2007**, *21*, 596-606.
198. Vingerhoeds, M. H.; Blijdenstein, T. B.; Zoet, F. D.; van Aken, G. A., Emulsion flocculation induced by saliva and mucin. *Food Hydrocolloids* **2005**, *19*, 915-922.
199. Bauer, E.; Jakob, S.; Mosenthin, R., Principles of physiology of lipid digestion. *Asian-Australasian Journal of Animal Sciences* **2005**, *18*, 282-295.
200. Maldonado-Valderrama, J.; Wilde, P.; Macierzanka, A.; Mackie, A., The role of bile salts in digestion. *Advances in Colloid and Interface Science* **2011**, *165*, 36-46.
201. Salvia-Trujillo, L.; Qian, C.; Martín-Belloso, O.; McClements, D., Influence of particle size on lipid digestion and β-carotene bioaccessibility in emulsions and nanoemulsions. *Food chemistry* **2013**, *141*, 1472-1480.
202. Sharma, R. A.; Steward, W. P.; Gescher, A. J., Pharmacokinetics and pharmacodynamics of curcumin. *Molecular Targets and Therapeutic Uses of Curcumin in Health and Disease* **2007**, *595*, 453-470.
203. Andersen, C. N., Vitamin and mineral dietary supplement and method of making. In Google Patents: 1946.
204. Desai, D.; Kothari, S.; Huang, M., Solid-state interaction of stearic acid with povidone and its effect on dissolution stability of capsules. *International journal of pharmaceutics* **2008**, *354*, 77-81.
205. Li, J.; Wu, Y., Lubricants in pharmaceutical solid dosage forms. *Lubricants* **2014**, *2*, 21-43.
206. Shokri, J.; Adibkia, K., Application of cellulose and cellulose derivatives in pharmaceutical industries. In *Cellulose-medical, pharmaceutical and electronic applications*, InTech: 2013.
207. Jannin, V.; Chevrier, S.; Michenaud, M.; Dumont, C.; Belotti, S.; Chavant, Y.; Demarne, F., Development of self emulsifying lipid formulations of BCS class II drugs with low to medium lipophilicity. *International Journal of Pharmaceutics* **2015**, *495*, 385-392.
208. Gómez-Estaca, J.; Gavara, R.; Hernández-Muñoz, P., Encapsulation of curcumin in electrosprayed gelatin microspheres enhances its bioaccessibility and widens its uses in food applications. *Innovative Food Science & Emerging Technologies* **2015**, *29*, 302-307.
209. Dave, R. H., Overview of pharmaceutical excipients used in tablets and capsules. *Drug Topics, Oct* **2008**, *24*, 1-13.
210. Schwarz, W., *PVP: a critical review of the kinetics and toxicology of polyvinylpyrrolidone (povidone)*. CRC Press: 1990.
211. Paradkar, A.; Ambike, A. A.; Jadhav, B. K.; Mahadik, K., Characterization of curcumin–PVP solid dispersion obtained by spray drying. *International journal of pharmaceutics* **2004**, *271*, 281-286.
212. Gangwar, R. K.; Dhumale, V. A.; Kumari, D.; Nakate, U. T.; Gosavi, S.; Sharma, R. B.; Kale, S.; Datar, S., Conjugation of curcumin with PVP capped gold nanoparticles for improving bioavailability. *Materials Science and Engineering: C* **2012**, *32*, 2659-2663.
213. Croy, S.; Kwon, G., Polymeric micelles for drug delivery. *Current pharmaceutical design* **2006**, *12*, 4669-4684.

214. Akbar, M. U.; Rehman, K.; Zia, K. M.; Qadir, M. I.; Akash, M. S. H.; Ibrahim, M., Critical Review on Curcumin as a Therapeutic Agent: From Traditional Herbal Medicine to an Ideal Therapeutic Agent. *Critical Reviews in Eukaryotic Gene Expression* **2018**, *28*, 17-24.
215. Hatcher, H.; Planalp, R.; Cho, J.; Tortia, F. M.; Torti, S. V., Curcumin: From ancient medicine to current clinical trials. *Cellular and Molecular Life Sciences* **2008**, *65*, 1631-1652.
216. Tsuda, T., Curcumin as a functional food-derived factor: degradation products, metabolites, bioactivity, and future perspectives. *Food & Function* **2018**, *9*, 705-714.
217. Kunwar, A.; Priyadarsini, K. I., Curcumin and Its Role in Chronic Diseases. In *Anti-Inflammatory Nutraceuticals and Chronic Diseases*, Gupta, S. C.; Prasad, S.; Aggarwal, B. B., Eds. 2016; Vol. 928, pp 1-25.
218. Zhou, H. Y.; Beevers, C. S.; Huang, S. L., The Targets of Curcumin. *Current Drug Targets* **2011**, *12*, 332-347.
219. Higdon, J.; Drake, V. J.; Delage, B.; Howells, L. Curcumin. http://lpi.oregonstate.edu/mic/dietary-factors/phytochemicals/curcumin
220. Heger, M.; van Golen, R. F.; Broekgaarden, M.; Michel, M. C., The Molecular Basis for the Pharmacokinetics and Pharmacodynamics of Curcumin and Its Metabolites in Relation to Cancers. *Pharmacological Reviews* **2014**, *66*, 222-307.
221. Stanic, Z., Improving therapeutic effects of curcumin - a review. *Journal of Food and Nutrition Research* **2018**, *57*, 109-129.
222. Nayak, P. A.; Mills, T.; Norton, I., Lipid Based Nanosystems for Curcumin: Past, Present and Future. *Current Pharmaceutical Design* **2016**, *22*, 4247-4256.
223. McClements, D. J., Nanoscale Nutrient Delivery Systems for Food Applications: Improving Bioactive Dispersibility, Stability, and Bioavailability. *Journal of Food Science* **2015**, *80*, N1602-N1611.
224. Krishnakumar, I.; Ravi, A.; Kumar, D.; Kuttan, R.; Maliakel, B., An enhanced bioavailable formulation of curcumin using fenugreek-derived soluble dietary fibre. *Journal of Functional Foods* **2012**, *4*, 348-357.
225. McClements, D. J., Delivery by Design (DbD): A Standardized Approach to the Development of Efficacious Nanoparticle- and Microparticle-Based Delivery Systems. *Comprehensive Reviews in Food Science and Food Safety* **2018**, *17*, 200-219.
226. Pan, K.; Luo, Y. C.; Gan, Y. D.; Baek, S. J.; Zhong, Q. X., pH-driven encapsulation of curcumin in self-assembled casein nanoparticles for enhanced dispersibility and bioactivity. *Soft Matter* **2014**, *10*, 6820-6830.
227. Peng, S. F.; Li, Z. L.; Zou, L. Q.; Liu, W.; Liu, C. M.; McClements, D. J., Improving curcumin solubility and bioavailability by encapsulation in saponin-coated curcumin nanoparticles prepared using a simple pH-driven loading method. *Food & Function* **2018**, *9*, 1829-1839.
228. Peng, S. F.; Li, Z. L.; Zou, L. Q.; Liu, W.; Liu, C. M.; McClements, D. J., Enhancement of Curcumin Bioavailability by Encapsulation in Sophorolipid-Coated Nanoparticles: An in Vitro and in Vivo Study. *Journal of Agricultural and Food Chemistry* **2018**, *66*, 1488-1497.
229. Zheng, B. J.; Peng, S. F.; Zhang, X. Y.; McClements, D. J., Impact of Delivery System Type on Curcumin Bioaccessibility: Comparison of Curcumin-Loaded Nanoemulsions with Commercial Curcumin Supplements. *Journal of Agricultural and Food Chemistry* **2018**, *66*, 10816-10826.

230. Zhang, R.; Zhang, Z.; Zhang, H.; Decker, E. A.; McClements, D. J., Influence of emulsifier type on gastrointestinal fate of oil-in-water emulsions containing anionic dietary fiber (pectin). *Food Hydrocolloids* **2015**, *45*, 175-185.
231. McClements, D. J., Colloidal basis of emulsion color. *Current opinion in colloid & interface science* **2002**, *7*, 451-455.
232. Chantrapornchai, W.; Clydesdale, F. M.; McClements, D. J., Understanding colors in emulsions. In *Color Quality of Fresh and Processed Foods*, Culver, C. A.; Wrolstad, R. E., Eds. American Chemical Society: Washington, D.C., 2008; Vol. 983, pp 364-387.
233. Robins, M. M., Emulsions—creaming phenomena. *Current opinion in colloid & interface science* **2000**, *5*, 265-272.
234. Chen, B. C.; McClements, D. J.; Gray, D. A.; Decker, E. A., Stabilization of Soybean Oil Bodies by Enzyme (Laccase) Cross-Linking of Adsorbed Beet Pectin Coatings. *Journal of Agricultural and Food Chemistry* **2010**, *58*, 9259-9265.
235. Iwanaga, D.; Gray, D. A.; Fisk, I. D.; Decker, E. A.; Weiss, J.; McClements, D. J., Extraction and characterization of oil bodies from soy beans: A natural source of pre-emulsified soybean oil. *Journal of Agricultural and Food Chemistry* **2007**, *55*, 8711-8716.
236. Chuang, R. L. C.; Chen, J. C. F.; Chu, J.; Tzen, J. T. C., Characterization of seed oil bodies and their surface oleosin isoforms from rice embryos. *Journal of Biochemistry* **1996**, *120*, 74-81.
237. Chang, Y.; McClements, D. J., Characterization of mucin–lipid droplet interactions: Influence on potential fate of fish oil-in-water emulsions under simulated gastrointestinal conditions. *Food Hydrocolloids* **2016**, *56*, 425-433.
238. Singh, H.; Ye, A.; Horne, D., Structuring food emulsions in the gastrointestinal tract to modify lipid digestion. *Progress in lipid research* **2009**, *48*, 92-100.
239. Hettiarachchy, N.; Kalapathy, U., Functional properties of soy proteins. **1998**.
240. Kinsella, J. E., Functional properties of soy proteins. *Journal of the American Oil Chemists' Society* **1979**, *56*, 242-258.
241. Ozturk, B.; McClements, D. J., Progress in natural emulsifiers for utilization in food emulsions. *Current Opinion in Food Science* **2016**, *7*, 1-6.
242. Chung, C.; Sher, A.; Rousset, P.; McClements, D. J., Use of natural emulsifiers in model coffee creamers: Physical properties of quillaja saponin-stabilized emulsions. *Food hydrocolloids* **2017**, *67*, 111-119.
243. Li, Y.; McClements, D. J., New mathematical model for interpreting pH-stat digestion profiles: Impact of lipid droplet characteristics on in vitro digestibility. *Journal of Agricultural and Food Chemistry* **2010**, *58*, 8085-8092.
244. Willett, W., Food in the Anthropocene: the EAT–Lancet Commission on healthy diets from sustainable food systems. *The Lancet* **2019**.
245. Poore, J.; Nemecek, T., Reducing food's environmental impacts through producers and consumers. *Science* **2018**, *360*, 987-+.
246. Springmann, M.; Clark, M.; Mason-D'Croz, D.; Wiebe, K.; Bodirsky, B. L.; Lassaletta, L.; de Vries, W.; Vermeulen, S. J.; Herrero, M.; Carlson, K. M.; Jonell, M.; Troell, M.; DeClerck, F.; Gordon, L. J.; Zurayk, R.; Scarborough, P.; Rayner, M.; Loken, B.; Fanzo, J.; Godfray, H. C. J.; Tilman, D.; Rockström, J.; Willett, W., Options for keeping the food system within environmental limits. *Nature* **2018**.
247. Sethi, S.; Tyagi, S. K.; Anurag, R. K., Plant-based milk alternatives an emerging segment of functional beverages: a review. *Journal of Food Science and Technology-Mysore* **2016**, *53*, 3408-3423.

248.Campbell, K. A.; Glatz, C. E.; Johnson, L. A.; Jung, S.; de Moura, J. M. N.; Kapchie, V.; Murphy, P., Advances in Aqueous Extraction Processing of Soybeans. *Journal of the American Oil Chemists Society* **2011**, *88*, 449-465.
249.Wang, W.; Cui, C. L.; Wang, Q. L.; Sun, C. B.; Jiang, L. Z.; Hou, J. C., Effect of pH on physicochemical properties of oil bodies from different oil crops. *Journal of Food Science and Technology-Mysore* **2019**, *56*, 49-58.
250.Qi, B. K.; Ding, J.; Wang, Z. J.; Li, Y.; Ma, C. G.; Chen, F. S.; Sui, X. N.; Jiang, L. Z., Deciphering the characteristics of soybean oleosome-associated protein in maintaining the stability of oleosomes as affected by pH. *Food Research International* **2017**, *100*, 551-557.
251.Chang, M. T.; Tsai, T. R.; Lee, C. Y.; Wei, Y. S.; Chen, Y. J.; Chen, C. R.; Tzen, J. T. C., Elevating Bioavailability of Curcumin via Encapsulation with a Novel Formulation of Artificial Oil Bodies. *Journal of Agricultural and Food Chemistry* **2013**, *61*, 9666-9671.
252.Sanidad, K. Z.; Sukamtoh, E.; Xiao, H.; McClements, D. J.; Zhang, G., Curcumin: Recent Advances in the Development of Strategies to Improve Oral Bioavailability. *Annual Reviews in Food Science and Technology* **2019**, *10*, 597–617.
253.Zou, L. Q.; Liu, W.; Liu, C. M.; Xiao, H.; McClements, D. J., Utilizing Food Matrix Effects To Enhance Nutraceutical Bioavailability: Increase of Curcumin Bioaccessibility Using Excipient Emulsions. *Journal of Agricultural and Food Chemistry* **2015**, *63*, 2052-2062.
254.Ichikawa, T.; Dohda, T.; Nakajima, Y., Stability of oil-in-water emulsion with mobile surface charge. *Colloids and Surfaces A: Physicochemical and Engineering Aspects* **2006**, *279*, 128-141.
255.Priyadarsini, K., The chemistry of curcumin: from extraction to therapeutic agent. *Molecules* **2014**, *19*, 20091-20112.
256.Kharat, M.; Du, Z. Y.; Zhang, G. D.; McClements, D. J., Physical and Chemical Stability of Curcumin in Aqueous Solutions and Emulsions: Impact of pH, Temperature, and Molecular Environment. *Journal of Agricultural and Food Chemistry* **2017**, *65*, 1525-1532.
257.McClements, D. J.; Li, F.; Xiao, H., The Nutraceutical Bioavailability Classification Scheme: Classifying Nutraceuticals According to Factors Limiting their Oral Bioavailability. In *Annual Review of Food Science and Technology, Vol 6*, Doyle, M. P.; Klaenhammer, T. R., Eds. 2015; Vol. 6, pp 299-327.
258.Kopec, R. E.; Failla, M. L., Recent advances in the bioaccessibility and bioavailability of carotenoids and effects of other dietary lipophiles. *Journal of Food Composition and Analysis* **2018**, *68*, 16-30.
259.Jones, P. J.; Jew, S., Functional food development: concept to reality. *Trends in Food Science & Technology* **2007**, *18*, 387-390.
260.Siro, I.; Kápolna, E.; Kápolna, B.; Lugasi, A., Functional food. Product development, marketing and consumer acceptance—A review. *Appetite* **2008**, *51*, 456-467.
261.Menrad, K., Market and marketing of functional food in Europe. *Journal of food engineering* **2003**, *56*, 181-188.
262.Daliu, P.; Santini, A.; Novellino, E., From pharmaceuticals to nutraceuticals: bridging disease prevention and management. *Expert Review of Clinical Pharmacology* **2019**, *12*, 1-7.
263.Abuajah, C. I.; Ogbonna, A. C.; Osuji, C. M., Functional components and medicinal properties of food: a review. *Journal of food science and technology* **2015**, *52*, 2522-2529.
264.Ameratunga, R.; Crooks, C.; Simmons, G.; Woon, S. T., Health Risks and Adverse Reactions to Functional Foods. *Critical Reviews in Food Science and Nutrition* **2016**, *56*, 318-325.

265. Shahbandeh, M. Revenue generated by the functional food market worldwide in 2017 and 2022 (in billion U.S. dollars). https://www.statista.com/statistics/252803/global-functional-food-sales/
266. Dwyer, J.; Coates, P.; Smith, M., Dietary supplements: regulatory challenges and research resources. *Nutrients* **2018**, *10*, 41.
267. Espin, J. C.; Garcia-Conesa, M. T.; Tomas-Barberan, F. A., Nutraceuticals: Facts and fiction. *Phytochemistry* **2007**, *68*, 2986-3008.
268. Varzakas, T.; Zakynthinos, G.; Verpoort, F., Plant food residues as a source of nutraceuticals and functional foods. *Foods* **2016**, *5*, 88.
269. Delgado-Vargas, F.; Paredes-Lopez, O., *Natural colorants for food and nutraceutical uses*. CRC press: 2002.
270. Hewlings, S. J.; Kalman, D. S., Curcumin: A Review of Its' Effects on Human Health. *Foods* **2017**, *6*.
271. Kocaadam, B.; Sanlier, N., Curcumin, an active component of turmeric (Curcuma longa), and its effects on health. *Critical Reviews in Food Science and Nutrition* **2017**, *57*, 2889-2895.
272. Pulido-Moran, M.; Moreno-Fernandez, J.; Ramirez-Tortosa, C.; Ramirez-Tortosa, M. C., Curcumin and Health. *Molecules* **2016**, *21*.
273. Stanic, Z., Curcumin, a Compound from Natural Sources, a True Scientific Challenge - A Review. *Plant Foods for Human Nutrition* **2017**, *72*, 1-12.
274. Carbonell-Capella, J. M.; Buniowska, M.; Barba, F. J.; Esteve, M. J.; Frígola, A., Analytical methods for determining bioavailability and bioaccessibility of bioactive compounds from fruits and vegetables: A review. *Comprehensive Reviews in Food Science and Food Safety* **2014**, *13*, 155-171.